Carbon TerraVault VI
Class VI Permit Application
Narrative Report

Submitted to:

U.S. Environmental Protection Agency Region 9
San Francisco, CA

Prepared by:

27200 Tourney Road, Suite 200
Santa Clarita, CA 91355
(888) 848-4754

ATTACHMENT A: NARRATIVE REPORT
[40 CFR 146.82(a)]
CTV VI

Table of Contents

List of Attachments

List of Appendices

Document Version History

Version	Revision Date	File Name	Description of Change
1	7/31/2024	Att A - CTV VI Narr.docx	Initial submission
2	8/26/2025	Att A - CTV VI Narr_v2.docx	Response to May 15, 2025 EPA Comments
3	11/21/2025	Att A - CTV VI Narr_v3.docx	Response to August 21, 2025 EPA Comments

1. Project Background and Contact Information

Carbon TerraVault Holdings, LLC (CTV), a wholly owned subsidiary of California Resources Corporation (CRC), proposes to construct and operate seven carbon dioxide (CO_2) geologic sequestration wells at the project area located in Fresno County, California. This application was prepared in accordance with the U.S. Environmental Protection Agency's (EPA's) Class VI regulations, in Title 40 of the Code of Federal Regulations (40 CFR 146.81). CTV is not requesting an injection depth waiver or aquifer exemption expansion.

CTV will obtain the required authorizations from applicable local and state agencies, including the associated environmental review process under the California Environmental Quality Act. **Appendix 1** outlines potential local, state and federal permits and authorizations. The project wells and facilities will not be located on Indian Lands. Federal act considerations and additional consultation, which includes the Endangered Species Act, the National Historic Preservation Act, and consultations with Tribes in the Area of Review (AoR), are presented in **Appendix 2**.

CTV forecasts the potential CO_2 stored in the Injection Zone (Domengine, Garzas, Blewett, and Tracy Formations) at 3.38 million metric tons (MMT) annually on average for 30 years for a total of 101.5 MMT.

CTV is planning to construct a carbon capture and sequestration "hub" project (i.e., a project that collects CO_2 from multiple sources over time and injects the CO_2 stream(s) via Class VI UIC permitted injection wells). Therefore, CTV is currently considering multiple sources of anthropogenic CO_2 for the project. Potential sources include capture from existing and potential future industrial sources in the San Joaquin Basin area, as well as direct air capture (DAC).

The CTV VI storage site is located in the Northern San Joaquin basin, in Fresno County, California (**Figure 1-1**). The project is comprised of seven injection wells, surface facilities, and monitoring wells. This supporting documentation applies to each of the seven injection wells.

CTV will actively communicate project details and submitted regulatory documents to County and State agencies:

- Fresno County
  District 5 Supervisor –Nathan Magsig
  2281 Tulare St. Room #300
  Fresno, CA 93721
  (559) 600-5000
- Fresno County Department of Public Works and Planning
  Director – Steven E. White
  2220 Tulare Street, 6th Floor
  Fresno, CA 93721
  (559) 600-4537
- California Geologic Energy Management Division (CalGEM)
  Senior Oil and Gas Engineer – Erwin Sison

715 P Street, MS 1804
Sacramento, CA 95814
(916) 203-7734

- CA Assembly District 27
  Assemblyman Esmeralda Soria
  512 West 18th Street
  Merced, CA 95340
  (209) 726-5465
- CA Senate District 14
  Senator Anna Caballero
  512 West 18th Street
  Merced, CA 95340
  (209) 726-5465
- US Congressional District 13
  Representative John S. Duarte
  90 S. First Street
  Turlock, CA 95380
  (209) 226-6880
- United States Senator
  Senator Laphonza Butler 2500 Tulare Street
  Suite 4290
  Fresno, CA 93721
  (559) 485-7430
- United States Senator
  Senator Alex Padilla 2500
  Tulare Street
  Suite 5290
  Fresno, CA 93721
  (559) 497-5109
- Region 9 Environmental Protection Agency
  David Albright
  75 Hawthorne Street
  San Francisco, CA 94105
  (415) 947-8000

2. Site Characterization

2.1 Regional Geology, Hydrogeology, and Local Structural Geology [40 CFR 146.82(a)(3)(vi)]

2.1.1 Geologic History

The CTV VI storage site is located in western Fresno County in the vicinity of several oil and gas fields (**Figure 1-1**). The small gas fields nearest to the project area are Ash Slough (13 miles

north), Cheney Ranch (10 miles south southwest), Gill Ranch (14 miles east), Merrill Avenue (8.2 miles northeast), Mint Road (18 miles north northwest), Moffat Ranch (9.3 miles east northeast), San Joaquin Northwest (19 miles southeast now abandoned), and Chowchilla Gas Field (22 miles north). These fields were discovered between 1935 and 1992 and produce from Late Cretaceous, Paleocene, Eocene, and/or Miocene reservoirs. The Raisin City Oil Field (30 miles southeast) and San Joaquin Oil Field (24 miles southeast) were discovered in 1941 and 1947, respectively, with Raisin City producing from Miocene reservoirs and San Joaquin producing from Eocene reservoirs.

Several exploration wells have been drilled in the region of the CTV VI project. There are three abandoned exploration wells within 1 mile of the Area of Review (AoR) and two abandoned exploration wells within the AoR; however, no hydrocarbon accumulations have been discovered within the project AoR (**Figure 1-1**).

The CTV VI Injection Zone consists of the Tracy, Blewett, Garzas, and Domengine storage reservoirs and several interbedded shales (Ragged Valley, Moreno, and Hall shales). The Kreyenhagen Shale will be the overriding Confining Zone. The Zilch is considered a Monitoring Zone overlying the Kreyenhagen.

The CTV VI AoR, shown as the red boundary in **Figure 2.1-1**, represents the combined project CO_2 plume areas for the Tracy, Blewett, Garzas, and Domengine Formations in the Injection Zone. The project AoR was determined based on computational modeling as described in **Attachment B: AoR and Corrective Action Plan** (**Attachment B**).

2.1.2 Geology Overview

The CTV VI storage site lies within the northern San Joaquin Basin in central California (**Figure 2.1-2**). The San Joaquin Basin is the southern, asymmetric sub-basin of the larger, Great Valley Forearc.

2.1.2.1 Basin Structure

The Great Valley was developed during mid to late Mesozoic time. The advent of this development occurred under convergent-margin conditions via eastward, Farallon Plate subduction of oceanic crust beneath the western edge of North America (Beyer, 1988). The convergent continental margin that characterized central California during the Late Jurassic through Oligocene time was later replaced by a transform-margin tectonic system. This occurred as a result of the northward migration of the Mendocino Triple Junction (from Baja California to its present location off the coast of Oregon), located along California's coast (**Figure 2.1-3**). Following this migrational event, the progressive cessation of both subduction and arc volcanism occurred as the progradation of a transform fault system moved in as the primary tectonic environment (Graham, 1984). The major present day fault, the San Andreas, intersects most of the Franciscan subduction complex, which consists of the exterior region of the extinct convergent-margin system (Graham, 1984).

2.1.2.2 Basin Stratigraphy

The structural trough that developed subsequent to these tectonic events ("the Great Valley") became a depocenter for eroded sediment, and therefore currently contains a thick infilled

sequence of sedimentary rocks. These sedimentary formations range in age from Jurassic to Holocene. The first deposits occurred as an ancient seaway that through time were built up by the erosion of the surrounding structures. The basin is constrained on the west by the Coast Range Thrust, on the north by the Stockton Arch, on the east by the Sierra Nevada, and on the south by the Wind Wolves Fault (**Figure 2.1-2**). To the west, the Coastal Range boundary was created by uplifted rocks of the Franciscan Assemblage (**Figure 2.1-4**). The Sierra Nevada, which make up the eastern boundary, are a result of a chain of ancient volcanos.

Basin development is broken out into evolutionary stages at the end of each time-period of the arc-trench system from Jurassic to Neogene in **Figure 2.1-5**. Sediment infill began as an ancient seaway and was later sourced from the erosion of the surrounding structures. Sedimentary infill consists of Cretaceous-Paleogene fluvial, deltaic, shelf and slope sediments. Due to the southward tilt of the basin, sedimentation thickens towards the southern end near the Wind Wolf Fault, creating sequestration quality sandstones toward the basin center and on the eastern margin of the basin.

In the northern San Joaquin Basin, the Cretaceous Tracy, Blewett, and Garzas Sandstones are deep marine units fed from the Starkey deltaic units shed from eastern Sierran basement. After a long hiatus, Eocene Domengine Sandstone was fed from the west and covered by Kreyenhagen shales (**Figure 2.1-6**). The Oligo-Miocene Zilch is an eastern sourced sandstone. All reservoir units are composed of thick-bedded sandstones. Shales separate the Cretaceous sands and cap the Eocene sand. Structure in this area is characterized as a flat basin floor with an eastern homocline that dips about 2 degrees to the southwest.

2.1.3 Geological Sequence

The seven injection wells for the project will inject CO_2 within the injection interval, which is comprised of the Tracy, Blewett, Garzas, and Domengine Formations. The injection depth for the project wells spans approximately 4,296 to 9,280 feet total vertical depth subsea (TVDSS).

Figure 2.1-7 is a schematic cross section depicting the stratigraphy in the region east of the San Joaquin Fault and west of the Sierran uplift, where the project area is located. The injection location on the west is stratigraphically separated from the non-associated gas fields to the east.

2.1.3.1 Basin Floor Fans

Eustatic sea level events and tectonics caused the northern San Joaquin Basin to undergo a series of shelf progradations and subsequent transgressions that resulted in a series of basin floor fan systems fed from erosive fan channel systems that dissected the shelf edge deltas. The Cretaceous Lathrop through Blewett sandstones are down slope equivalents of Starkey deltaic sandstones. The Garzas Sandstone is a deltaic to shallow marine sandstone that prograded westward across the east side, onto slope and basin floor Moreno Shale.

Following deposition of each of the prospective reservoir units (**Figures 2.1-6 and 2.1-7**), they were overlain by a succession of shales. The Lathrop was overlain by the Sawtooth Shale, the Tracy was overlain by the Ragged Valley Shale, and the Blewett Sandstone was overlain by the Moreno Shale. In the late Cretaceous, the Moreno was overlain by the progradational Garzas Sandstone. After a 10 million-year hiatus, the Garzas was overlain by the Eocene Domengine

Formation Sandstone, which is in turn overlain by the Eocene Kreyenhagen Formation Shale. The shales that separate the Cretaceous sandstone reservoir units cover much of the northern San Joaquin. The Kreyenhagen Shale caps the Domengine and overlies the entire injection interval. The Kreyenhagen is found throughout the northern San Joaquin basin and serves as the Confining Zone for the project due to its low permeability, adequate thickness (approximately 500 to 650 feet within the AoR), and regional continuity that spans beyond the AoR (**Figure 2.1-8**). Above the Kreyenhagen Shale lies the Zilch Formation (Monitoring Zone) and the basal shale of the Santa Margarita Formation.

2.2 Maps and Cross Sections of the AoR [40 CFR 146.82(a)(2), 146.82(a)(3)(i)]

2.2.1 Data

To date, two exploration wells have been drilled within the project AoR (**Figure 2.2-1**). In addition to well log data from the vicinity of the project, this project uses seismic coverage, core, and reservoir performance data such as production and pressure to give an adequate description of the reservoir. Wells with data used to inform the development of the conceptual geologic model are shown in **Figure 2.2-2(a)** and **2.2-2(b)**.

Well data are used in conjunction with two-dimensional (2D) and three-dimensional (3D) seismic to define the structure and stratigraphy of the injection zones and confining layers. **Figure 2.2-3** shows outlines of the seismic data used within the area of the model boundary. Also shown are the seismic well ties made to the 2D and 3D data, along with velocity data from wellbores with available checkshot surveys. Available 3D seismic data were used as the basis for phase- and time-matching the 2D seismic lines so that the surfaces were mapped on a consistent datum. The 2D and 3D data were mapped for the following surfaces:

- Santa Margarita Formation
- Domengine Formation
- Garzas Formation
- Blewett Formation
- Tracy Formation
- Lathrop Formation
- A seismic basement reflector used to look for deep faulting in the area but not part of the simulation model

The interpretation of these layers began with a series of well ties at well locations shown in **Figure 2.2-3**. These well ties create an accurate relationship between wells which are in depth and the seismic which is in time. The well tie time-depth relationships are used in conjunction with available checkshot data to confirm the well picks relative to the seismic data. The layers listed above were mapped in time across the 2D and 3D seismic data and then gridded. Alongside this mapping was the interpretation of any faulting in the area, which is discussed further in the Faults and Fracture section of this document.

The gridded time maps are sampled to well pick tops across the model area to create time-depth pairs, which are used to calculate an average velocity. Average velocity maps are then created for each of the layers listed above to convert the gridded time maps into depth for input into the simulation model. Intermediate layers between the mapped seismic surfaces are developed using a framework using conformance relationships to create a series of depth grids that are controlled by formation well tops picked on well logs. The seismic mapped depth grids are used as structural control between these well tops to incorporate the detailed mapping of the seismic data. A separate 3D velocity model was created to depth convert any interpreted faults from the seismic data into the depth domain.

2.2.2 Stratigraphy

Major stratigraphic intervals within the project area, from oldest to youngest, include the Sawtooth Shale, the Tracy Formation, the Blewett Formation, the Garzas Formation, the Domengine Formation, the Kreyenhagen Shale, the Zilch Formation, and the Santa Margarita Formation (**Figures 2.2-4 and 2.2-5**). As shown in **Figure 2.2-5**, the Kreyenhagen Shale is the sealing rock that separates the injection zone from the overlying formations and underground sources of drinking water (USDWs). Injection Zone, Confining Zone, and Monitoring Zone formations are described in the following subsections. Shallower formations are described in Section 2.7.

2.2.2.1 Cretaceous Sandstones (Blewett and Tracy Formations, Injection Zone)

The Cretaceous-age sandstones, locally known as the Blewett and Tracy Formations, represent deep-water submarine-fan systems. Average gross thicknesses across the northern San Joaquin Basin region of the Blewett and Tracy Formations are approximately 660 feet and 650 feet, respectively. Reservoir depths average approximately 5,300 feet and 6,200 feet regionally for the Blewett and Tracy Formations, respectively. The submarine fan deposits pinch out against flanking shale facies up-dip to the east. To the west, the sands grade laterally into offshore deep marine deposits and outcrop near the western edge of the study area.

2.2.2.2 Paleogene Sandstones (Domengine and Garzas Formations, Injection Zone)

The Paleogene-age sandstones, locally known as the Domengine and Garzas Formations, are Injection Zone targets. They represent lower shoreface to deltaic sandstones. Across the northern San Joaquin Basin region, the shallower of the two reservoirs, the Domengine, lies at depths on average of approximately 3,400 feet below ground surface (bgs). Regionally, the thickness of the Domengine Formation averages 490 feet and reservoir porosity and permeability average 29 percent and 155 millidarcies (mD), respectively. The regional thickness of the Garzas Formation averages 760 feet with an average porosity and permeability of 28 percent and 91 mD, respectively. Garzas Formation depths average 4,200 feet bgs regionally. At the eastern edge of the basin, the Domengine and Garzas both thin and pinch out against the Sierran basement complex (Scheirer and Magoon, 2008). On the basin's west side, the sandstones grade laterally into slope shales and basin-plain shales (Nilsen and Moore, 1997).

2.2.2.3 Kreyenhagen Shale (Confining Zone)

The Kreyenhagen Shale conformably overlies the Domengine and serves as the primary Confining Zone. It is composed of a firm, brown shale with low average permeability

(<0.001 mD as measured in core in the northern San Joaquin Basin region), average regional thickness (280 feet), and regional continuity that spans beyond the vicinity of the project (Scheirer and Magoon, 2008). As shown in **Figure 2.7-6**, the Kreyenhagen maintains a thickness of greater than 500 feet throughout the AoR and displays a consistent log signature characterized by high clay content typical of deepwater transgressive marine shales. While some logs in the model area show evidence of thin stringers of what are interpreted as distal, downdip sand deposits within the Kreyenhagen, these units are infrequent and thin (less than 20 feet) and are discontinuous from one well to another. The thickness of the Kreyehagen is constrained by wireline data toward the basin center as shown in **Figures 2.2-5** and **2.7-6**. At the basin margins, Kreyenhagen thickness is extrapolated to 0 thickness. These areas are sufficiently far from the project AoR and do not impact confinement.

2.2.2.4 Zilch Formation (Monitoring Zone)

Above the Kreyenhagen Shale lies the Zilch Formation, which is expected to serve as a Monitoring Zone and will be routinely sampled in accordance with **Attachment C: Testing and Monitoring Plan** (**Attachment C**). The Miocene, nonmarine Zilch sandstones tend to be relatively thin across the northern San Joaquin Basin region, ranging between approximately 10 and 100 feet thick, within an otherwise large section of interbedded sands, siltstones, and mudstones. Zilch sandstones are stratigraphically controlled lenticular sands with an average depth of 2,700 feet regionally. The Zilch Formation is overlain by a Miocene Shale deposit that is coeval with the McLure Shale Member of the Monterey Formation, a widespread transgression surface. The Monterey Formation is a deepwater mudstone that is present throughout most of the southern Sacramento and northern San Joaquin Basins.

2.2.3 Maps of the Area of Review

As required by 40 CFR 146.82(a)(2), **Figure 2.2-6** is a summary map of the oil and gas wells, water wells, State- or EPA-approved subsurface cleanup sites, and surface features in the project area and the project AoR. AoR delineation is presented in **Attachment B**. **Tables 2.2-1 and 2.2-2** list water supply wells and the oil and gas wells present in the AoR. Water wells were identified using the California Department of Water Resources (DWR) Well Completion Report (WCR) and California State Water Resources Control Board Groundwater Ambient Monitoring Assessment Program (GAMA) databases and are shown in **Figure 2.2-6**.

Major surface water bodies located in the area include agricultural canals associated with the San Joaquin River. Some canals extend into the AoR. More details concerning these surface water bodies are included in Section 2.7.

The project AoR is in Fresno County. **Figure 2.2-6** does not show the surface traces of known or suspected faults because there are no known surface faults in the AoR. Based on publicly available data from the Conservation Division of Mine Reclamation (DMR) and the U.S. Geological Survey (USGS), there are also no known mines or quarries in the AoR.

Figures 2.2-6 and 2.2-7 also show the locations of State- or EPA-approved subsurface cleanup sites. This cleanup site information obtained from the State Water Resources Control Board (SWRCB) GeoTracker database contains records for sites that impact, or have the potential to

impact, groundwater quality. Water wells within and adjacent to the AoR are discussed in Section 2.7 of this document.

40 CFR 146.82(a)(2) requires that the application includes a map showing the injection wells, the AoR, and the following list of items, and these are shown on the indicated maps where present:

- Existing injection wells, producing wells, abandoned wells, plugged wells or dry holes, deep stratigraphic boreholes (**Figures 2.2-1 and 2.2-6**).
- Surface bodies of water, springs, mines (surface and subsurface), quarries, State, Tribal, and Territory boundaries, roads and other pertinent surface features (**Figure 2.2-6**).
- State- or EPA-approved subsurface cleanup sites (**Figures 2.2-6 and 2.2-7**).
- Water wells (**Figure 2.2-6**; also see Section 2.7)
- **Figure 2.2-6** is a compilation of the above data including index numbers to well names. Referenced index numbers are listed in **Tables 2.2-1 and 2.2-2**.

Figure 2.2-8 displays the location of CTV VI project injection and monitoring wells and maximum CO_2 plume extent within each injection zone interval from modeling presented in **Attachment B**.

2.3 Faults and Fractures [40 CFR 146.82(a)(3)(ii)]

A combination of 3D seismic, 2D seismic, and well control data were used to define the structure and any faulting within the model area (**Figure 2.2-3**). No faults are identified within or near the AoR. The nearest fault is approximately 8 miles northeast of the edge of the AoR. In addition to the reviewed sub-surface data, public data from the USGS Quaternary Fault map support a general absence of faulting within the vicinity of the project AoR. **Figure 2.3-1** shows the Quaternary Fault Map generated by the USGS in collaboration with the California Geologic Survey (CGS) over a region surrounding the model area. USGS does not document a fault of any classification within the AoR. **Figure 2.3-2** shows a combination of the fault traces taken from the USGS map and fault traces identified using the seismic and well data.

Seismic-based depth conversion of the northwest-southeast trending thrust faults to the northeast of the AoR showed minimal offset across the injection zones on the order of zero to approximately 400 feet. These faults are around 8 to 10 miles northeast of the AoR. Representative schematics of 2D seismic sections are provided in **Figure 2.3-3** and **Figure 2.3-4**. These Figures show the interpreted seismic surfaces described in Section 2.2.1, spatial location and offset of the largest fault to the northeast of the AoR, and a number of wells including that from **Figure 2.2-4** and three of the wells from **Figure 2.2-5**. Due to the high net to gross of the injection zones and small offsets, the faults to the northeast are not considered to seal or limit flow or pressure in the simulation model. In addition to this, testing of these fault traces as sealing in simulations showed no material change to the AoR/ plume boundary (less than 0.1 percent area change). The structural expression of these faults are captured in the geologic model through the integration of the dense 2D seismic line interpretation. While the structural impact of the faults are accurately captured in the surfaces in the simulation grid, the grid itself is not explicitly faulted in order to maintain computational efficiency. The model geometry is

shown in **Figure 2.3-3** and **2.3-4.** This assumption is justified considering the distal nature of the faults to the AoR and minimal vertical offset.

The northwest-southeast trending fault system to the southwest of the AoR forms part of the Great Valley thrust fault system (Bryant, 2017). The nearest distance from these faults to the AoR is approximately 9 miles. This system of basin-bounding faults separates the Great Valley sequence from the Coast Ranges to the west. The system is described as a series of shallow-dipping east vergent blind thrust faults with associated west vergent backthrusts. The limited available seismic data in the western portion of the model boundary support this description with steeply dipping reflectors at the basin edge beneath a low-angle thrust with poor reflectivity in the western hanging wall of the fault. Due to thinning of the Injections Zones toward this margin and basin bounding nature of this fault system, this boundary is closed in the simulation model. Testing was also performed where this boundary was treated as open in simulations and showed similar negligible change to the AoR/plume boundary.

2.4 Injection and Confining Zone Details [40 CFR 146.82(a)(3)(iii)]

2.4.1 Mineralogy

No quantitative mineralogy information exists within the AoR boundary. Several wells outside the AoR have mineralogy over the formations of interest, and those data are presented below. The location of wells used for mineralogy are shown in **Figure 2.4-1**, and the mineralogy data are shown in **Table 2.4-1**. Additional mineralogy data from within the AoR will be collected during the pre-operational period as discussed in **Attachment I: Pre-operational Testing Plan**.

2.4.1.1 Monitoring Zone (Zilch Formation)

Mineralogy data are available for the Monitoring Zone in the form of semi-quantitative X-ray diffraction (XRD) data from one well outside the AoR, the PACLAND_THREE_36-4 (04019219300000) well located in Raisin City oil field. Two reservoir sand samples from this well contain on average 30 percent quartz, 50 percent plagioclase and potassium feldspar, and 20 percent total clay. The primary clay mineral is mixed layer illite/smectite. Calcite and dolomite were not detected in either of the samples. Additional mineralogy data from within the AoR will be collected during the pre-operational period as discussed in **Attachment I**.

2.4.1.2 Confining Zone (Kreyenhagen Shale)

Mineralogy data are available for the Confining Zone in the form of XRD data from two wells outside the AoR; the BRUMM_846-15 (04019253230000) well located in Riverdale oil field, and the RIPPERDAN_544-13 (04019253280000) well located in Raisin City oil field. A total of 10 shale samples from these wells average 19 percent quartz, 20 percent plagioclase and potassium feldspar, and 50 percent total clay. Additional minerals include on average 5 percent pyrite and in the RIPPERDAN_544-13 well, Opal-CT was detected with an average weight percent of 8 percent. The primary clay minerals are illite and mixed layer illite/smectite. Calcite and dolomite were detected in nominal amounts in the samples. This mineralogy is similar to outcrop samples of the Confining Zone from adjacent to the model boundary (Hurst et al., 2021; Lewan et al., 2014). Additional mineralogy data from within the AoR will be collected during the pre-operational period as discussed in **Attachment I**.

2.4.1.3 Domengine Formation

Mineralogy data are available for the Domengine Formation in the form of XRD data from one well outside the AoR, the WILCOX_20 (04067205140000) well located in Rio Vista Gas Field. The one sample in this well contains 43 percent quartz, 26 percent plagioclase and potassium feldspar, and 25 percent total clay. Additional minerals include 6 percent pyrite. The primary clay mineral is kaolinite. Calcite and dolomite were not detected in the sample.

Rough sand grain count mineralogy of the Domengine Formation in the project vicinity was conducted by Daviess (1946). A total of 4 outcrop samples from the Los Banos area average 39 percent quartz and 60 percent plagioclase and potassium feldspar. No effort was made to determine clay mineralogy or content. Additional mineralogy data from within the AoR will be collected during the pre-operational period as discussed in **Attachment I**.

2.4.1.4 Garzas Formation

No mineralogy data are currently available for the Garzas Formation inside the model area (**Attachment B**). Therefore, data from the shallower Domengine Formation, similar in age, was used as an analog. The Domengine Formation mineralogy is described in Section 2.4.1.3.

Rough sand grain count mineralogy of Paleocene sandstone in the project vicinity was conducted by Daviess (1946). A total of 14 outcrop samples from the Los Banos area average 44 percent quartz and 56 percent plagioclase and potassium feldspar. No effort was made to determine clay mineralogy or content. Additional mineralogy data from within the AoR will be collected during the pre-operational period as discussed in **Attachment I**.

2.4.1.5 Blewett Formation

No mineralogy data are available for the Blewett Formation, even from outside the AoR. Therefore, data from the deeper Lathrop formation, also Late Cretaceous in age, were used as an analog. The NAPA_AVE_A1 (04019225380000) well, located near the Gill Ranch Gas Field, has 3 samples of reservoir sand within the Lathrop formation. These samples average 35 percent quartz, 54 percent plagioclase and potassium feldspar, and 9 percent total clay. The primary clay minerals are kaolinite and illite. Calcite and dolomite were not detected in the samples. Additional mineralogy data from within the AoR will be collected during the pre-operational period as discussed in **Attachment I**.

2.4.1.6 Tracy Formation

No mineralogy data are available for the Tracy Formation, even from outside the AoR. Therefore, data from the deeper Lathrop Formation, also Late Cretaceous in age, were used as an analog. This mineralogic composition is described in Section 2.4.1.5. Additional mineralogy data from within the AoR will be collected during the pre-operational period as discussed in **Attachment I**.

2.4.2 Porosity and Permeability

Wireline log data were acquired with measurements that include but are not limited to spontaneous potential, natural gamma ray, borehole caliper, compressional sonic, resistivity, neutron porosity, and bulk density.

Formation porosity is determined one of two ways: from bulk density using 2.65 grams per cubic centimeter (g/cc) matrix density as calibrated from core grain density and core porosity data, or from compressional sonic using 55.5 microseconds per foot (μsec/ft) matrix slowness and the Wyllie time average equation. The compaction coefficient (Hilchie, 1978) was calculated using a depth dependent shale travel time.

Volume of clay is determined by spontaneous potential and is calibrated to core data.

Log-derived permeability is determined by applying a core-based transform that uses capillary pressure porosity and permeability along with clay values from XRD or FTIR. Core data from 16 wells of similar age formations (Eocene, Paleocene, and Late Cretaceous) in the Sacramento Basin and the Northern San Joaquin Basin were used to develop a permeability transform (**Figure 2.4-2**). The transform and core data is illustrated in **Figure 2.4-3.**

Comparison of log calculated porosity and the permeability transform to core permeability is shown in **Figure 2.4-4** for the GILL_RANCH_34-18-202 (04039201180000) well in Gill Ranch Gas Field. This well, while outside the AoR, has abundant core data across two of the main Injection Zones for comparison to the permeability transform. Both core porosity and permeability are matched well by the log calculated curves.

A log plot for the DOW_PRICE_GIFEN_1 (04019209700000) is included in **Figure 2.4-5**, showing the calculated model curves directly adjacent to the AoR.

2.4.2.1 Monitoring Zone

The average porosity of the Monitoring Zone is 32.1 percent, based on 39 wells with porosity logs and 10,424 individual logging data points. See **Figure 2.4-6** for the locations of wells used for porosity and permeability averaging. The geometric average permeability of the Monitoring Zone is 77 mD, based on 30 core data points from 3 wells (see **Figure 2.2-2(b)** for well locations). Core porosity was measured, and is in agreement with the log averages (see **Table 2.4-2**).

2.4.2.2 Confining Zone

The average porosity of the confining zone is 26.3 percent, based on 92 wells with porosity logs and 70,165 individual logging data points. The geometric average permeability of the confining zone is 1.62 nanodarcies (nD), based on core permeability measurements performed on 32 samples from 2 wells; the BRUMM_846-15 (04019253230000) well located in Riverdale oil field and the RIPPERDAN_544-13 (04019253280000) well located in Raisin City oil field (see **Table 2.4-3**). These samples were analyzed using the Gas Research Institute (GRI) crushed rock method, and the permeability reported is representative of the matrix permeability.

2.4.2.3 Domengine Formation

The average porosity of the Domengine Formation is 30.6 percent, based on 90 wells with porosity logs and 70,766 individual logging data points. The geometric average permeability of the Domengine Formation is 145 mD, based on 82 wells with porosity logs and 61,507 individual logging data points. A total of 11 core data points from 3 wells are from the

Domengine Formation (see **Table 2.4-4**). The porosity and permeability measurements from core were used to calibrate log permeability and porosity.

2.4.2.4 Garzas Formation

The average porosity of the Garzas Formation is 29.4 percent, based on 80 wells with porosity logs and 55,954 individual logging data points. The geometric average permeability of the Garzas Formation is 106 mD, based on 74 wells with porosity logs and 50,926 individual logging data points. A total of 42 core data points from 5 wells are from the Garzas Formation (see **Table 2.4-5)**. The porosity and permeability measurements from core were used to calibrate log permeability and porosity.

2.4.2.5 Blewett Formation

The average porosity of the Blewett Formation is 26.4 percent, based on 86 wells with porosity logs and 59,117 individual logging data points. The geometric average permeability of the Blewett Formation is 85 mD, based on 89 wells with porosity logs and 57,705 individual logging data points. A total of 375 core data points from 14 wells are from the Blewett Formation (see **Table 2.4-6**). The porosity and permeability measurements from core were used to calibrate log permeability and porosity.

2.4.2.6 Tracy Formation

The average porosity of the Tracy Formation is 22.7 percent, based on 34 wells with porosity logs and 24,170 individual logging data points. The geometric average permeability of the Tracy Formation is 23 mD, based on 34 wells with porosity logs and 22,462 individual logging data points. A total of 181 core data points from the 7 wells are from the Tracy Formation (see **Table 2.4-7**). The porosity and permeability measurements from core were used to calibrate log permeability and porosity.

2.4.3 Injection and Confining Zone Capillary Pressure

Capillary pressure is the difference across the interface of two immiscible fluids. Capillary entry pressure is the minimum pressure required for an injected phase to overcome capillary and interfacial forces and enter the pore space containing the wetting phase.

No capillary pressure data were available for the Confining Zone or any of the Injection Zones. These data will be acquired as part of pre-operational testing.

For computational modeling purposes, capillary pressure data obtained from the similar geologic age and setting Winters Formation in the Union Island Gas Field were used. The Winters Formation data from well SONOL_SECURITIES_5 (04077201910000) are deemed adequate for modeling purposes until site and zone-specific data can be obtained as part of the pre-operational testing program (see **Figure 2.4-2** for well location). **Figure 2.4-7** shows the capillary pressure curve used for the computational modeling. In addition, sensitivity cases were run to gauge the effect of varying the capillary pressure curve on the CO_2 plume and reservoir pressure behavior and the effect was minimal (Attachment B).

Caprock threshold entry pressure tests were available for two of the internal shales, namely the Moreno Shale and the Ragged Valley Shale, from the Gill Ranch gas field (Core Laboratories, 2010). A total of 12 samples from 2 wells (GILL_RANCH_11-21-101 and GILL_RANCH_34-18-202) were tested; 5 of the samples showed no brine production at the highest delta pressure of 2,000 pounds per square inch (psi), 1 sample showed brine breakthrough at the last pressure tested of 2,000 psi, 1 sample showed brine breakthrough at 800 psi, 4 samples showed brine breakthrough at 600 psi, and 1 sample showed brine breakthrough at 400 psi. A comparison of measured air permeability on these samples versus threshold entry pressure is shown in **Figure 2.4-8**. Any sample with air permeability less than 0.1 mD showed no brine breakthrough even at the highest measured delta pressure of 2,000 psi. Because measured permeability on core samples from the Confining Zone are much lower than 0.1 mD (see Section 2.4.2), it can be assumed that the Confining Zone is an impermeable seal at reservoir conditions.

2.4.4 Depth and Thickness

Depth and thickness of the Confining Zone and Injection Zone (**Table 2.4-8**) are determined by structural and isopach maps based on well data (wireline logs) and seismic data. Structure maps of the Injection and Confining Zone, presented in **Figures 2.4-9(a)** through **2.4-9(d)** are provided to indicate a depth to formation adequate for supercritical-state injection.

Isopach maps of the Injection and Confining Zones are also presented in **Figures 2.4-9(a)** through **2.4-9(d)**. Spontaneous potential (SP) logs from surrounding gas wells were used to identify sandstones. Negative millivolt (mV) deflections on these logs, relative to a baseline response in the enclosing shales, define the sandstones. These logs were shale baseline-shifted to 0 mV. Due to the log vintage variability, there is an effect on quality which creates a degree of subjectivity within the gross sand; however, this will not have a material impact on the maps.

Variability in the thickness and depth of the Confining Zone and the Injection Zone will not impact confinement. CTV will use the thicknesses and depths shown when determining operating parameters and assessing project geomechanics.

2.5 Geomechanical and Petrophysical Information [40 CFR 146.82(a)(3)(iv)]

2.5.1 Caprock Ductility

Ductility and the unconfined compressive strength (*UCS*) of shale are two properties used to describe geomechanical behavior. Ductility refers to how much a rock can be distorted before it fractures, while the *UCS* is a reference to the resistance of a rock to distortion or fracture. Ductility generally decreases as compressive strength increases (IEAGHG, 2011).

Ductility and rock strength calculations were performed based on the methodology and equations from Ingram & Urai (1999) and Ingram et al. (1997). Brittleness is determined by comparing the log-derived *UCS* to an empirically derived *UCS* for a normally consolidated rock (UCS_{NC}).

$$\log UCS = -6.36 + 2.45 \log\left(0.86 V_p - 1172\right) \quad (1)$$

$$\sigma' = OB_{pres} - P_p \quad (2)$$

$$UCS_{NC} = 0.5\sigma' \quad (3)$$

$$BRI = \frac{UCS}{UCS_{NC}} \quad (4)$$

Units for the *UCS* equation are *UCS* in megapascals (MPa) and V_p (compressional velocity) in meters per second (m/s). OB_{pres} is overburden pressure, P_p is pore pressure, σ' is effective overburden stress, and *BRI* is brittleness index.

If the value of *BRI* is less than 2, empirical observation shows that the risk of embrittlement is lessened, and the confining zone is sufficiently ductile to accommodate large amounts of strain without undergoing brittle failure. However, if *BRI* is greater than 2, the "risk of development of an open fracture network cutting the whole seal depends on more factors than local seal strength, and therefore the *BRI* criterion is likely to be conservative, so that a seal classified as brittle may still retain hydrocarbons" (Ingram & Urai, 1999).

2.5.1.1 Confining Zone

Within the project area, 40 wells had compressional sonic and bulk density data over the confining zone to calculate ductility, comprising 31,800 individual logging data points (pink squares in **Figure 2.2-2(a)**). In addition, 87 wells were used to calculate *UCS*, comprising 67,692 individual logging data points. The average ductility of the confining zone based on the mean value is 0.95. The average rock strength of the confining zone, as determined by the log-derived *UCS* equation above, is 882 psi.

An example calculation for the well DOW_PRICE_GIFEN_1 (04019209700000) is shown in **Figure 2.5-1**. UCS_CCS_VP is the UCS based on the compressional velocity, UCS_NC is the UCS for a normally consolidated rock, and *BRI* is the calculated brittleness using this method. Brittleness less than 2 (representing ductile rock) is shaded red.

Within the Confining Zone, the brittleness calculation drops to a value less than 2. Additionally, almost all of the shales within and between the injection zones have BRI values of less than 2. Using this methodology, all of these caprocks would be classified as "Very Good" based on Kivior et al. (2002). As a result of the Confining Zone ductility, there are no fractures that will act as conduits for fluid migration from the Injection Zone.

2.5.2 Stress Field

The stress of a rock can be expressed as three principal stresses. Formation fracturing will occur when the pore pressure exceeds the least of the stresses. In this circumstance, fractures will propagate in the direction perpendicular to the least principal stress (**Figure 2.5-2**).

Stress orientations in central California have been studied using both earthquake focal mechanisms and borehole breakouts (Hickman and Zoback, 2004; Townend and Zoback, 2004; Mount and Suppe, 1987, 1992). The general azimuth of maximum principal horizontal stress is that of being fault perpendicular to the strike of the San Andreas fault (Townend and Zoback, 2004; Zoback et al., 1987). Data from the World Stress Map 2016 release (Heidbach et al., 2016, 2018) shows an average S_{Hmax} azimuth of N55ºE ± 6º once several S_{Hmax} indicators with very low-quality grades (D or less) are excluded (**Figure 2.5-3**). This is consistent with

Townend and Zoback (2004) (**Figure 2.5-4)**. Mount and Suppe (1987) determined a regional S_{Hmax} azimuth of N43.9ºE ± 1.9º for the area just to the south of the project area near the town of Coalinga. The earthquakes in the area indicate a strike-slip faulting regime (Lund-Snee and Zoback, 2020).

There are no site-specific fracture gradient data for the injection or confining layers. A step-rate test (SRT) will be conducted per **Attachment I** in the Injection Zones. However, several wells in the project vicinity do have fracture gradient data either in the Injection Zones or in formations of similar age and depth. An SRT was performed in HILMAR_WD2 well within the Domengine Formation with a resultant fracture gradient of 0.82 pounds per square inch per foot (psi/ft). An additional seven wells in the vicinity have formation integrity tests (FITs) or leak-off tests (LOTs) performed at similar depth ranges to the project Injection and Confining Zones. A total of 11 tests from these wells average 0.825 psi/ft from tests in the depth range of 3,000 to 12,350 feet true vertical depth (TVD). See **Figure 2.5-5** for the locations of the wells. For the computational simulation modeling and well-performance modeling, a frac gradient of 0.8 psi/ft was assumed for now for all zones as a safety factor.

The overburden stress gradient in the confining and injection zones is 0.87 to 0.94 psi/ft. The method for calculating the overburden gradient was to integrate density logs using methodology laid out in Fjaer et al. (2008):

$$\sigma_v = \int_0^D \rho(z) g \, dz \quad (5)$$

where ρ is the density of the sediments, g is the acceleration due to gravity, D is the depth of interest, z is the vertical depth interval, and σ_v is the vertical stress. This calculation was completed using the "Overburden Gradient Calculation" module in the software Interactive Petrophysics 5.1.0. **Figure 2.5-6** displays the overburden gradient calculation inputs and outputs from the software. The overburden gradient was calculated using 53 density logs. See **Table 2.5-1** for a list of the wells used for overburden stress gradient calculations.

No data currently exist for the pore pressure of the confining zone. This will be determined as part of the preoperational testing.

2.6 Seismic History [40 CFR 146.82(a)(3)(v)]

2.6.1 Recent Seismicity

As discussed in prior sections, 2D and 3D seismic along with well data were used to create depth surfaces within the model area and AoR. No faults were mapped within the AoR, with the nearest faults identified on seismic data approximately 8 to 10 miles northeast of the AoR edge. Nearest mapped faults shown in the USGS Quaternary Fault map are approximately 9 miles southwest of the edge of the AoR (**Figure 2.3-2**).

USGS (2024) provides an earthquake catalog tool that can be used to search for recent seismicity that could be associated with faults for movement. A search was made for earthquakes in the greater vicinity of the project area from 1850 to June 17, 2024 with events of a magnitude greater

than 2.5. This threshold is used to account for "felt" seismicity across the catalog time record. **Figure 2.6-1** shows the results of this search.

There are nine documented events within a 7-mile radius of the edge of the AoR. **Table 2.6-1** summarizes some of the data taken from them. All of the events were less than a 3.0 magnitude. There are clearly depth errors with four of the events showing depths above ground surface; taking an average of the remaining five shows an average depth of 5.2 kilometers (km), or approximately 17,000 feet. The largest magnitude event cataloged within the model boundary was a 4.84 on September 5, 1974. This event is approximately 16 miles to the south of the AoR edge located close to the northwest-southeast trending fault trace that forms part of the Great Valley thrust system shown on the map by the USGS (**Figure 2.3-1**). There are no events within the AoR boundary.

Lund-Snee and Zoback (2020) published updated maps for crustal stress estimates across North America. **Figure 2.6-2** shows a modified image from Lund-Snee (2020) work highlighting the project area. This work agrees with previous estimates of maximum horizontal stress in the region of approximately N55°E in a predominantly strike-slip regime (see Section 2.5-2). **Attachment C** discusses the seismicity monitoring plan for this injection site.

2.6.2 Seismic Hazard Mitigation

CTV VI is in an area of little historical seismicity, and no active faults have been documented by USGS within the AoR. This document defines the confining zone that separate the injection intervals from USDW.

The following is a summary of CTVs seismic hazard mitigation for CTV VI:

The project has a geologic system capable of receiving and containing the volumes of CO_2 proposed to be injected

- Extensive historical operations in the San Joaquin Basin, across multiple geologic formations, provides valuable experience to understand operating conditions such as injection volumes and reservoir containment.
- There are no faults or fractures identified in the AoR that will impact the confinement of CO_2 injectate. The nearest identified fault is approximately eight miles from the edge of the AoR.

Will be operated and monitored in a manner that will limit risk of endangerment to USDWs, including risks associated with induced seismic events

- Injection pressure will be lower than the fracture gradient of the sequestration reservoir with a safety factor (90 percent of the fracture gradient).
- Injection and monitoring well pressure monitoring will ensure that pressures are beneath the fracture pressure of the sequestration reservoir.
- A seismic monitoring program will be designed to detect events lower than seismic events that can be felt. This will ensure that operations can be modified with early warning events, before a felt seismic event.

Will be operated and monitored in a way that in the unlikely event of an induced event, risks will be quickly addressed and mitigated

- Via monitoring and surveillance practices (pressure and seismic monitoring program), CTV personnel will be notified of events that are considered an early warning sign. Early warning signs will be addressed to ensure that more significant events do not occur.
- CTV will establish a central control center to ensure that personnel have access to the continuous data being acquired during operations.

Minimizing potential for induced seismicity and separating any events from natural to induced

- Pressure will be monitored in each injector and sequestration monitoring well to ensure that pressure does not exceed the fracture pressure of the reservoir or Confining Zone.
- Seismic monitoring program will be installed pre-injection for a period to monitor for any baseline seismicity that is not being resolved by current monitoring programs.
- Average depth of prior seismic hazard in the region based on reviewed historical seismicity has been approximately 5.2 km. Significantly deeper than the proposed Injection Zones.

2.7 Hydrologic and Hydrogeologic Information [40 CFR 146.82(a)(3)(vi), 146.82(a)(5)]

DWR has defined 515 groundwater basins and subbasins within California. The project AoR lies entirely within the western part of the San Joaquin Valley Groundwater Basin (DWR Basin No. 5-022) and encompasses portions of the Westside Subbasin (DWR Basin No. 5-022.09) and Delta-Mendota Subbasin (DWR Basin No. 5-022.07) (DWR, 2020). **Figures 2.7-1 and 2.7-2** illustrate the project AoR, subbasins, and the surrounding areas.

The AoR lies primarily within the northern boundary of the Westside Subbasin and hydrologic information presented here is largely based on data compiled from within that subbasin, as summarized in Luhdorff & Scalmanini (2022). The Westside Subbasin is bounded on the west by the Diablo Range and on the north, east, and south by other subbasins. The project area lies at the northernmost extent of the Westside subbasin and the adjacent southwestern portion of the Delta-Mendota Subbasin, a boundary roughly defined by the Third Lift Canal and land survey lines (**Figures 2.7-1 and 2.7-2**).

2.7.1 Hydrologic Information

The arid climate in the rain shadow of the Coast Ranges limits the occurrence of natural surface water bodies. In the vicinity of the project area, natural surface water consists primarily of ephemeral streams originating from the Coast Range, which flow eastward into the San Joaquín Basin. The closest such stream to the AoR is Panoche Creek, located approximately 20 miles southwest of the project area. Panoche Creek is the largest surface drainage emanating from the Diablo Range (Luhdorff & Scalmanini, 2022).

The San Joaquin River is the principal surface drainage in the region, and lies within the Delta-Mendota Subbasin approximately 5 miles to the east of the AoR (EKI, 2022). Diversions from

this and other rivers entering the Central Valley are imported to the Westside Subbasin to meet local irrigation demand (Luhdorff & Scalmanini, 2022). The Third Lift, Delta-Mendota, and Outside Canals are located within or adjacent to the AoR on the north side of the project area (**Figure 2.7-2**).

2.7.2 Base of Fresh Water and Base of USDWs

The owner or operator of a proposed Class VI injection must define the general vertical and lateral limits of all USDWs and their positions relative to the Injection and Confining Zones. The intent of this information is to demonstrate the relationship between the proposed injection formation and any USDWs, and it will support an understanding of the water resources near the proposed injection well. A USDW is defined as an aquifer or its portion that (a) (1) supplies any public water system or (2) contains a sufficient quantity of groundwater to supply a public water system and (i) currently supplies drinking water for human consumption or (ii) contains less than 10,000 milligrams per liter (mg/L) total dissolved solids (TDS) and (b) which is not an exempted aquifer. For the purpose of the California Sustainable Groundwater Management Act (SGMA), the bottom of the groundwater basin is defined as the base of fresh groundwater (BFW), which is approximately 2,000 to 3,000 mg/L TDS (Luhdorff & Scalmanini, 2022).

2.7.2.1 Base of Fresh Water

BFW helps define the aquifers that are used for public water supply and is by definition shallower than the base of the lowermost USDW. Local water agencies in the subbasins have participated in various studies to comply with SGMA. There is a significant thickness of sedimentary strata overlying basement bedrock. Therefore, it is appropriate to consider water quality when delineating the basin bottom.

USGS mapped the BFW based on measured specific conductance of less than 3,000 micromhos per centimeter (µmhos/cm), which is approximately 2,000 mg/L TDS (Page, 1971 and 1973). A similar dataset was presented by Kang (2020). Based on these data, the BFW in the vicinity of the AoR varies from approximately 450 to 600 feet bgs (**Figure 2.7-3**).

2.7.2.2 Base of Lowermost USDW

Borehole sampling data presented in Kang (2020) suggested that the deepest USDW in the project area would be at a depth greater than 1,500 feet but less than 4,000 feet. CTV has used geophysical logs to investigate the USDWs and the base of the USDWs. Salinity logs from well bores in the project vicinity indicate that the base of the deepest observed USDW corresponds to the base of the Santa Margarita Sandstone (the shallower portion of the Santa Margarita Formation), and this horizon has been adopted as a conservative proxy for the overall depth to USDW within the AoR. Based on well log correlation, the depth to the base of the Santa Margarita Sandstone in the project area ranges from approximately 3,000 to 3,800 feet bgs, which is consistent with the depth range for lowermost USDW estimated from the sampling data. **Figure 2.7-4(a)** presents depth contours to the base of the Santa Margarita Sandstone (assumed to be base of the lowermost USDW). **Figure 2.7-4(b)** is an isopach map illustrating the thickness between the base of USDW and the top of Kreyenhagen. The separation between the lowermost USDW and the uppermost confining layer is variable but never less than 234 feet.

The calculation of salinity from logs used by CRC is a four-step process:

1. Convert measured density or sonic to formation porosity, using the following equation:

$$POR = \frac{(Rhom - RHOB)}{(Rhom - Rhof)} \quad (6)$$

where POR = formation porosity
Rhom = formation matrix density, g/cc; 2.65 g/cc is used for sandstones
RHOB = calibrated bulk density taken from well log measurements (g/cc)
Rhof = fluid density (g/cc); 1.00 g/cc is used for water-filled porosity

The equation to convert measured sonic slowness to porosity is:

$$POR = -1\left(\frac{\Delta tma}{2\Delta tf} - 1\right) - \sqrt{\left(\frac{\Delta tma}{2\Delta tf} - 1\right)^2 + \frac{\Delta tma}{\Delta tlog} - 1} \quad (7)$$

where POR = formation porosity
Δtma = formation matrix slowness (μs/ft); 55.5 μs/ft is used for sandstones
Δtf = fluid slowness (μs/ft); 189 μs/ft is used for water-filled porosity
Δtlog = formation compressional slowness from well log measurements (μs/ft)

2. Calculate apparent water resistivity using the Archie equation:

$$Rwah = \frac{POR^m R_t}{a} \quad (8)$$

where Rwah = apparent water resistivity (ohm-m)
POR = formation porosity
m = the cementation factor; 2 is the standard value
R_t = deep reading resistivity taken from well log measurements (ohm-m)
a = the archie constant; 1 is the standard value

3. Correct apparent water resistivity to a standard temperature of 75°F:

$$Rwahc = Rwah\frac{TEMP + 6.77}{75 + 6.77} \quad (9)$$

where Rwahc = apparent water resistivity (ohm-m), corrected to surface temperature
TEMP = downhole temperature based on temperature gradient (°F)

4. Convert temperature-corrected apparent water resistivity to salinity (Davis 1988):

$$SAL\_a\_EPA = \frac{5500}{Rwahc} \quad (10)$$

where SAL_a_EPA = salinity from corrected Rwahc (parts per million [ppm])

2.7.3 Formations with USDWs

The principal aquifers in AoR vicinity are termed the Upper and Lower Aquifers, which are hosted within a thick sequence of Pleistocene terrestrial sediments. Formations hosting potential

USDWs extend to depth below the principal aquifers and comprise over 3,000 feet of terrestrial and marine sediments of Holocene to Miocene age. The groundwater basin within the project area is composed of at least five formations with the potential to store and transmit water meeting the criteria for USDW: (1) shallow Alluvium, (2) Tulare Formation, (3) San Joaquin Formation, (4) Undivided Pliocene to Miocene terrestrial and marine sediments, and (5) Santa Maria sands of the Monterey Formation.

2.7.3.1 Shallow Alluvium

Groundwater encountered in the upper most part of the shallow aquifer, above the highest regionally extensive lacustrine clay layer where present, is locally named the "shallow zone," and is defined by wells that are screened generally within the first 100 feet from ground surface. This area is not considered a principal aquifer or hydrologically connected to a principal aquifer. Groundwater in this zone is often degraded and locally may not meet USDW criteria (Kang, 2020).

2.7.3.2 Tulare Formation (Upper)

The terrestrial alluvial deposits overlying the uppermost Pliocene marine unit (San Joaquin Formation) was named the Tulare Formation by Anderson (1905). The Tulare Formation was also defined as the youngest deformed deposits along the western margin of the Central Valley. Historically, the term "Tulare Formation" was specific to sedimentary deposits derived from the Coast Ranges to the west, while Sierra-derived sediments were termed simply "alluvium" (L&S, 2022). However, due to the similarity of depositional setting and style, complex interfingering relationships, and difficulty discriminating provenance from borehole data, Pleistocene terrestrial clastic sediments underlying the AoR are referred to collectively as the Tulare Formation.

The overall age of the Tulare Formation is considered to be late Pliocene to late Pleistocene. The Tulare Formation above the Cocoran Clay is middle to late Pleistocene in age and consists primarily of alluvial fan and associated fluvial deposits, within the project area derived largely from the Diablo Range to the west. It is difficult to differentiate the upper Tulare Formation from overlying younger alluvium from driller's reports and geophysical logs due to the similar age, source of sediments (Coast Range), and depositional setting of alluvial sediments. The overall thickness of the upper Tulare Formation and the overlying younger alluvium is about 400 to 600 feet in the project area.

2.7.3.3 Corcoran Clay

The fine-grained Cocoran Clay member of the Tulare Formation provides a regionally extensive confining layer between the Upper and Lower Aquifers. The Corcoran Clay was deposited in a widespread lake which inundated much of the Valley during the middle Pleistocene between 740,000 and 615,000 years ago (Lettis, 1988). In the vicinity of the AoR, the top of the Cocoran Clay is encountered between 400 and 600 feet bgs, and the unit is between 76 and 100 feet thick (Luhdorff & Scalmanini, 2022).

2.7.3.4 Tulare Formation (lower)

The Tulare Formation below the Cocoran Clay is a terrestrial fluvial and floodplain deposit sourced from both the Sierra (east) and Diablo (west) ranges, and characterized by interbedded

thin sand, silt and clay beds. Thick, regionally extensive beds are sparse, and correlation of discrete geologic units within this interval is relatively poor. The base of the non-marine Tulare Formation is considered the base of the lower principal aquifer and is estimated to be encountered at approximately 1,200 feet bgs in the project area, although potential USDWs continue to greater depth. The basal deposits of the Lower Aquifer overlie and may interfinger with the uppermost marine deposits of the San Joaquin Formation.

2.7.3.5 San Joaquin Formation

The Pliocene-age San Joaquin Formation records the final presence of the sea within the San Joaquin Basin (Loomis, 1990). The lowermost terrestrial beds of the Tulare Formation overlie and interfinger with the waning or marginal marine deposition recorded by the San Joaquin Formation. Sediments of the San Joaquin Formation are predominantly fine-grained, consisting of silty sandstone, silt, and clay (Foss and Blaisdell, 1968). The base of the San Joaquin Formation has not been formally defined in boring logs in the vicinity of the AoR.

2.7.3.6 Undifferentiated Pliocene and Miocene Units

Undifferentiated Miocene to Pliocene-age sedimentary deposits underlie the San Joaquin Formation and may be correlative with the regionally recognized Pliocene-age Etchegoin Formation and undivided upper marine units of the Miocene-age Monterey Formation (Scheirer, 2008). These deposits extend to the top of the Santa Maria Sandstone member of the Monterey Formation. The Monterey Formation is a deep-water mudstone that is present throughout most of the southern Sacramento and northern San Joaquin Basins.

2.7.3.7 Santa Margarita Sands (Monterey Formation)

The Santa Margarita Sandstone member of the Monterey Formation is the lowermost geologic unit potentially hosting an USDW in the project area, based on salinity logs of regional well bores. The Santa Margarita Sandstone member is a locally fossiliferous marine sandstone of Late Miocene age (Scheirer, 2007), and is approximately 200 to 300 feet thick in the vicinity of the AoR.

Although the depth of lower-most groundwater with TDS <10,000 mg/L may cross formation boundaries regionally, the base of the Santa Margarita Sandstone is considered a conservative proxy for the overall deepest extent of potential USDW within the project area. The Santa Margarita Sandstone is underlain by the locally designated Santa Margarita Shale, a Miocene-age marine shale equivalent to the lower members of the Monterey Formation.

2.7.4 Geologic Cross Sections Illustrating Formations with USDWs

No published geologic cross sections are available for the project area showing details of the shallow (i.e., post-Miocene) stratigraphy and the formations hosting potential USDWs. Cross Sections A-A' and B-B' of Miller et al (1971) show detail of the principal aquifers and Pleistocene sedimentary system, and are located to the west and south of the project area, respectively. These cross sections are reproduced in the Westside Subbasin GSP (Luhdorff & Scalmanini, 2022). These cross sections do not intersect the AoR, present only generalized information with respect to pre-Pleistocene formations, and do not extended to the base of the USDWs. The hydrogeological conceptual model for the site is depicted in **Figure 2.7-5,** and

provides a clear illustration of the structure of the principal aquifer units, but does not provide a detailed stratigraphy or information regarding USDWs below the Lower Aquifer.

CTV has prepared a geologic cross section based on boreholes with wire-line geophysical logs within the project AoR. This cross section is provided in **Figure 2.7-6**. Features of the cross section include the following:

- The base of the Tulare Formation non-marine clastic sediments is evident at approximately 1,000 to 1,200 feet TVDSS, which closely agrees with the thickness of the Tulare Formation shown on Cross Section A-A' of Miller et al. (1971).
- Shallower units such as the Cocoran Clay, upper Tulare Formation, and Holocene alluvium are not depicted on the wireline logs.
- Log interpretation suggests 200 to 400 feet of Pliocene marine sediments of the San Joaquin Formation, and over 1,500 feet of undivided Miocene and Pliocene sediments.
- The top of the Santa Margarita Sandstone member of the Miocene-age Monterey Formation is encountered between 2,600 and 3,200 feet TVDSS. The Santa Margarita Sandstone is considered the lowest stratigraphic unit to potentially host a USDW.

The BFW in the project vicinity is roughly 450 to 600 feet TVDSS and is also not depicted on the logs. The base of the Santa Margarita Sandstone is considered the base of the USDW, and is depicted at a depth of approximately 3,400 feet TVDSS within the AoR.

2.7.5 Principal Aquifers

In the SGMA regulations, principal aquifers are defined as aquifers or aquifer systems that store, transmit, and yield significant or economic quantities of groundwater to wells, springs, or surface water systems. There are two separate principal aquifers in the project area, designated the Upper and Lower Aquifer, each of which is primarily composed of terrestrial sedimentary deposits. These aquifer zones are separated by the lacustrine Cocoran Clay member of the Tulare Formation, which acts as a confining layer for the Lower Aquifer. A conceptual model of the primary aquifer system is presented in **Figure 2.7-5**.

The primary uses for groundwater extracted from the principal aquifers are irrigated agriculture, public supply, and rural/domestic. Most municipal (community) water systems in the Westside Subbasin rely on surface water from the California Aqueduct and not on groundwater. Available data on domestic well construction and monitoring are limited. Based on available data, most domestic wells within the subbasin are constructed in the Upper Aquifer, or are composite wells that are constructed in the Upper Aquifer and Lower Aquifer with the shallow zone of the Upper Aquifer sealed to prevent downward percolation of poor-quality water (Luhdorff & Scalmanini, 2022). Water wells drilled in western Fresno County are typically screened in the Lower Aquifer to achieve adequate yields. Localized groundwater interaction may occur between the Upper and Lower Aquifers where wells have penetrated both aquifers and are perforated above and below the Corcoran Clay (Williamson et al., 1989).

2.7.6 Groundwater Levels and Flow

This section summarizes water level data and analysis for the two primary aquifers (Upper and Lower Aquifers) in the Westside Subbasin, as presented in Luhdorff & Scalmanini (2022). Groundwater level data were obtained from several sources including the Westside Water District, USGS, DWR, and the SWRCB GeoTracker database. Groundwater level data were classified by primary aquifer unit based on available well construction information. Depth to the groundwater potentiometric surface in the site vicinity can range from near ground surface to 500 feet bgs, estimated from measurements provided by DWR (2024).

2.7.6.1 Upper Aquifer

Although considerable local variability is observed, many of the wells for which data are available displayed increasing groundwater levels prior to the early 2000s, followed by stable water levels in some wells after 2000. Data suggest that although temporal trends in groundwater levels tend to be similar at various depths within the Upper Aquifer, pressure head variations can exist within the Upper Aquifer due to well construction details (i.e., screened intervals), local influences from groundwater pumping, and geological variability such as local confining layers or vertical head gradients. Recent groundwater level data (2008-2018) indicate a variable decline in groundwater elevation across the Subbasin, indicative of an extended period of drought coupled with temporary increases in groundwater pumping. This trend is most evident in deeper wells within the Upper Aquifer. Many of the Upper Aquifer wells show significant seasonal variations of groundwater elevation up to hundreds of feet.

A general trend of decreasing water levels toward the Subbasin's eastern boundary is observed, indicating that the groundwater flow directions are influenced by groundwater development in the adjoining subbasins to the east. Groundwater elevation contours indicate that the flow direction in the Upper Aquifer was generally northeastward to northward during the time periods for which data were analyzed. Although data in the project vicinity are sparse, potentiometric surface maps presented in Luhdorff & Scalmanini (2022) indicate water levels ranging from near ground surface to 100 feet bgs in the Upper Aquifer in the site vicinity.

2.7.6.2 Lower Aquifer

Historically low groundwater levels within the lower aquifer occurred in the 1950s and 1960s, with a dramatic rise of water levels after completion of the Central Valley Project and delivery of surface water began in 1968. Groundwater levels remained relatively stable during the 1980s though early 2000s. Since 2010, however, groundwater levels in the Lower Aquifer declined significantly, with some wells declining by as much as 200 feet in the five years between 2010 and 2015. Water levels have continued to vary with seasonal and climatic conditions. Although the decline in groundwater elevations has been dramatic, note that this represents potentiometric surface changes in a confined aquifer, which may not be equivalent to elevation changes in an unconfined system in terms of change in aquifer storage.

Generally, groundwater elevation contours from 2015 show the lowest groundwater elevations along a north-south axis in the central portion of the Westside Subbasin, with the lowest groundwater levels at around 160 feet below sea level. Groundwater levels typically increase toward the western and eastern boundaries of the Westside Subbasin. Winter/spring contours of

groundwater elevations from 2006/2007 and 2014/2015 indicate that groundwater in the Lower Aquifer flows eastward out of the subbasin during wet years and into the subbasin during extended drought periods. During the periods for which data are presented in Luhdorff & Scalmanini (2022), the groundwater flow direction in the Lower Aquifer in the project vicinity is generally southward. Although data in the project vicinity are sparse, potentiometric surface maps presented in Luhdorff & Scalmanini (2022) indicate potentiometric water levels ranging from approximately 100 to 150 feet bgs in the Lower Aquifer in the site vicinity.

2.7.7 Water Supply and Groundwater Monitoring Wells

The California State Water Resources Control Board GAMA, DWR, California Statewide Groundwater Elevation Monitoring (CASGEM), and other public databases were searched to identify any water supply and groundwater monitoring wells within the AoR. DWR's Water Data Library reports groundwater data collected from a variety of well types including irrigation, stock, domestic, and public supply wells. The State Water Board's GAMA Program was established in 2000 to create a comprehensive groundwater monitoring program throughout California and increase public availability and access to groundwater quality and contamination information (State Water Board, 2018).

A total of 136 wells were identified from DWR and GAMA databases within the AoR (**Figure 2.2-6** and **Table 2.2-1**); however, many of these are dedicated monitoring wells. A total of 29 known water supply wells were identified within the AoR. Data provided from public databases indicate that the wells identified are completed much shallower than the proposed injection zone.

2.8 Geochemistry [40 CFR 146.82(a)(6)]

2.8.1 Formation Geochemistry

All formation geochemistry information is presented in the mineralogy section (Section 2.4.1). However, almost all of the injection zones are lacking quantitative mineralogy data. For this reason, analogous data were used for the mineralogic inputs for the geochemical modeling as explained in Section 2.4.1.

2.8.2 Fluid Geochemistry

No water samples from the storage zones exist within the AoR, so samples from surrounding oil and gas fields in close proximity to the AoR have been used (see **Figure 2.8-1** for well locations).

2.8.2.1 Monitoring Zone

For the Monitoring Zone, a water sample was available from the nearby Raisin City oil field. Well NOBLE_WI_1 (04019209310000) was sampled in 1984. The measurement of TDS for the sample is 41,835 mg/L. The complete water chemistry is shown in **Figure 2.8-2**.

2.8.2.2 Confining Zone

For the Confining Zone, a water sample was available from the nearby Gill Ranch gas field. Well GILL_RANCH_18X-17 (04039200560000) was sampled in 1995. The measurement of TDS for the sample is 31,200 mg/L. The complete water chemistry is shown in **Figure 2.8-3**.

2.8.2.3 Domengine

No complete water chemistry for the Domengine Formation was found. However, a partial analysis was available from well LAWTON_1-23 (04019219800000) (**Figure 2.8-4)**. The chloride content of this water (13,116 mg/L) is very similar to the chloride content of the deeper Blewett and Tracy Formations. For this reason, the water chemistry from the Blewett Formation was assumed to be analogous, with an assumed TDS of 20,700 mg/L, which is within the range for the Domengine Formation from the surrounding Helm, Raisin City, and Riverdale oil fields based on data presented in Sullivan (1971).

2.8.2.4 Garzas

No water samples were found for the Garzas Formation. For this reason, the water chemistry from the Blewett Formation was assumed to be analogous.

2.8.2.5 Blewett

For the Blewett Formation, a water sample was available from the nearby Gill Ranch gas field. Well GILL_RANCH_12-20 (04039200570000) was sampled in 1995. The measurement of TDS for the sample is 20,700 mg/L. The complete water chemistry is shown in **Figure 2.8-5**.

2.8.2.6 Tracy

For the Tracy Formation, a water sample was available from the nearby Gill Ranch gas field. Well GILL_RANCH_A-3 (04039200510000) was sampled in 1995. The measurement of TDS for the sample is 21,100 mg/L. The complete water chemistry is shown in **Figure 2.8-6**.

2.8.2.7 Geochemical Modeling

Using fluid geochemistry data for the Injection Zones and the available mineralogy data for the Injection Zones and Confining Zone, geochemical modeling was conducted using PHREEQC (ph-REdox-Equilibrium), the USGS geochemical modeling software, to evaluate the compatibility with formation rocks and fluid of the injectates being considered for the project.

The PHREEQC software was used to evaluate the behavior of minerals and changes in aqueous chemistry and mineralogy over the life of the project, and to identify major potential fluid/rock reactions that may affect injection or containment.

Based on the geochemical modeling, the injection of CO_2 at the CTV VI site does not cause significant reactions that will affect injection or containment. Detailed methodology and results are presented in **Appendix 3**.

2.9 Other Information (Including Surface Air and/or Soil Gas Data, if Applicable)

No additional information necessary.

2.10 Site Suitability [40 CFR 146.83]

Sufficient data from both wells and seismic demonstrate the integrity through lateral continuity of the storage reservoirs as well as the Confining Zone. Oil and gas fields in the vicinity of the project AoR demonstrate adequate seal capacity in the Confining Zone. Corrosion-resistant alloy (CRA) will be used for completion of the injection and monitoring wells, inhibiting any reaction between CO_2 and wellbores.

The Kreyenhagen Shale (Confining Zone) is regionally continuous, thick, and has low permeability, providing confinement for CO_2 storage and safely separating the Injection Zone from the Monitoring Zone and overlying USDWs.

CTV's estimated storage for the project is 101.5 MMT of CO_2. This mass was determined using the computational modeling presented in **Attachment B**. As discussed in **Attachment B,** a dynamic model was generated for the target Injection Zones with data from:

- The static model (structure, porosity, absolute permeability, net to gross ratio, facies)
- Special core analysis (relative permeability and capillary pressure)
- Pressure, volume, temperature (PVT) analysis (fluid PVT)
- Geochemical analysis (water salinity)

Injection well locations are based on geologic interpretation, petrophysical properties, and economic optimization. Injection rates were analyzed with flexibility to handle offset well failure during the project period. Injection wells were also designed with a maximum allowable injection pressure limit.

3. AoR and Corrective Action

Pursuant to 40 CFR 146.82(a)(4), 40 CFR 146.82(a)(13) and 146.84(b), and 40 CFR 146.84(c), **Attachment B** describes the process, software, and results to establish the AoR, and the wells that require corrective action.

AoR and Corrective Action GSDT Submissions
GSDT Module: AoR and Corrective Action ***Tab(s):*** All applicable tabs Please use the checkbox(es) to verify the following information was submitted to the GSDT: ☒ Tabulation of all wells within AoR that penetrate confining zone ***[40 CFR 146.82(a)(4)]*** ☒ AoR and Corrective Action Plan ***[40 CFR 146.82(a)(13) and 146.84(b)]***

☒ Computational modeling details ***[40 CFR 146.84(c)]***

4. Financial Responsibility

CTV's Financial Responsibility demonstration pursuant to 140 CFR 146.82(a)(14) and 40 CFR 146.85 (**Attachment H**) is met with a line of credit for Injection Well Plugging and Post-Injection Site Care and Site Closure and insurance to cover Emergency and Remedial Responses.

Financial Responsibility GSDT Submissions
GSDT Module: Financial Responsibility Demonstration ***Tab(s):*** Cost Estimate tab and all applicable financial instrument tabs Please use the checkbox(es) to verify the following information was submitted to the GSDT: ☒ Demonstration of financial responsibility ***[40 CFR 146.82(a)(14) and 146.85]***

5. Injection and Monitoring Well Construction

Appendix 5: Injection and Monitoring Well Schematics (Appendix 5) provides casing diagram figures for all injection and monitoring wells with construction specifications and anticipated completion details in graphical and/or tabular format.

5.1 Proposed Stimulation Program [40 CFR 146.82(a)(9)]

In the event stimulation is necessary, a stimulation plan has been added as **Attachment J: Stimulation Plan.**

5.2 Construction Procedures [40 CFR 146.82(a)(12)]

CTV has created Construction and Plugging documents for each project well pursuant to 40 CFR 146.82(a)(8). Each well-specific plan within **Attachment G: Well Construction and Plugging Plan (Attachment G)** document includes well construction information based on requirements defined within 40 CFR 146.82.

6. Pre-Operational Logging and Testing

CTV has indicated a proposed pre-operational logging and testing plan throughout the application documentation pursuant to 40 CFR 146.82(a)(8). Each **Attachment G** document (listed in Section 5.2) includes logging and testing plans for each individual project well based

on requirements defined within 40 CFR 146.87. **Attachment I** summarizes pre-operational testing.

Pre-Operational Logging and Testing GSDT Submissions
GSDT Module: Pre-Operational Testing ***Tab(s):*** Welcome tab Please use the checkbox(es) to verify the following information was submitted to the GSDT: ☒ Proposed pre-operational testing program ***[40 CFR 146.82(a)(8) and 146.87]***

7. Well Operation

7.1 Operational Procedures [40 CFR 146.82(a)(10)]

The Operational Procedures for all injectors associated with the project are detailed in **Appendix 4: Operational Procedures**.

7.2 Proposed Carbon Dioxide Stream [40 CFR 146.82(a)(7)(iii) and (iv)]

CTV is planning to construct a carbon capture and sequestration "hub" project (i.e., a project that collects CO_2 from multiple sources over time. Therefore, CTV is currently considering multiple sources of anthropogenic CO_2 for the project. Potential sources include capture from existing and potential future industrial sources in the San Joaquin Basin area, as well as DAC. CTV would expect the CO_2 stream to be sampled at the transfer point from the source and between the final compression stage and the wellhead. Samples will be analyzed according to the analytical methods described in the Table 4 of **Appendix 10: QASP** (**Appendix 10**) and Table C-1 of **Attachment C**.

For the purposes of geochemical modeling, CO_2 plume modeling, AoR determination, and well design, two major types of injectate compositions were considered based on the source:

- Injectate 1: A potential injectate stream composition from DAC or a pre-combustion source (such as a blue hydrogen facility that produces hydrogen using steam methane reforming process) or a post-combustion source (such as a natural gas fired power plant or steam generator). The primary impurity in the injectate is nitrogen.
- Injectate 2: A potential injectate stream composition from a biofuel capture source (such as a biodiesel plant that produces biodiesel from a biologic source feedstock) or from an oil and gas refinery. The primary impurity in the injectate is light-end hydrocarbons (methane and ethane).

The compositions for these two injectates are shown in **Table 7.2-1** and are based on engineering design studies and literature.

For geochemical and plume modeling scenarios, these injectate compositions were simplified to a four-component system, shown in **Table 7.2-2**, and then normalized for use in the modeling. The four-component simplified compositions cover 99.9 percent by mass of Injectates 1 and 2 and cover particular impurities of concern (H_2S and SO_2). The estimated properties of the injectates at downhole conditions are specified in **Table 7.2-3**.

The anticipated injection temperature at the wellhead is 90 to 130°F.

No corrosion is expected in the absence of free-phase water provided that the entrained water is kept in solution with the CO_2. This is ensured by maintaining a <25 pounds per million cubic feet (lb/mmscf) injectate specification limit, and this specification will be a condition of custody transfer at the capture facility. For transport through pipelines, which typically use standard alloy pipeline materials, this specification is critical to the mechanical integrity of the pipeline network, and out-of-specification product will be immediately rejected. Therefore, all product transported through pipeline to the injection wellhead is expected to be dry-phase CO_2 with no free-phase water present.

Injectate water solubility will vary with depth and time as temperature and pressures change. The water specification is conservative to ensure water solubility across supercritical operating ranges. CRA tubing will be used in the injection wells to mitigate any potential corrosion impact should free-phase water from the reservoir become present in the wellbore, such as during shut-in events when formation liquids, if present, could backflow into the wellbore. CTV may further optimize the maximum water content specification prior to injection based on technical analysis.

8. Testing and Monitoring

CTV's Testing and Monitoring Plan (**Attachment C**) pursuant to 40 CFR 146.82 (a) (15) and 40 CFR 146.90 describes the strategies for testing and monitoring to ensure protection of the USDW, injection well mechanical integrity, and plume monitoring.

Testing and Monitoring GSDT Submissions
GSDT Module: Project Plan Submissions ***Tab(s):*** Testing and Monitoring tab Please use the checkbox(es) to verify the following information was submitted to the GSDT: ☒ Testing and Monitoring Plan **[40 CFR 146.82(a)(15) and 146.90]**

9. Injection Well Plugging

CTV's Injection Well Plugging Plan pursuant to 40 CFR 146.92 (**Attachment D and Attachment G**) describes the process, materials and methodology for injection well plugging.

Injection Well Plugging GSDT Submissions
GSDT Module: Project Plan Submissions ***Tab(s):*** Injection Well Plugging tab Please use the checkbox(es) to verify the following information was submitted to the GSDT: ☒ Injection Well Plugging Plan **[40 CFR 146.82(a)(16) and 146.92(b)]**

10. Post-Injection Site Care (PISC) and Site Closure

CTV has developed **Attachment E: Post-Injection Site Care and Site Closure Plan (Attachment E)** pursuant to 40 CFR 146.93 (a) to define post-injection testing and monitoring.

CTV is proposing an alternative PISC time frame as described in **Attachment E**.

PISC and Site Closure GSDT Submissions
GSDT Module: Project Plan Submissions ***Tab(s):*** PISC and Site Closure tab Please use the checkbox(es) to verify the following information was submitted to the GSDT: ☒ PISC and Site Closure Plan **[40 CFR 146.82(a)(17) and 146.93(a)]**
GSDT Module: Alternative PISC Timeframe Demonstration ***Tab(s):*** All tabs (only if an alternative PISC timeframe is requested) Please use the checkbox(es) to verify the following information was submitted to the GSDT: ☒ Alternative PISC timeframe demonstration ***[40 CFR 146.82(a)(18) and 146.93(c)]***

11. Emergency and Remedial Response

Pursuant to 40 CFR 164.94, **Attachment F: Emergency and Remedial Response Plan** (**Attachment F**) describes the process and response to emergencies to ensure USDW protection.

Emergency and Remedial Response GSDT Submissions
GSDT Module: Project Plan Submissions ***Tab(s):*** Emergency and Remedial Response tab Please use the checkbox(es) to verify the following information was submitted to the GSDT: ☒ Emergency and Remedial Response Plan ***[40 CFR 146.82(a)(19) and 146.94(a)]***

12. Injection Depth Waiver and Aquifer Exemption Expansion

No depth waiver or aquifer exemption expansion is being requested as part of this application.

Injection Depth Waiver and Aquifer Exemption Expansion GSDT Submissions
GSDT Module: Injection Depth Waivers and Aquifer Exemption Expansions ***Tab(s):*** All applicable tabs Please use the checkbox(es) to verify the following information was submitted to the GSDT: ☐ Injection Depth Waiver supplemental report ***[40 CFR 146.82(d) and 146.95(a)]*** ☐ Aquifer exemption expansion request and data ***[40 CFR 146.4(d) and 144.7(d)]***

13. References

Anderson, F.M. 1905. A stratigraphic study in the Mount Diablo Range of California. *Third Series, California Academy of Science, Proceedings* 2: 155-248.

Beyer, L.A. 1988. Summary of geology and petroleum plays used to assess undiscovered recoverable petroleum resources of Sacramento Basin province*, California.* U.S. Geological Survey Open-File Report 71-223.

Bryant, W.A. (compiler). 2017. Fault number 28j, Great Valley thrust fault system, Panoche Hills (GV 10) section, in Quaternary fault and fold database of the United States. U.S. Geological Survey website. https://earthquakes.usgs.gov/hazards/qfaults.

California Air Resources Board (CARB). 2018. *Carbon capture and sequestration protocol under the Low Carbon Fuel Standard*. August 13, 2018.

Core Laboratories. 2010. Special core analysis study, 11-21-101 & 34-18-202 Wells, Gill Ranch Field, Final Report. California Department of Conservation File Request website. https://filerequest.conservation.ca.gov/.

Department of Water Resources (DWR), State of California. 2020. 5-021.65 Sacramento Valley—South American Basin Boundaries. May 2020.

DWR. 2024. California's Groundwater Live: Groundwater Levels. https://storymaps.arcgis.com/stories/b3886b33b49c4fa8adf2ae8bdd8f16c3

Daviess, S.N. 1946. Mineralogy of Late Upper Cretaceous, Paleocene, and Eocene Sandstones of Los Banos District, West Border of San Joaquin Valley, California. *AAPG Bulletin* 30(1): 63–83. doi: https://doi.org/10.1306/3D9337C6-16B1-11D7-8645000102C1865D.

Davis, K.E., 1988. Survey of Methods to Determine Total Dissolved Solids Concentrations. U.S. Environmental Protection Agency Underground Injection Control Program. Prepared by Ken E. Davis Associates under subcontract to Engineering Enterprises, INC. EPA LOE Contract No. 68-03-3416, Work Assignment No. 1-0-13, Keda Project No. 30-956.

EKI Environment and Water (EKI). 2022. *DRAFT Delta-Mendota Region Groundwater Sustainability Plan, Public Review Draft*. June 24, 2022

Fjaer, E., R.M. Holt, A.M. Raaen, and P. Horsrud. 2008. *Petroleum related rock mechanics* (2nd ed.). Elsevier Science.

Foss, C.D., and R. Blaisdell. 1968. Stratigraphy of the west side southern San Joaquin Valley. p. 33-43 in Karp, S.E. (Ed.), *Guidebook, Geology and oil fields, West side southern San Joaquin Valley: Pacific Sections, American Association of Petroleum Geologists, Society of Exploration Geophysicists, Society of Economic Paleontologists and Mineralogists, 43rd Annual Meeting*.

Graham, S.A., C. McCloy, M. Hiltzman, R. Ward, and R. Turner. 1984. Basin evolution during change from convergent to transform continental margin in Central California. *AAPG Bulletin* 68(3): 233-249. doi: https://doi.org/10.1306/AD460A03-16F7-11D7-8645000102C1865D.

Heidbach, O. M. Rajabi, K. Reiter, M. Ziegler, and WSM Team. 2016. World Stress Map Database Release 2016. GFZ Data Services, doi:10.5880/WSM.2016.001.

Hickman, S. and M. Zoback. 2004/ Stress orientations and magnitudes in the SAFOD pilot hole, *Geophys. Res. Lett.* 31, L15S12, doi:10.1029/2004GL020043.

Hilchie, D.W. 1978. Applied Openhole Log Interpretation: Golden, CO., D.W. Hilchie Inc.

Hurst, A., M.J. Wilson, A. Grippa, L. Wilson, G. Palladino, C. Belviso, and F. Cavalcante. 2021. Provenance and sedimentary context of clay mineralogy in an evolving forearc basin, Upper Cretaceous-Paleogene and Eocene mudstones, San Joaquin Valley, California. *Minerals* 11(1): 1-18. Article 71. https://doi.org/10.3390/min11010071.

IEAGHG. 2011. Caprock Systems for CO_2 Geologic Storage. May 2011.

Ingram G.M., J.L. Urai, and M.A. Naylor. 1997. In Hydrocarbon Seals: Importance for Exploration and Production, Sealing processes and top seal assessment, *Norwegian Petroleum Society (NPF) Special Publication*, eds Moller-Pedersen P., Koestler A. G. 7, pp 165–175.

Ingram, G. and J. Urai. 1999. Top-seal leakage through faults and fractures: the role of mudrock properties. *Geological Society, London, Special Publications* 158. 125-135. 10.1144/GSL.SP.1999.158.01.10.

Kang, M., D. Perrone, Z. Wang, S. Jasechko, and M.M. Rohde. 2020. Base of fresh water, groundwater salinity, and well distribution across California. *Proceedings of the National Academy of Sciences of the United States of America*.

Kivior, T., J. Kaldi, and S. Lang. 2002. Seal potential in Cretaceous and Late Jurassic rocks of the Vulcan Sub-basin, Northwest Shelf Australia. *Australian Petroleum Production and Exploration Association Journal* 42. 203-224. 10.1071/AJ01012.

Lettis, W.R. 1988. Quaternary geology of the northern San Joaquin Valley. p. 333-351 in Graham, S.A. and H.C. Olson (eds.), *Studies of the geology of the San Joaquin Basin: Los Angeles, Pacific Section*, Society of Economic Paleontologists and Mineralogists, Book 60.

Lewan, M., M. Dolan, and J. Curtis. 2014. Effects of smectite on the oil-expulsion efficiency of the Kreyenhagen Shale, San Joaquin Basin, California, based on hydrous-pyrolysis experiments. *AAPG Bulletin* 98: 1091-1109. 10.1306/10091313059.

Loomis, K.B. 1990. Depositional environments and sedimentary history of the Etchegoin Group, West-central San Joaquin Valley, California. p. 231-246 in Kuespert, J.G. and S.A. Reid (eds.), *Structure, stratigraphy, and hydrocarbon occurrences of the San Joaquin Basin, California: Bakersfield, Calif., Pacific Sections*, Society of Economic Paleontologists and Mineralogists and American Association of Petroleum Geologists, v. 64.

Luhdorff and Scalmanini. 2022. *Westside Subbasin Groundwater Sustainability Plan*. Prepared for Westlands Water District GSA and County of Fresno GSA-Westside. July 2022.

Lund-Snee, J.-E. 2020. *State of stress in North America: Seismicity, tectonics, and unconventional energy development*. 10.13140/RG.2.2.27217.07523/1.

Lund-Snee, J.-E. and M. Zoback. 2020. Multiscale variations of the crustal stress field throughout North America. *Nature Communications* 11: 1951.

Miller, R.E., J.H. Green, and G.H. Davis. 1971. Geology of the compacting deposits in the Los Banos-Kettleman City subsidence area, California. *U.S. Geological Survey Professional Paper* 497-E.

Mount, V.S. and J. Suppe. 1987. State of stress near the San Andreas fault: Implications for wrench tectonics. *Geology* 15: 1143-1146.

Mount, V. and J. Suppe. 1992. Present-day stress orientations adjacent to active strike-slip faults, California and Sumatra. *Journal of Geophysical Research* 971: 11995-12013. 10.1029/92JB00130.

Nilsen, T.H. and D.W. Moore. 1997. Regional Upper Cretaceous stratigraphy and depositional systems of the northern San Joaquin Basin, California. p. 1-12 in Cressy, F.B. Jr. and M.L. Simmons (eds.), *Geology of the northern San Joaquin Basin gas province: Bakersfield, Calif., Pacific Section*, American Association of Petroleum Geologists, MP 43.

Page, R.W. 1971. Base of fresh ground water (approximately 3,000 micromhos) in the San Joaquin Valley, California. U.*S. Geological Survey Open-File Report* 71-223.

Page, R.W. 1973. Base of fresh ground water (approximately 3,000 micromhos) in the San Joaquin Valley, California. *U.S. Geological Hydrologic Investigations Atlas* HA-489.

Scheirer, A.H. 2007. Petroleum systems and geologic assessment of oil and gas in the San Joaquin Basin Province, California. *U.S. Geological Survey Professional Paper* 1713.

Scheirer, A.H. and L.B. Magoon, 2008. Age, distribution, and stratigraphic relationship of rock units in the San Joaquin Basin Province, California: Chapter 5 in Petroleum systems and geologic assessment of oil and gas in the San Joaquin Basin Province, California. *U.S. Geological Survey Professional Paper* 1713-5.

State Water Resources Control Board. 2018. GAMA Program—About. Accessed June 24, 2020.

Sullivan, J.C. 1971. Oil and Gas Field Waters in Central San Joaquin Valley—Fresno, Kings, and Madera Counties, *California: Division of Oil and Gas Summary of Operations—California Oil Fields*, 57(1).

Townend, J. and M.D. Zoback. 2004. Regional tectonic stress near the San Andreas fault in central and southern California. *Geophys. Res. Lett.* 31: L15S11, doi:10.1029/2003GL018918.

U.S. Geological Survey (USGS). 2024. Earthquake Catalog Tool. https://earthquake.usgs.gov/earthquakes/search/.

Williamson, A.K., D.E. Prudic, and L.A. Swain. 1989. *Ground-water flow in the Central Valley, California: Regional aquifer-system analysis—Central Valley, California*. U.S. Geological Survey Professional Paper 1401-D.

Zoback, M.D., M.L. Zoback, V.S.Mount, J. Suppe, J.P. Eaton, J.H. Healy, D. Oppenheimer, P. Reasenberg, L. Jones, C.B. Raleigh, I.G. Wong, O. Scotti, and C. Wentworth. 1987. New evidence on the state of stress of the san andreas fault system. *Science* 238(4830):1105-11. doi: 10.1126/science.238.4830.1105. PMID: 17839366.

Figures

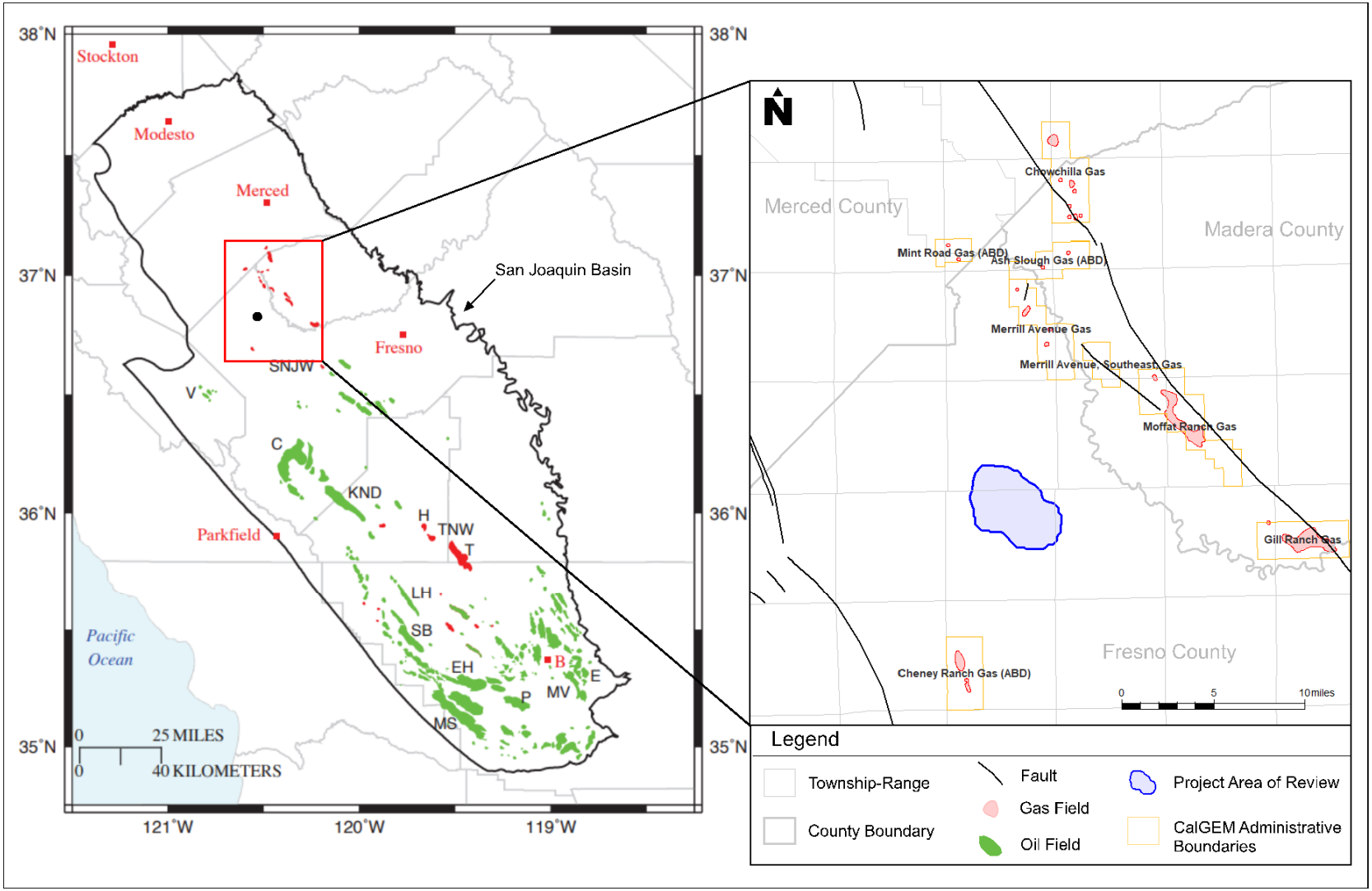

Figure 1-1. Location map of the project AoR in relation to the San Joaquin Basin. In the leftmost figure, city locations are labeled in red text. The city of Bakersfield is abbreviated with the letter B. Oil and Gas field locations are abbreviated in black text and are as follows: C, Coalinga; E, Edison; EH, Elk Hills; H, Harvester; KND, Kettleman North Dome; LH, Lost Hills; MS, Midway Sunset; MV, Mountain View; P, Paloma; SB, South Belridge; SJNW, San Joaquin Northwest; T, Trico; TNW, Trico Northwest; V, Vallecitos; Figure modified from (Scheirer, 2008).

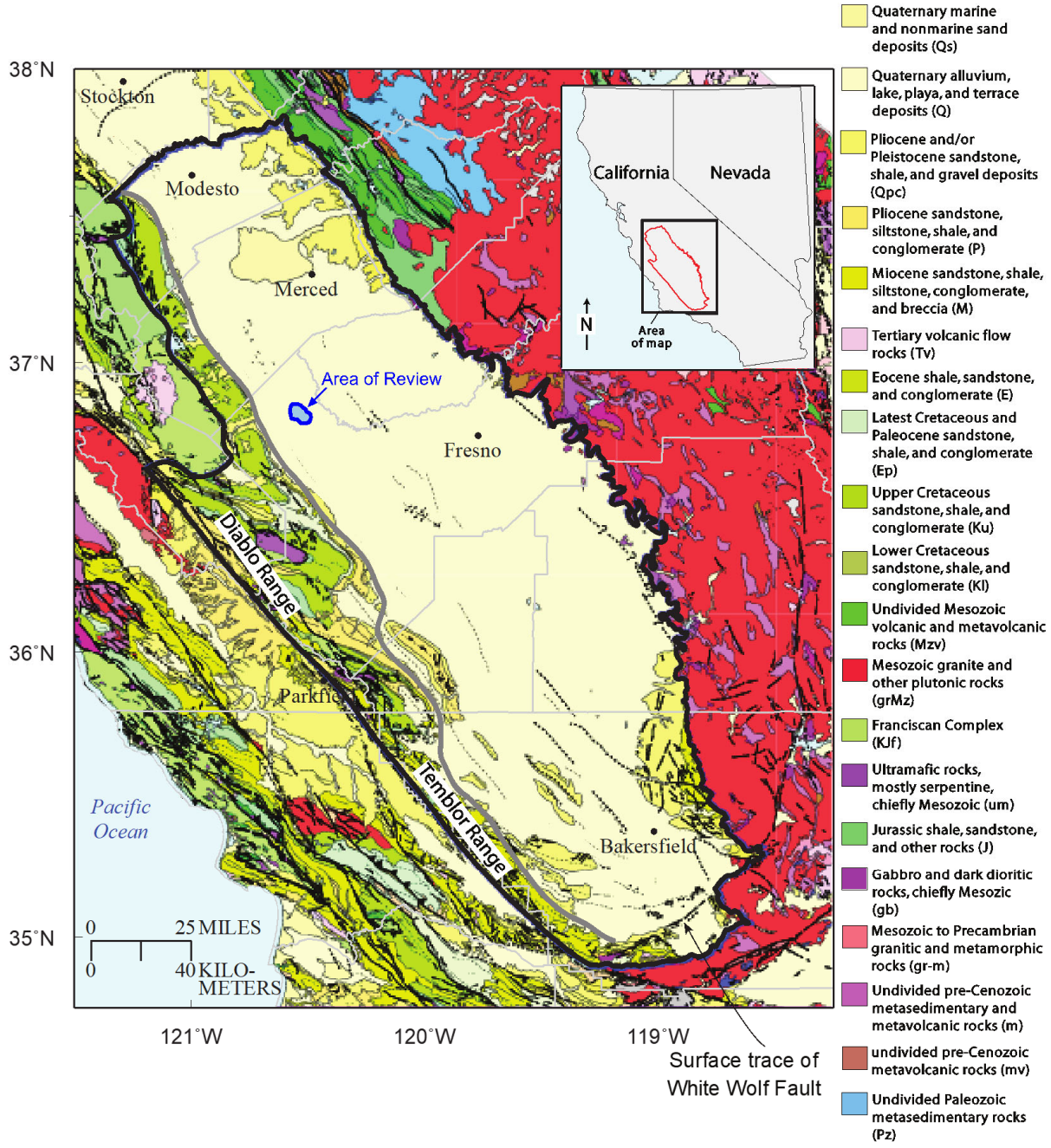

Figure 2.1-1. Surface Geologic Map of the San Joaquin Basin, California, showing the AoR. Figure modified from (Scheirer, 2008).

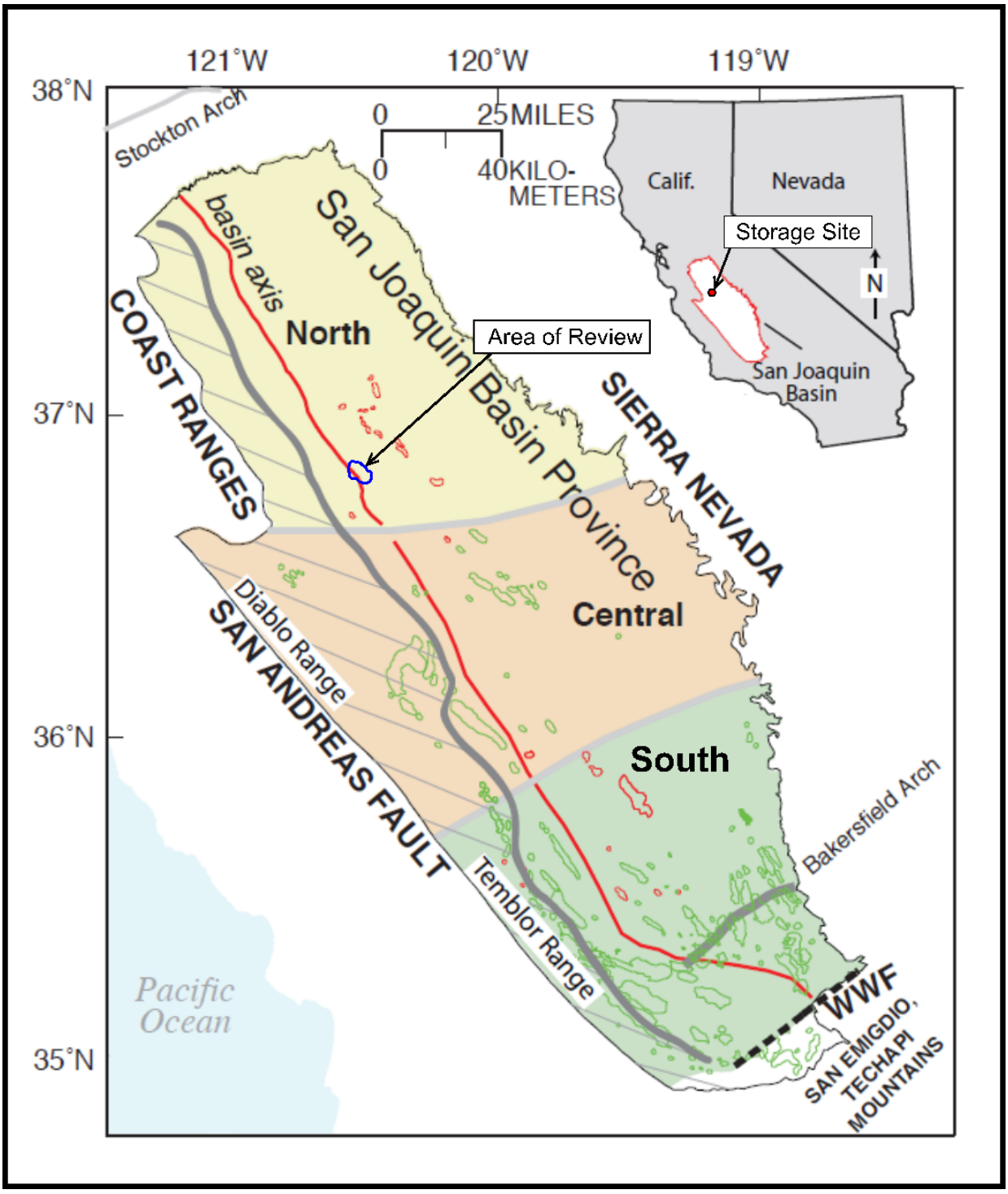

Figure 2.1-2. Project location map of California modified from (Scheirer, 2008) Gas field outlines are shown in red and oil field boundaries are shown in green.

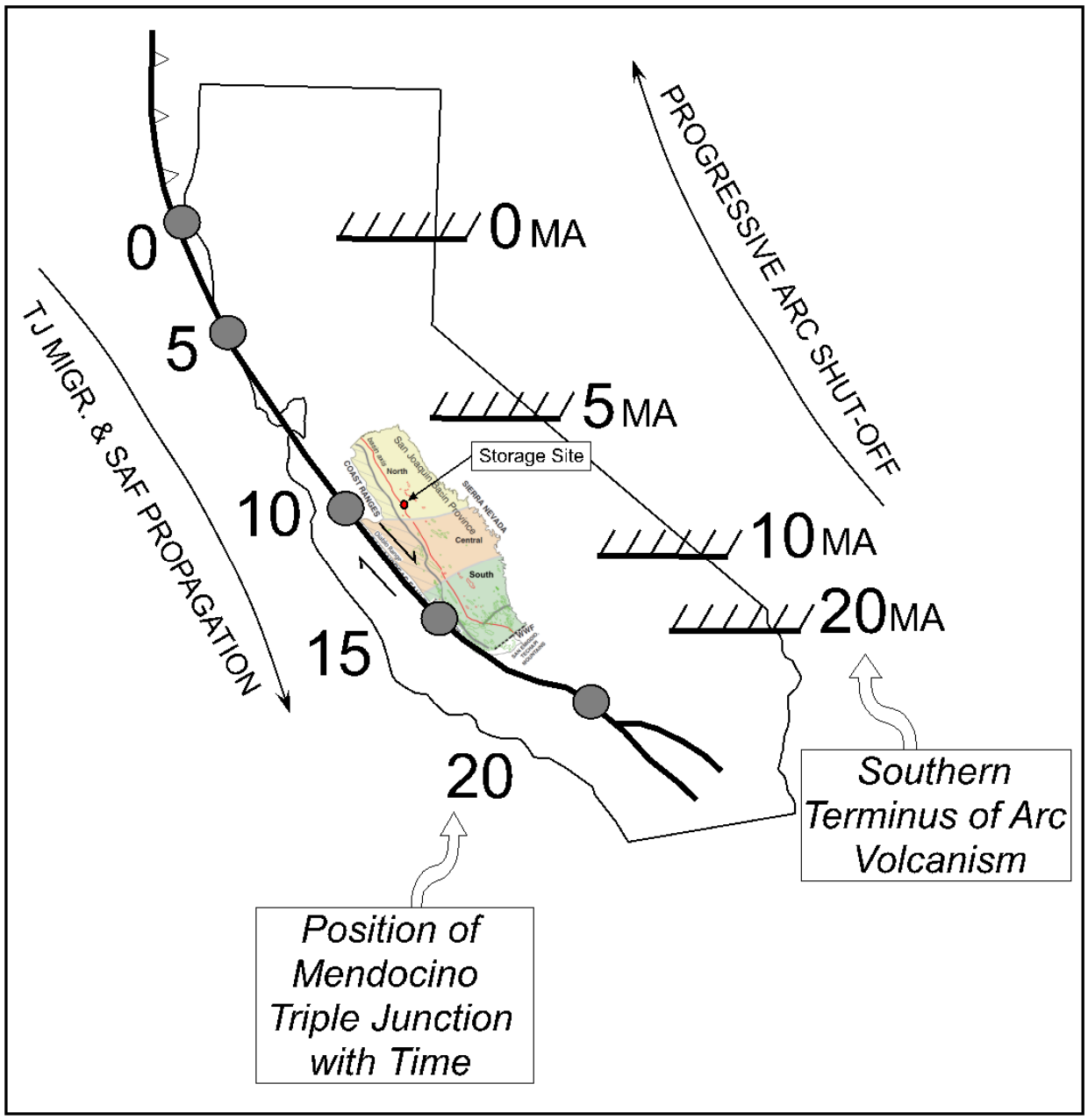

Figure 2.1-3. Migrational position of the Mendocino triple junction (Connection point of the Gorda, North American and Pacific plates) on the west and migrational position of Sierran Arc volcanism in the east (Graham, 1984). The figure indicates space-time relations of major continental-margin tectonic events in California during the Miocene. San Joaquin Basin figure modified from (Scheirer, 2008).

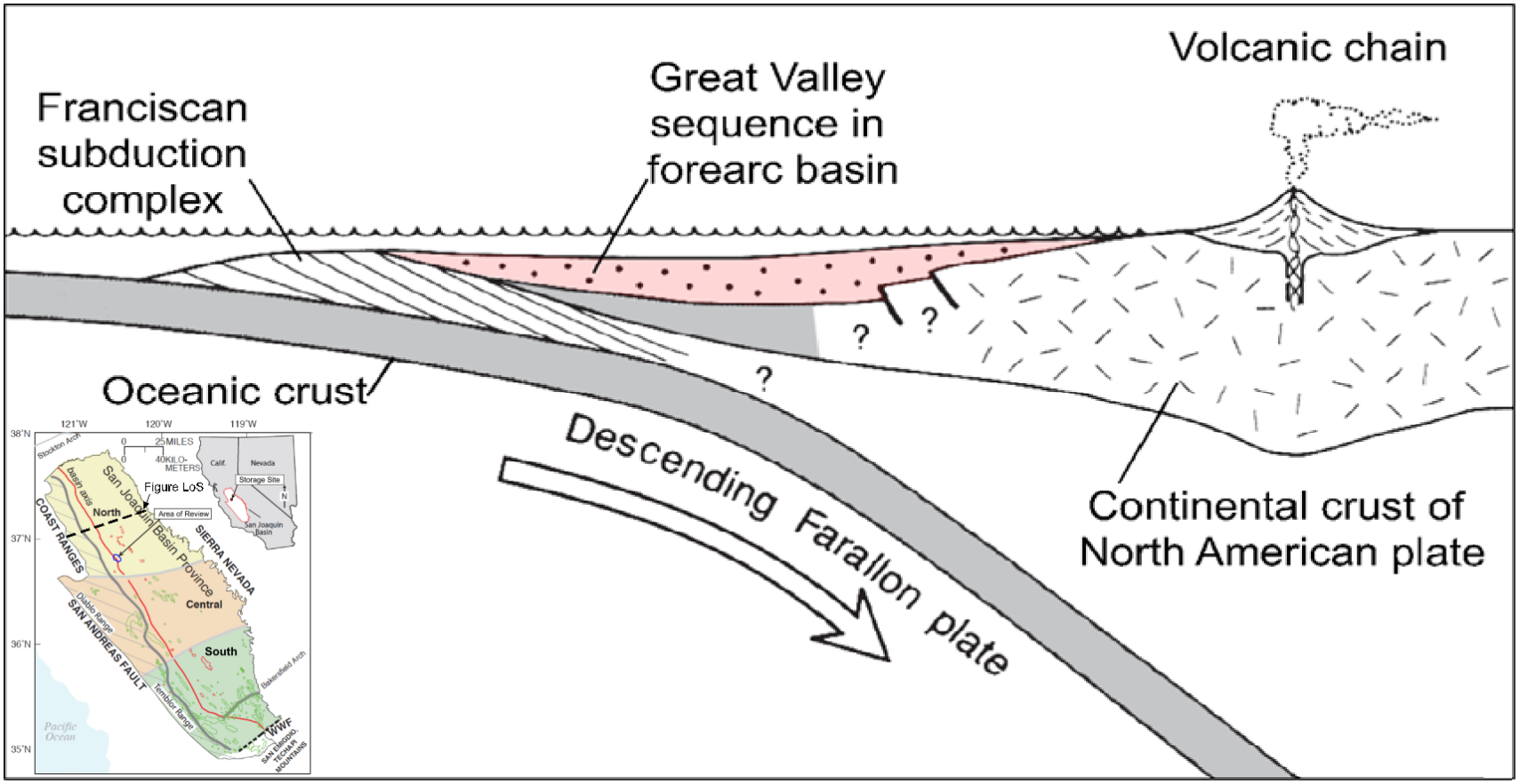

Figure 2.1-4. Schematic W-E cross-section of California, highlighting the San Joaquin Basin, as a continental margin during late Mesozoic. The oceanic Farallon plate was forced below the west coast of the North American continental plate. San Joaquin Basin figure modified from (Scheirer, 2008).

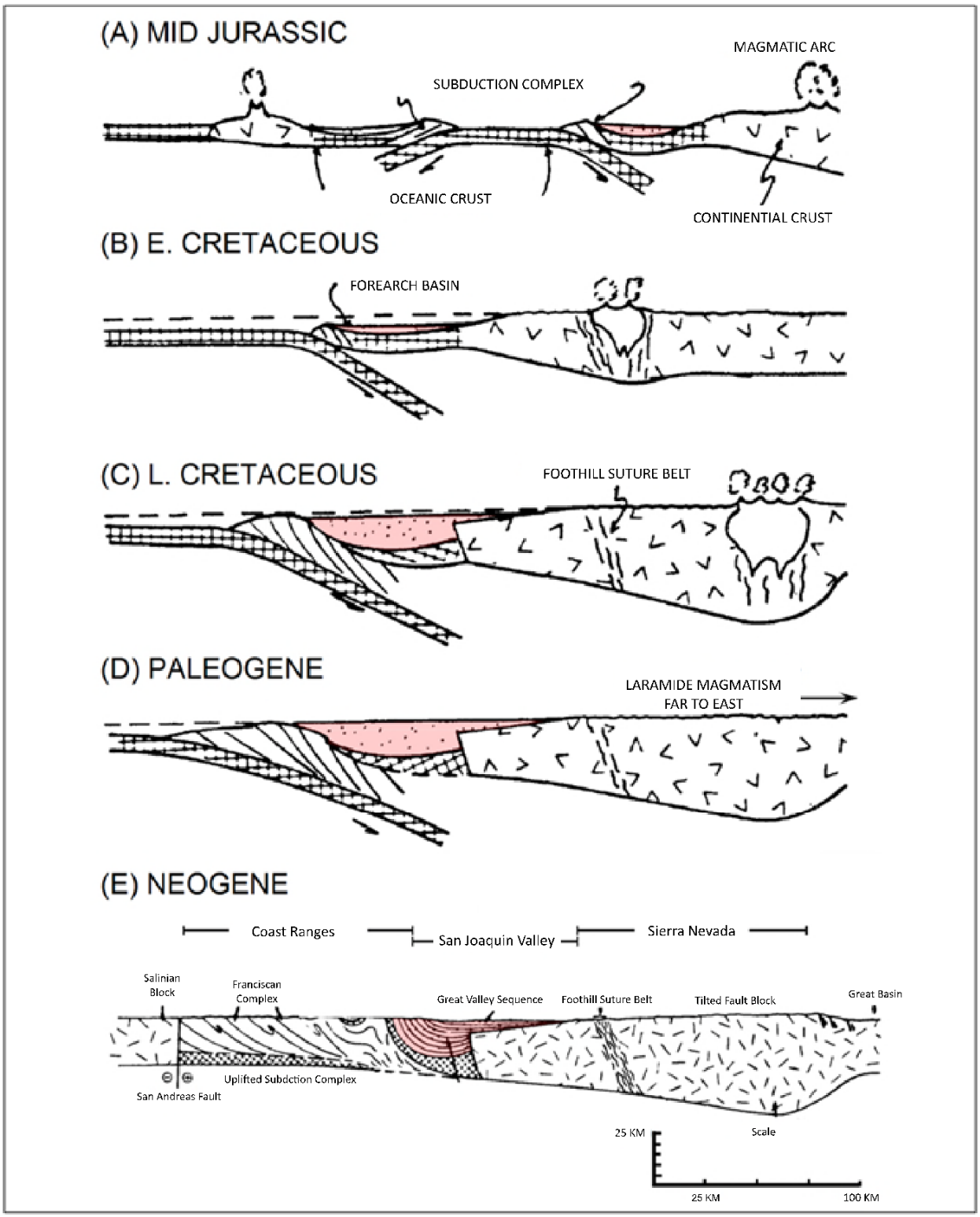

Figure 2.1-5. Evolutionary stages showing the history of the arc-trench system of California from Jurassic (A) to Neogene (E). Figure modified from (Beyer, 1988).

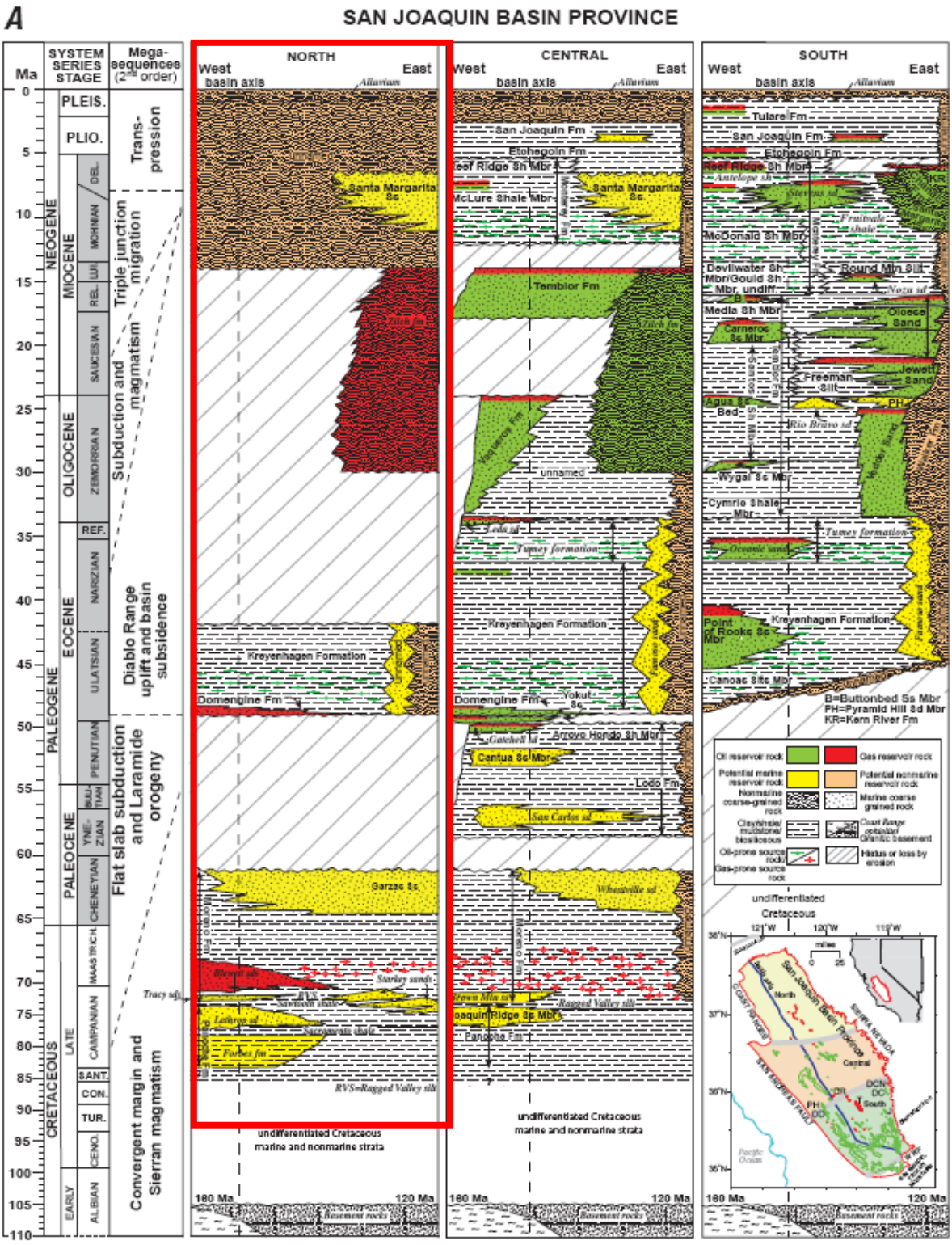

Figure 2.1-6. Stratigraphic column of the San Joaquin basin (Scheirer, 2008). The stratigraphy associated with project area is outlined red.

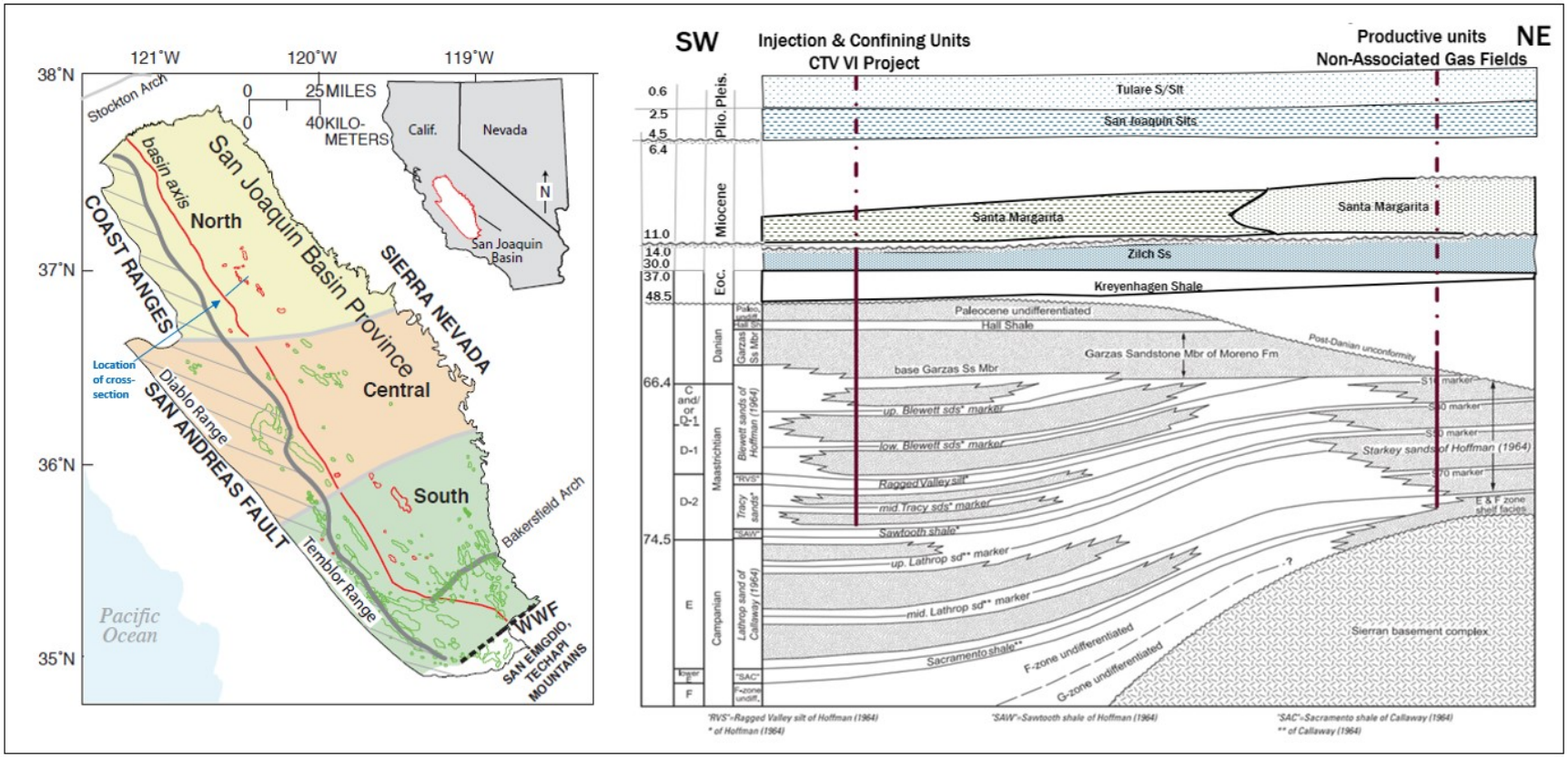

Figure 2.1-7. Detailed portion of the greater project area Stratigraphy. It also annotates the depositional age of the units. Figure modified from (Scheirer, 2008).

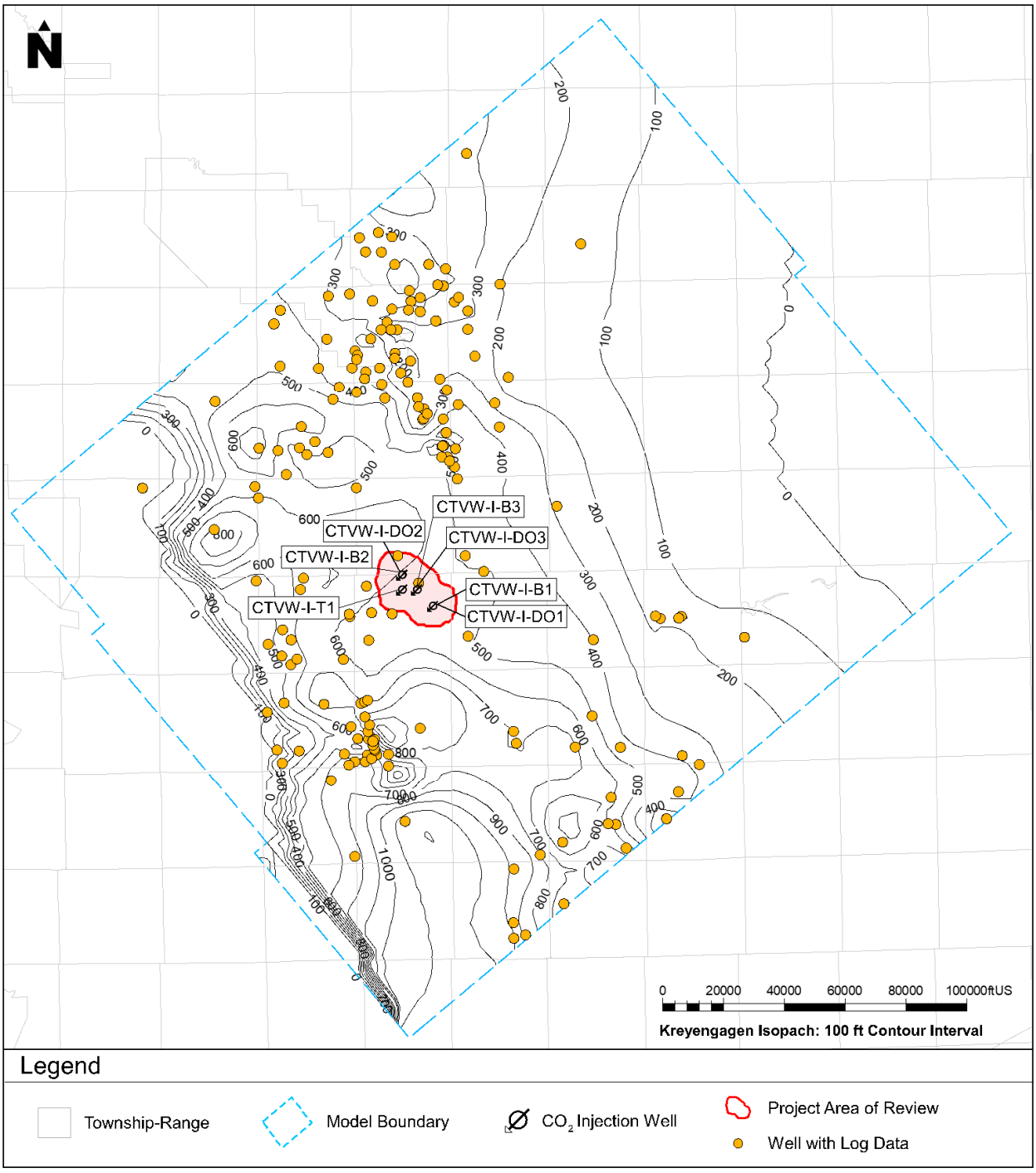

Figure 2.1-8. Kreyenhagen Shale isopach map for the greater project area. Wells shown as orange dots on the map penetrate the Kreyenhagen Shale and have open-hole logs.

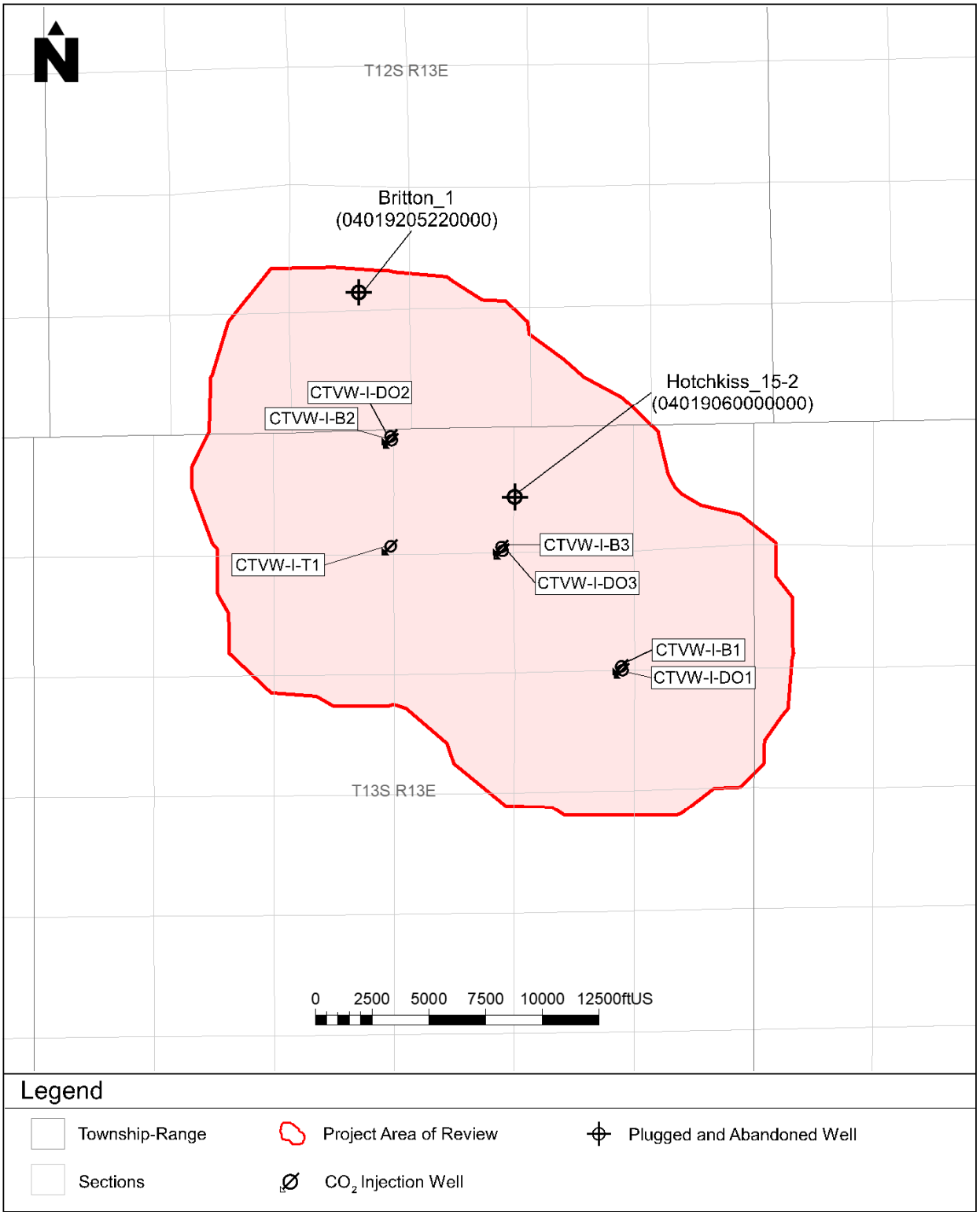

Figure 2.2-1. Existing oil/gas wells and injector well locations in the AoR. There are two oil/gas wells in the AoR.

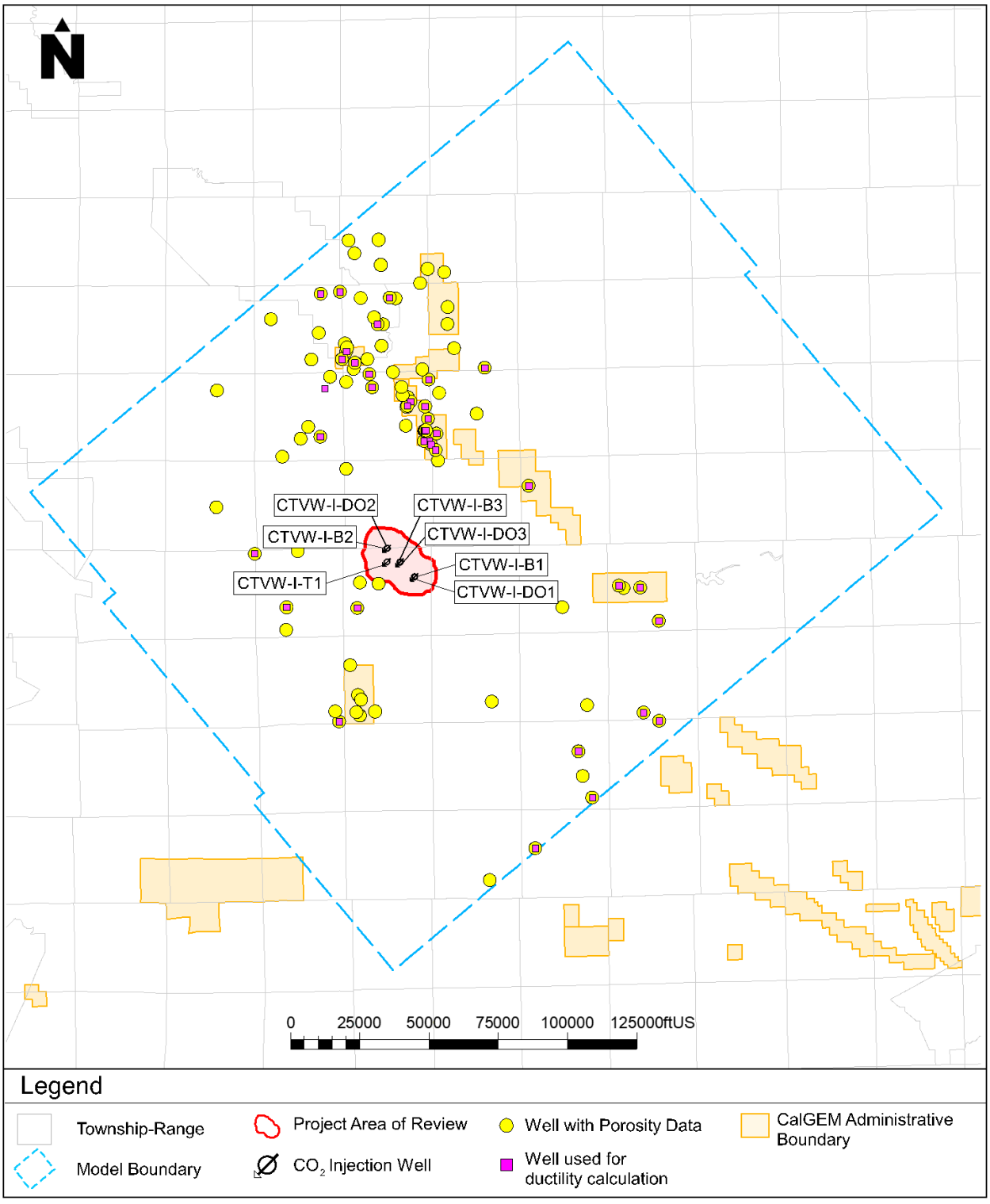

Figure 2.2-2(a). Wells drilled in the project area with porosity data are shown in yellow and wells used for ductility calculation are shown in pink.

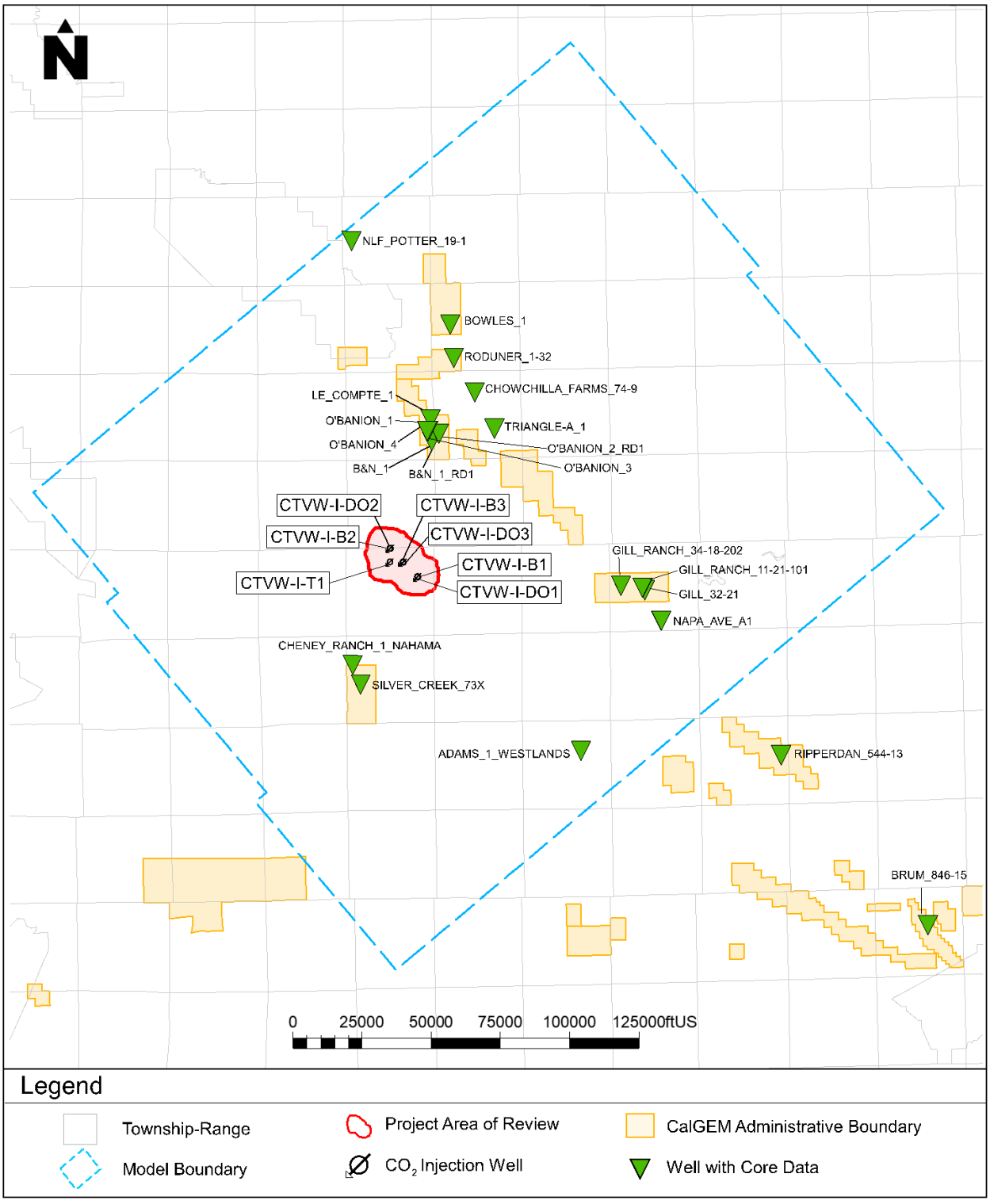

Figure 2.2-2(b). Wells drilled in the project area with core.

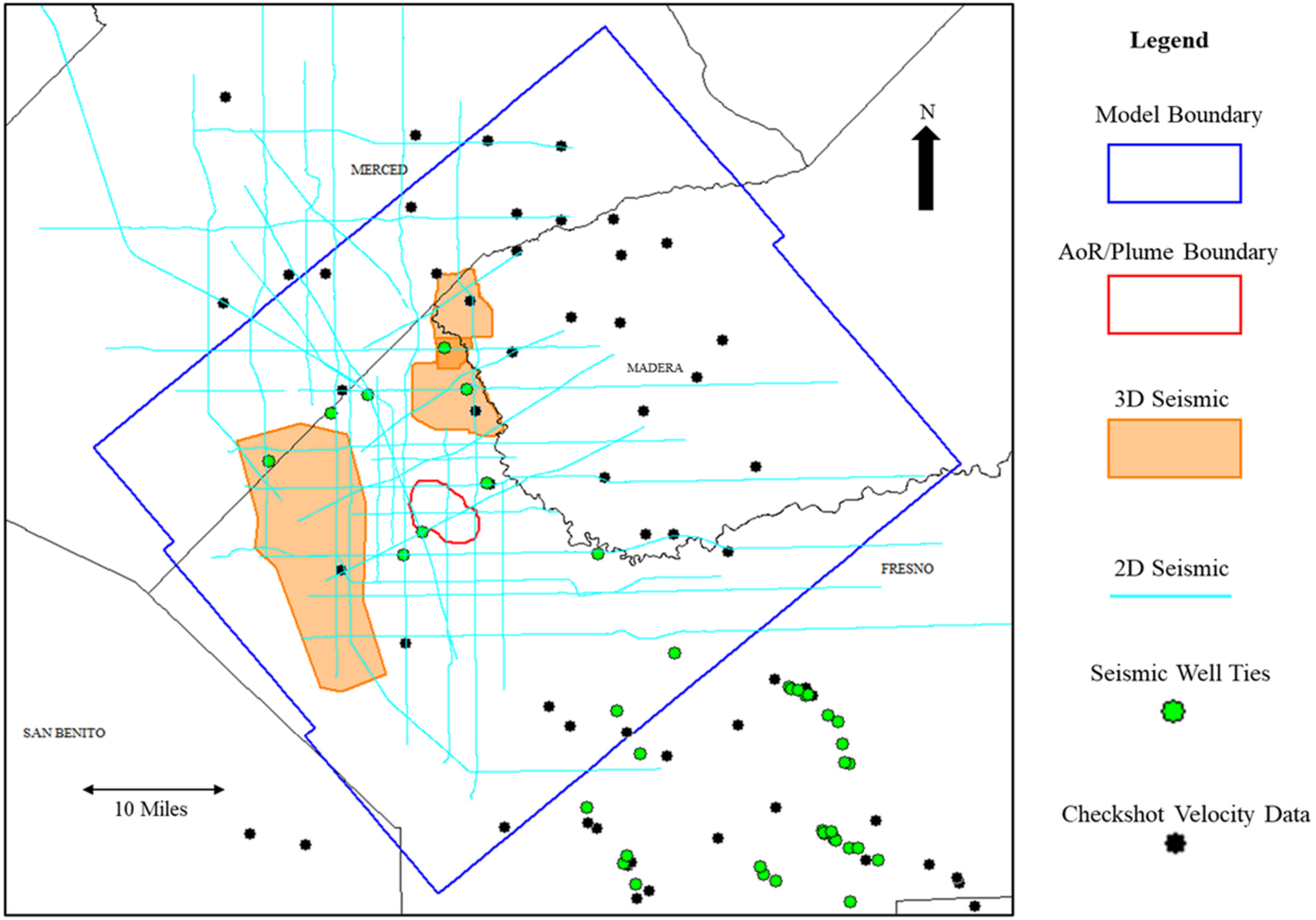

Figure 2.2-3. Summary map of seismic data used to build structural model within the model boundary. The 3D surveys were acquired between 2003 and 2007. The 2D seismic were acquired between 1979 and 1991.

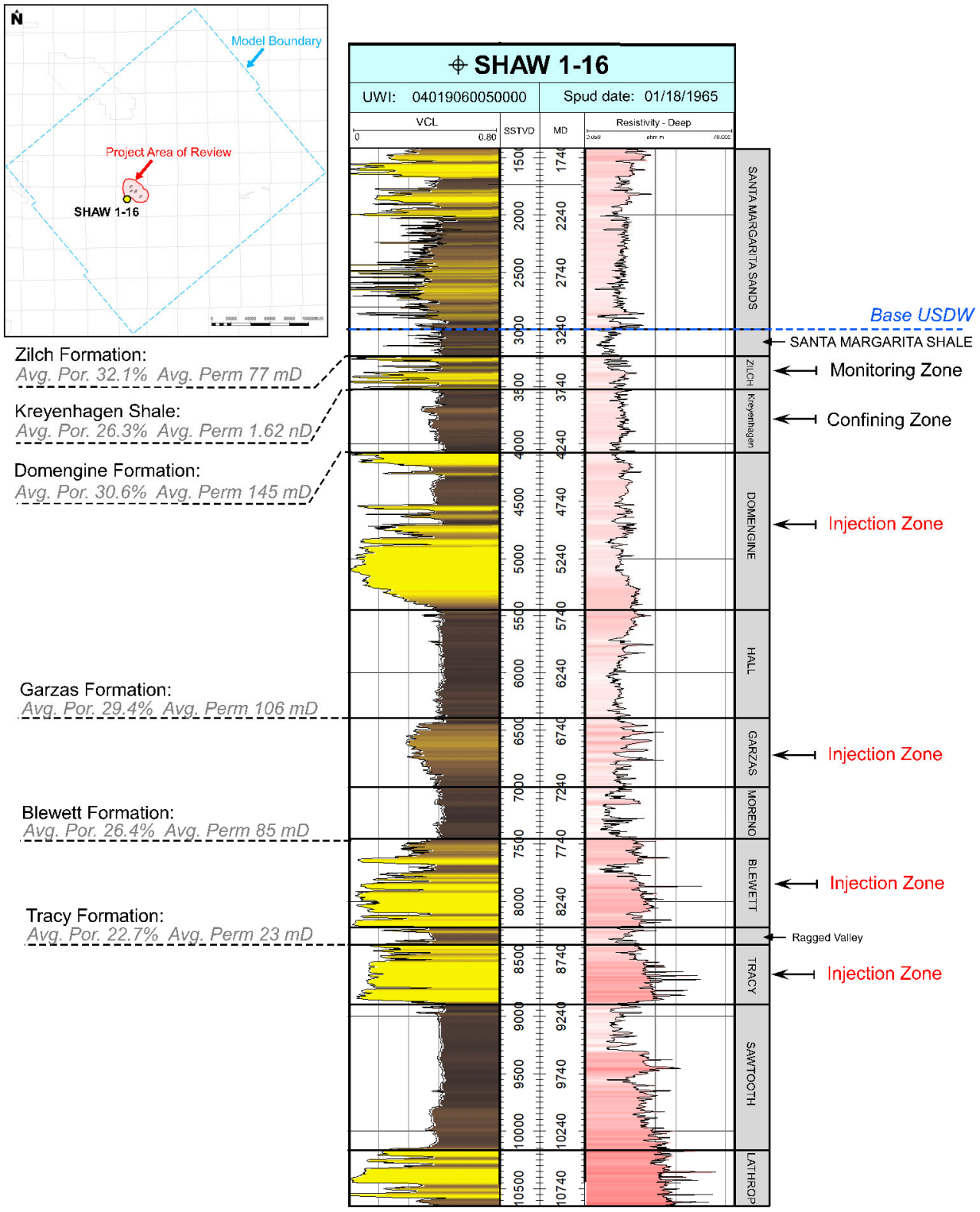

Figure 2.2-4. Type well showing average rock properties for the confining zones and injection zones within the project AoR.

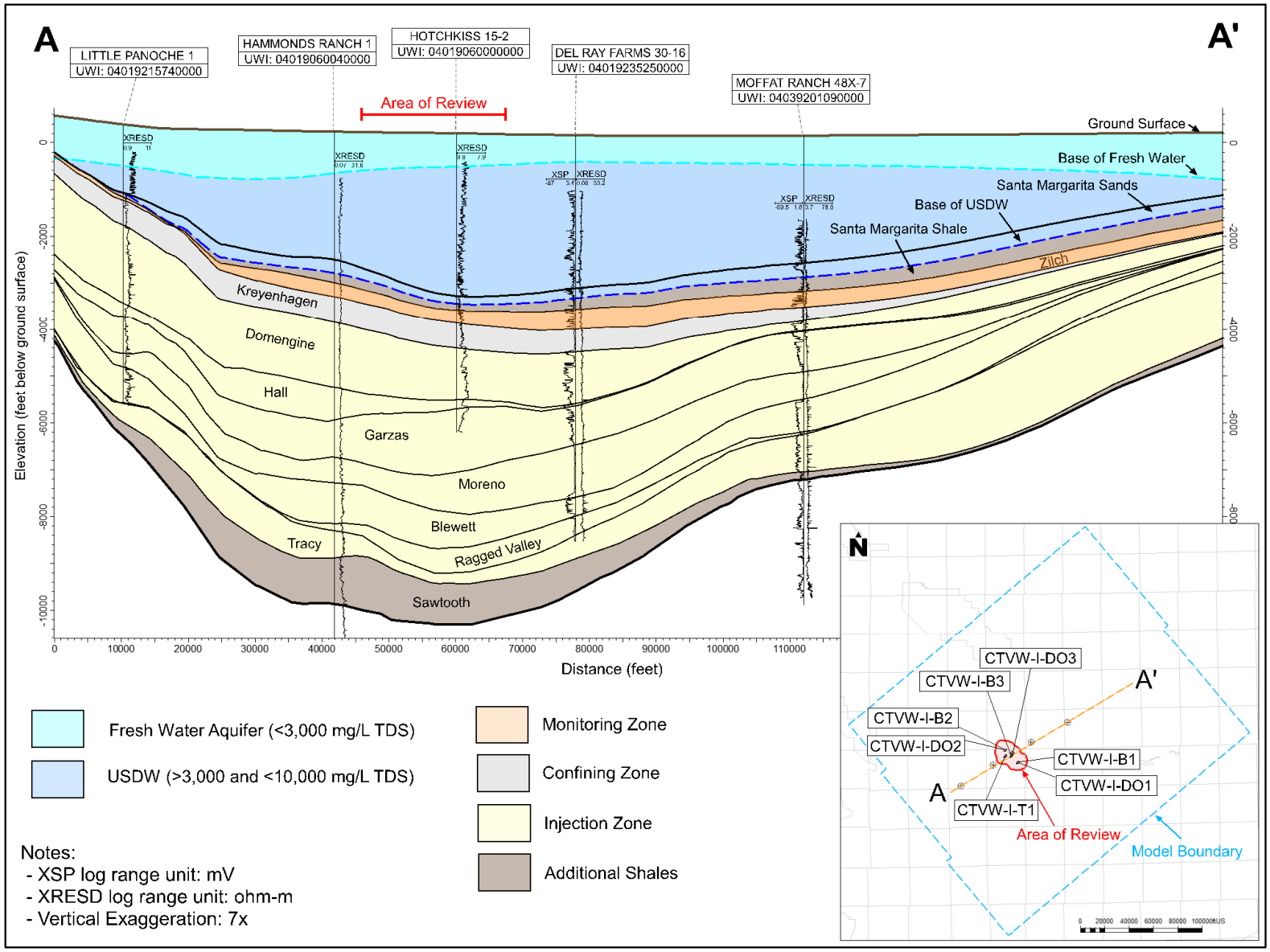

Figure 2.2-5. Cross section showing stratigraphy and lateral continuity of major formations across the AoR.

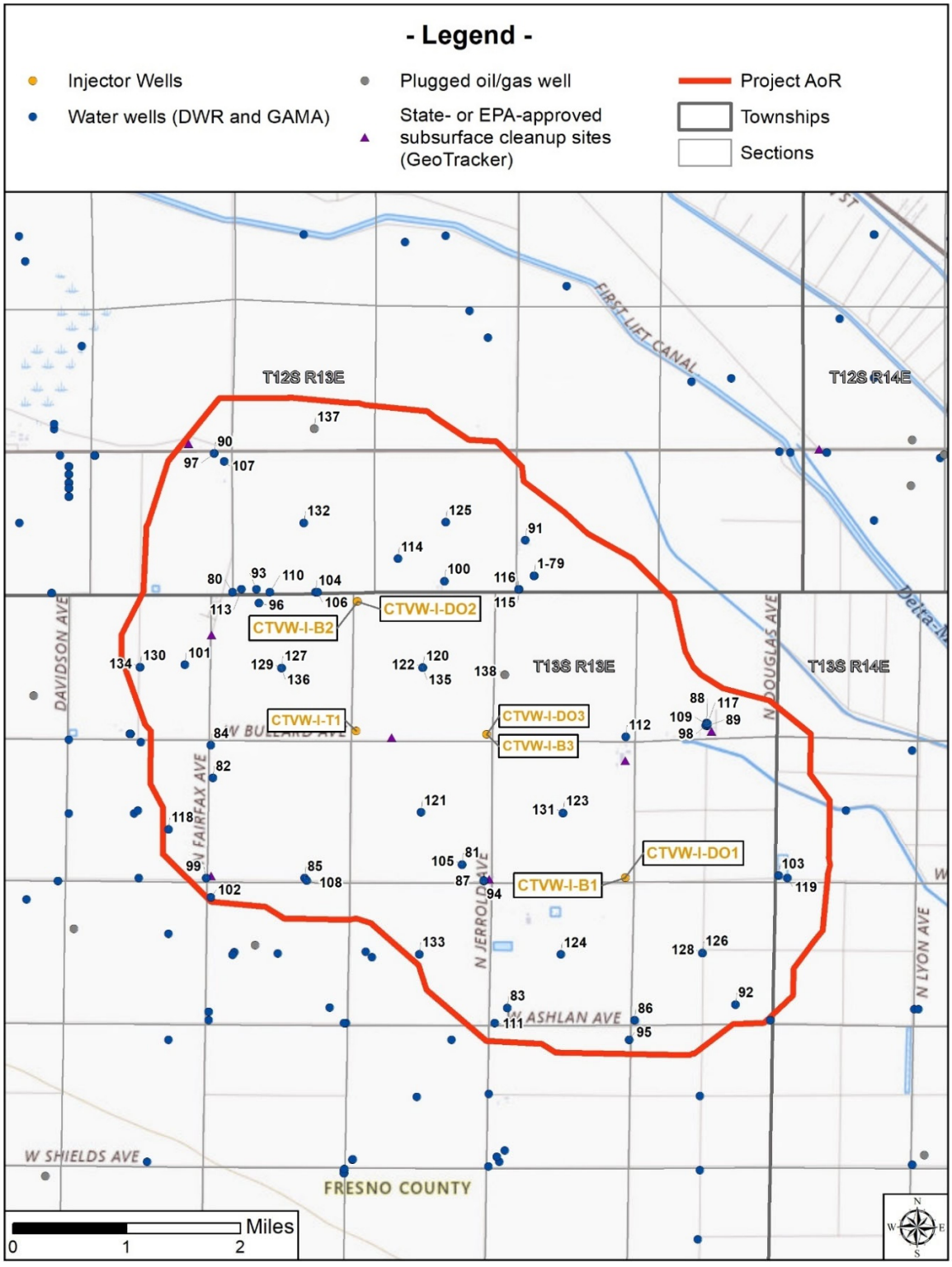

Figure 2.2-6. Summary map of the AoR, oil or gas wells, water wells, State- or EPA-approved subsurface cleanup sites, and surface features in the project area. Water wells from California Division of Drinking Water (DWR) and Groundwater Ambient Monitoring and Assessment (GAMA) program. No Mines, quarries, springs or tribal lands are identified near the AoR.

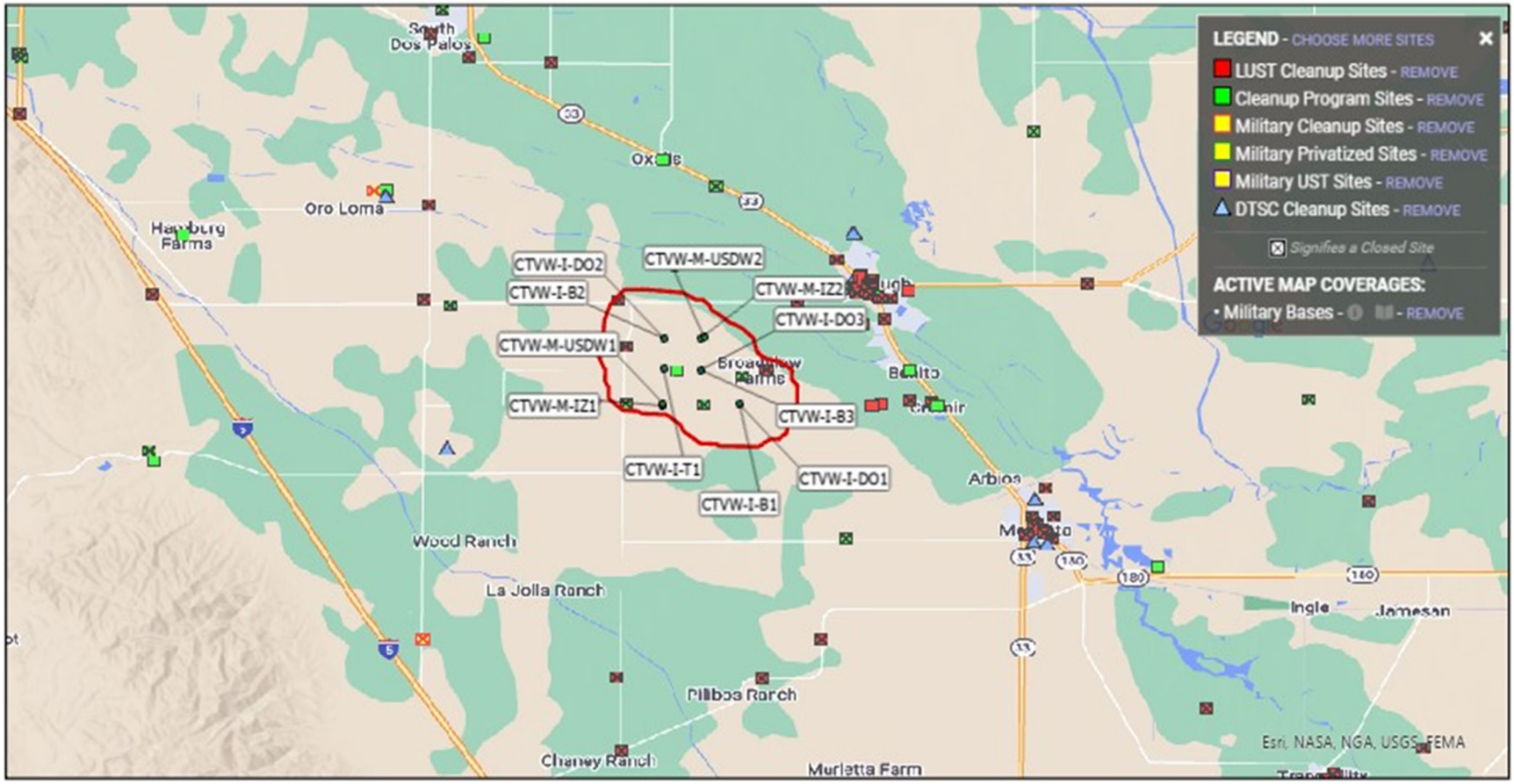

Figure 2.2-7. State- or EPA-approved subsurface cleanup sites. Source: California State Water Resources Control Board GeoTracker website.

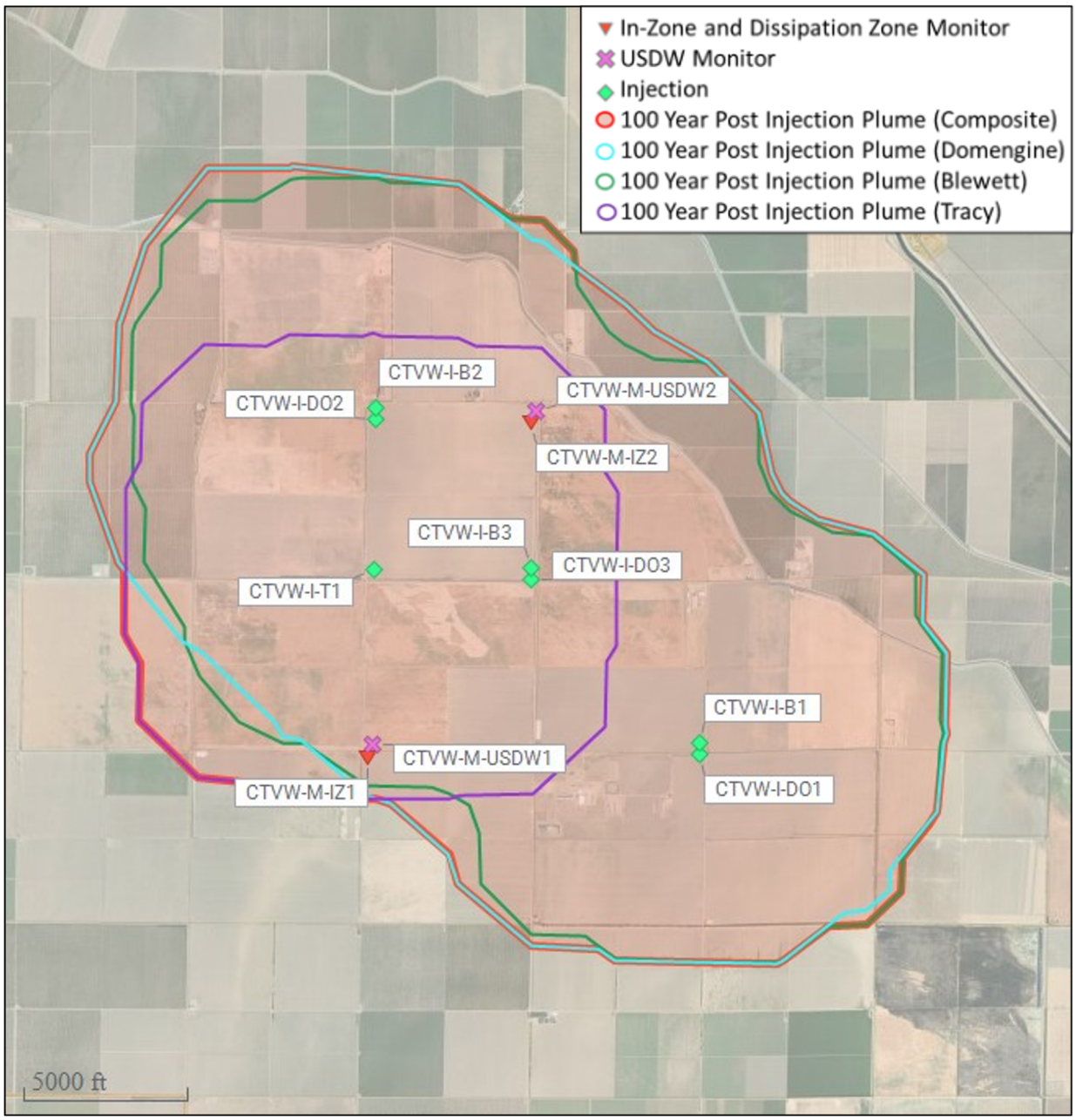

Figure 2.2-8. Locations of injection and monitoring wells

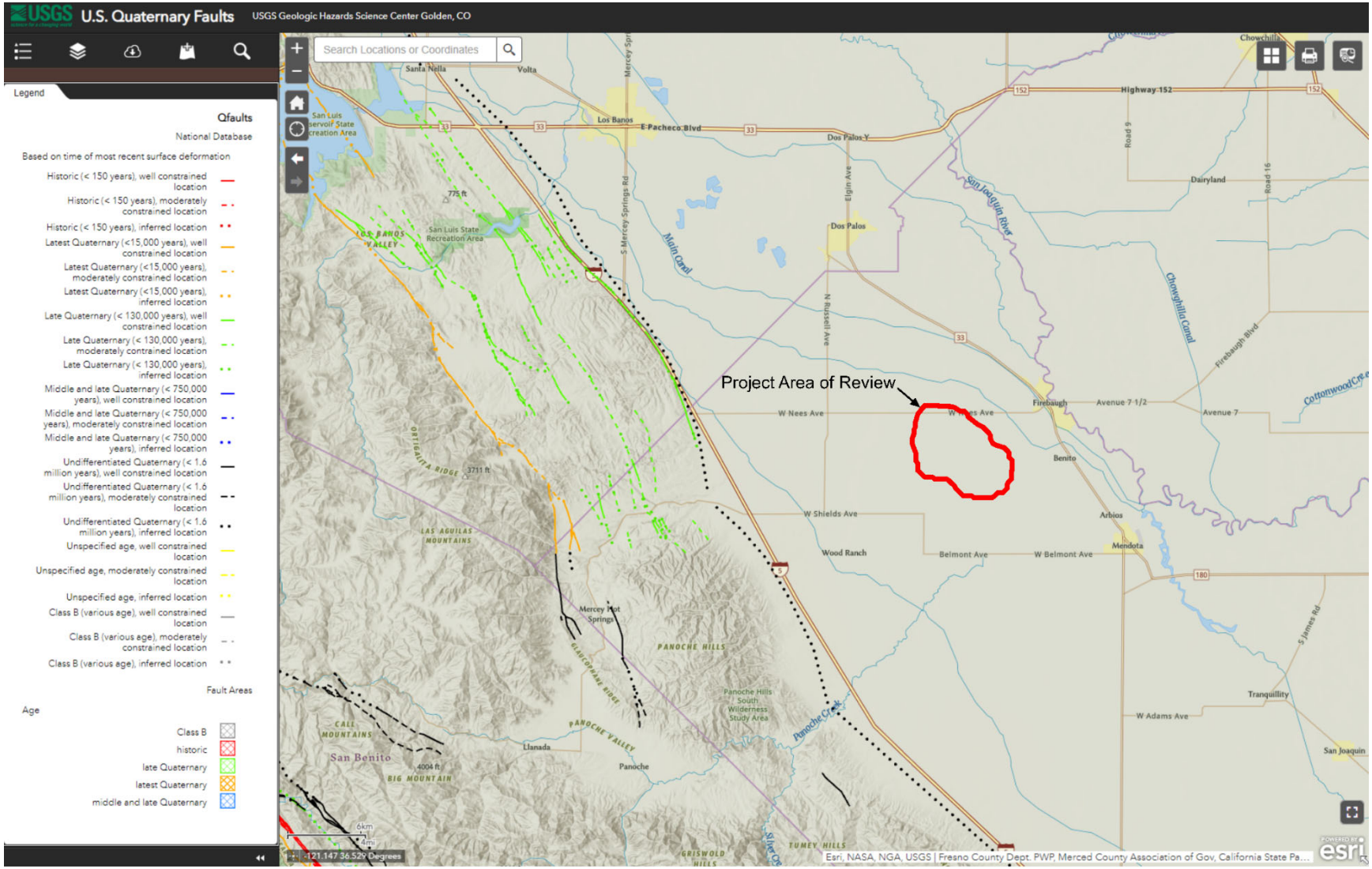

Figure 2.3-1. Fault activity map from the California Geologic Survey which shows no mapped faults within the project AoR. (https://maps.conservation.ca.gov/cgs/fam/)

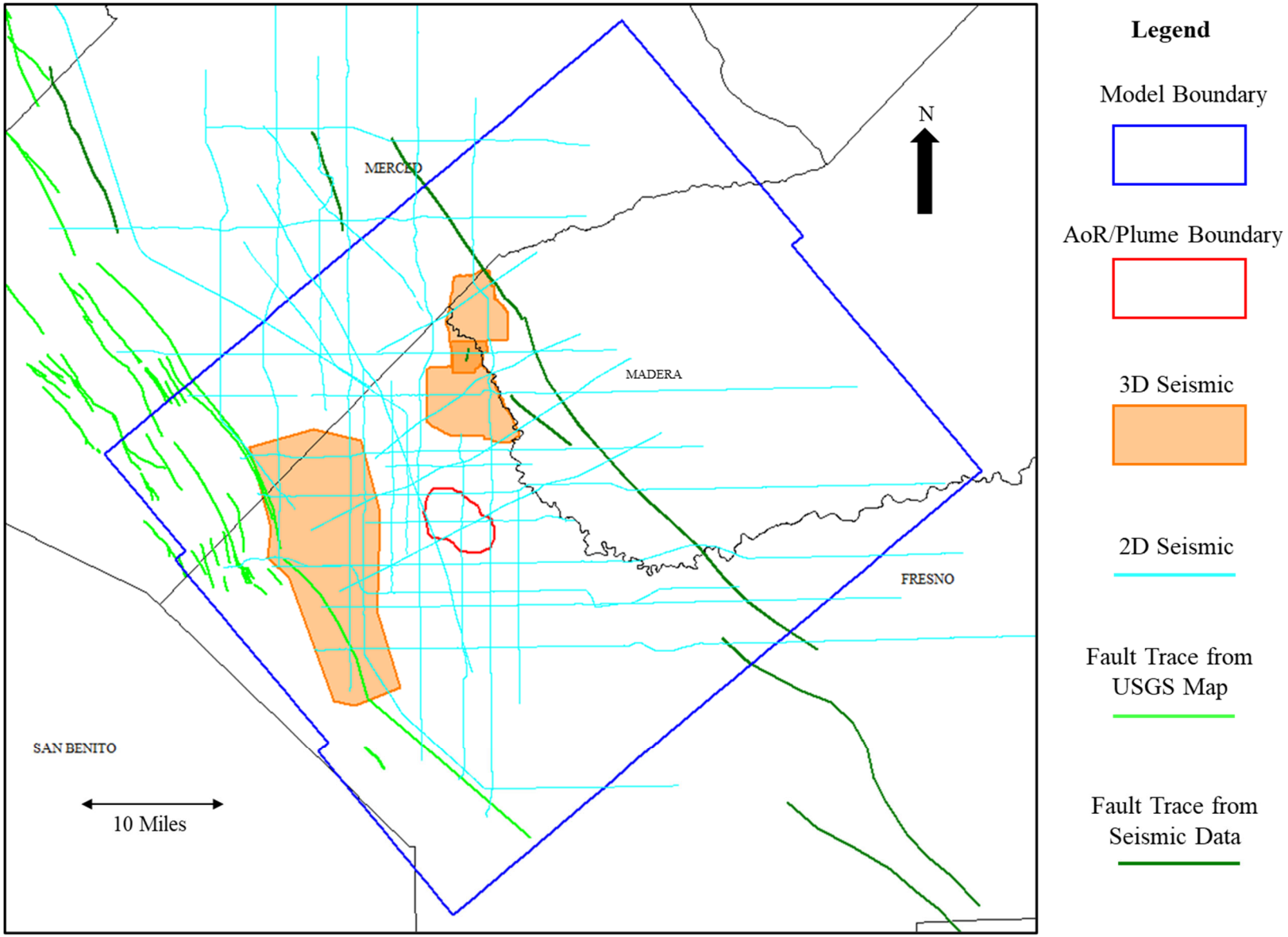

Figure 2.3-2. Faults interpreted from seismic, well, and published data within the extended region of the model boundary.

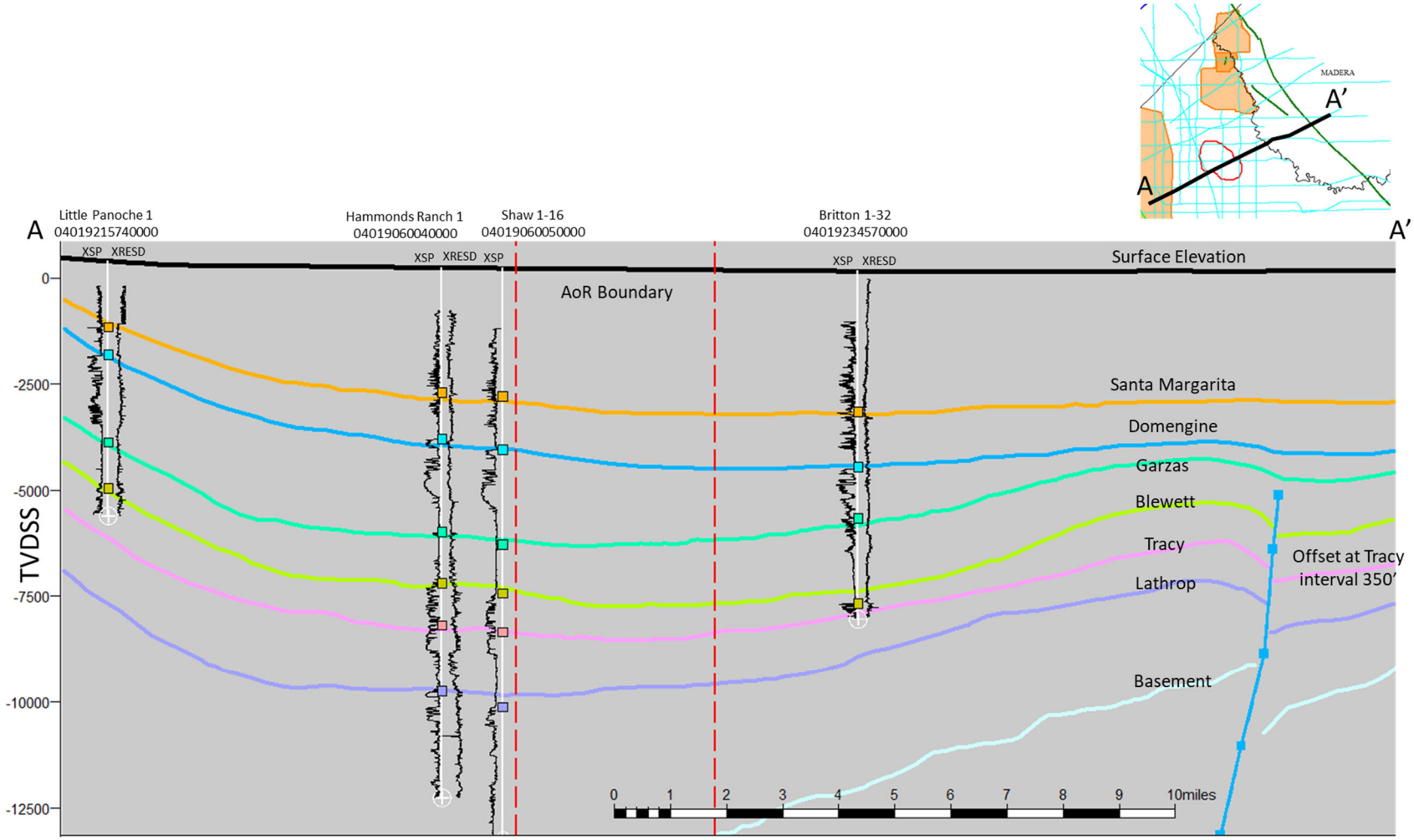

Figure 2.3-3. Schematic section from 2D seismic interpretation. Seismic surfaces are shown color matched with well picks from geophysical logs. Wells are projected in up to 3000ft into this line explaining some of the mismatch between surfaces and well picks. Maximum offset for an injection zone is at the Tracy interval of approximately 350'. The AoR boundary is delineated by the red striped vertical lines.

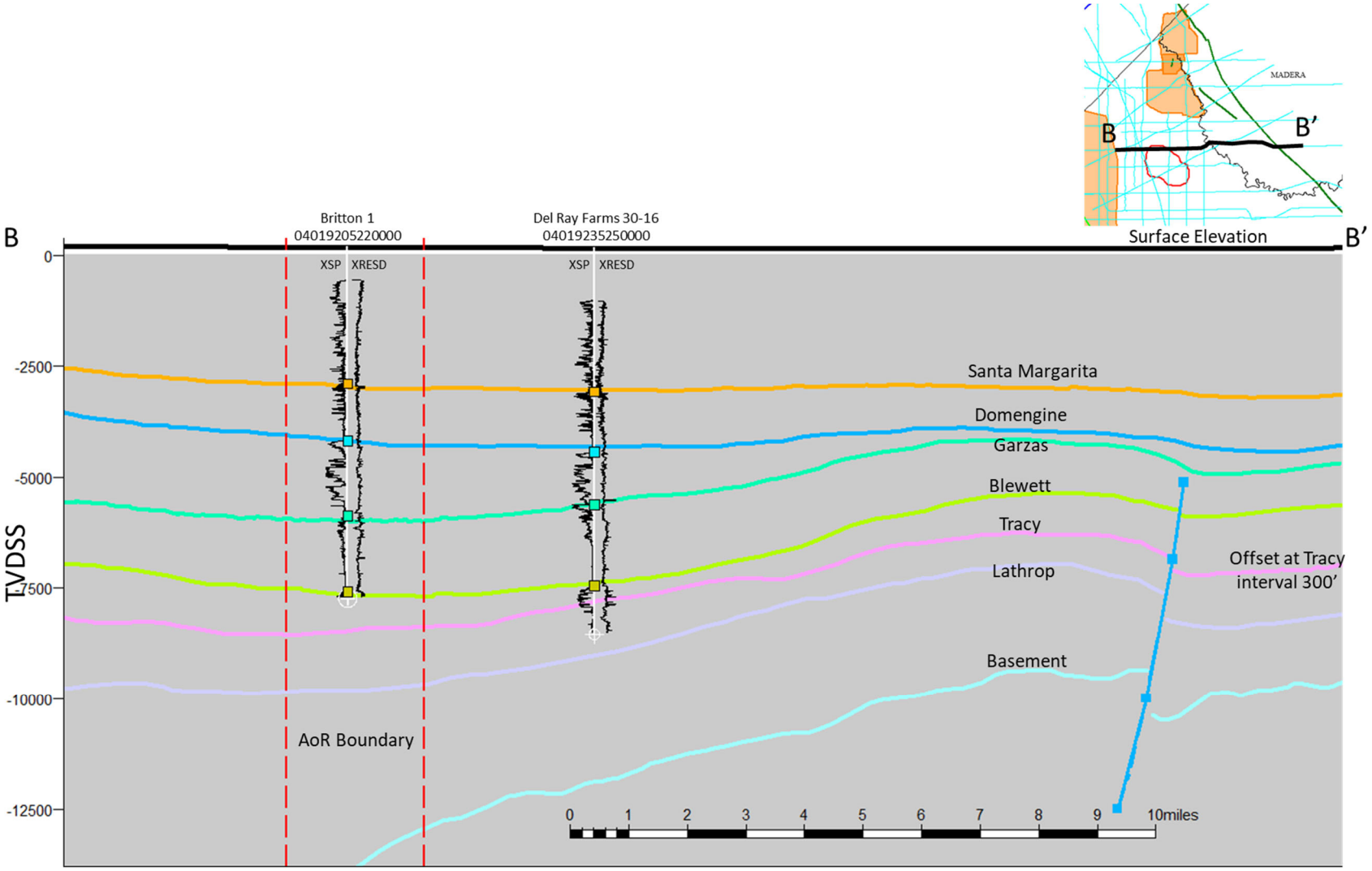

Figure 2.3-4. Schematic section from 2D seismic interpretation. Seismic surfaces are shown color matched with well picks from geophysical logs. Wells are projected in up to 900ft into this line explaining some of the mismatch between surfaces and well picks. Maximum offset for an injection zone is at the Tracy interval of approximately 300'. The AoR boundary is delineated by the red striped vertical lines.

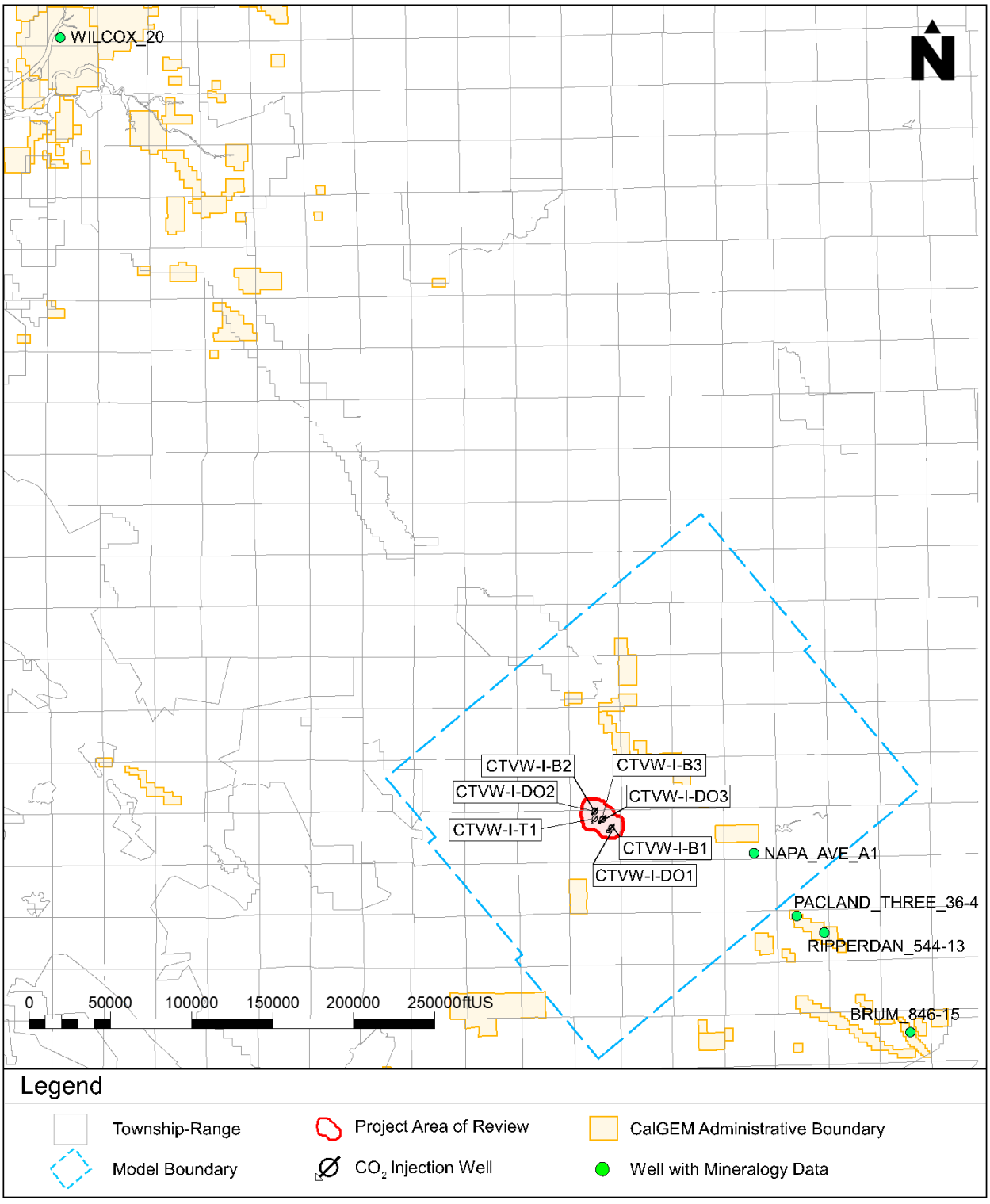

Figure 2.4-1. Map showing the location of wells with mineralogical data.

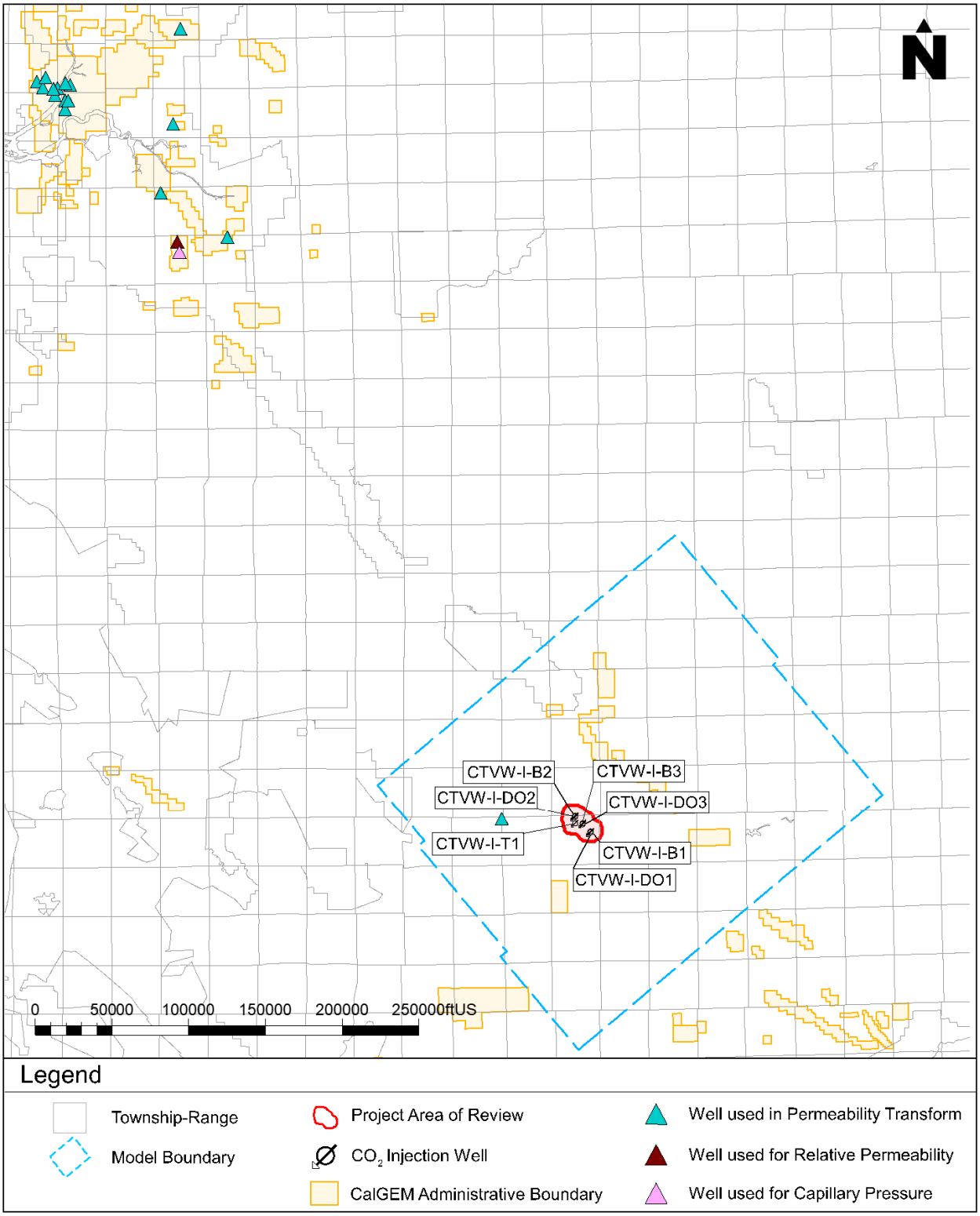

Figure 2.4-2. Map showing the location of wells used in the permeability transform.

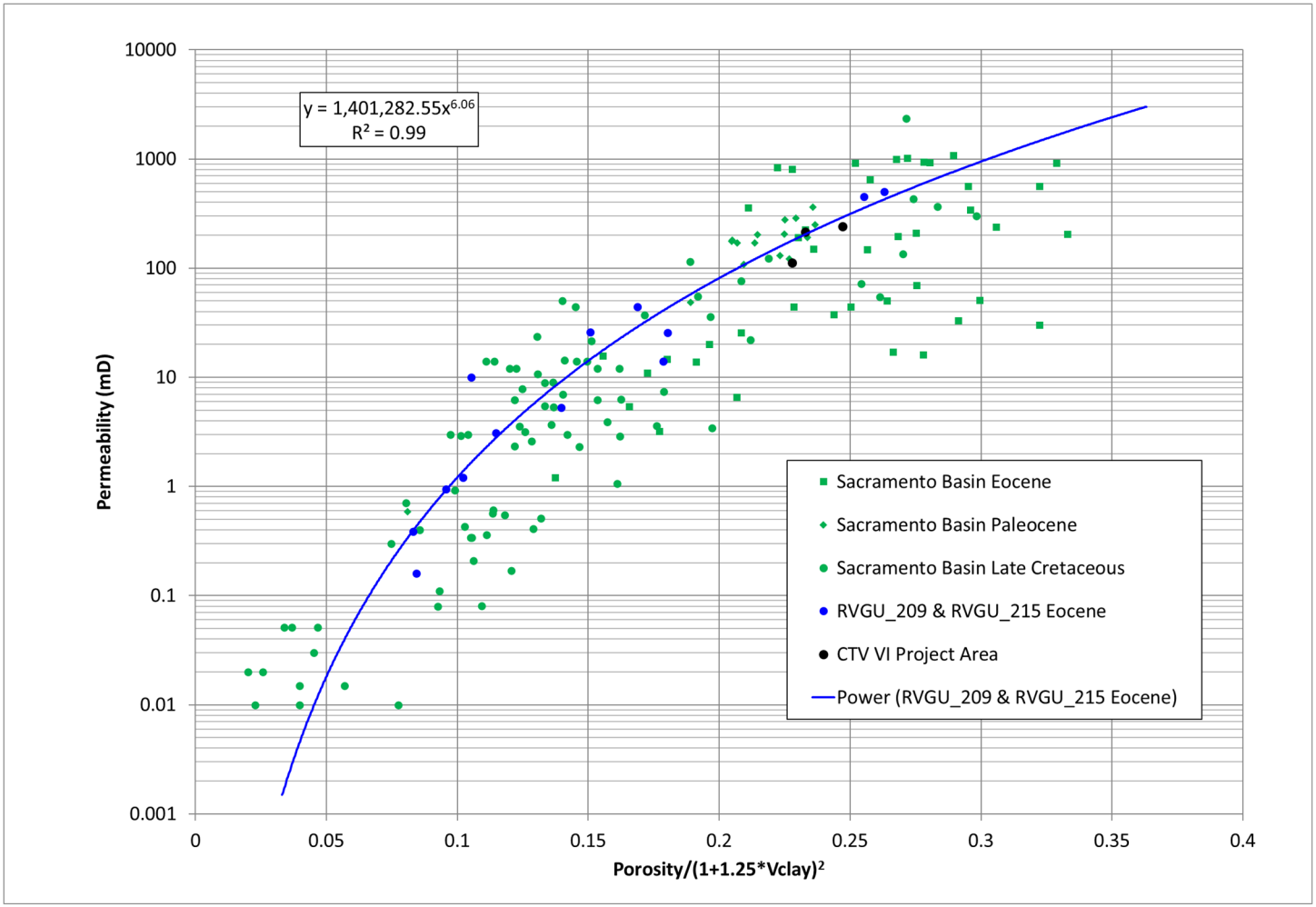

Figure 2.4-3. Permeability transform for CTV VI Injection zones. The blue data points are from two wells in Rio Vista gas field (RVGU_209 & RVGU_215) and are the basis for the permeability transform. Additional core data from the Sacramento basin is also shown in green, with circles corresponding to Late Cretaceous age rock, diamonds corresponding to Paleocene age rock, and squares corresponding to Eocene age rock. The black data points are core from a well specific to the CTV VI model area. Data shown is limited to those core data points representing sand, with a clay volume from XRD of less than 25% clay and exclude any percussion sidewall derived permeability values.

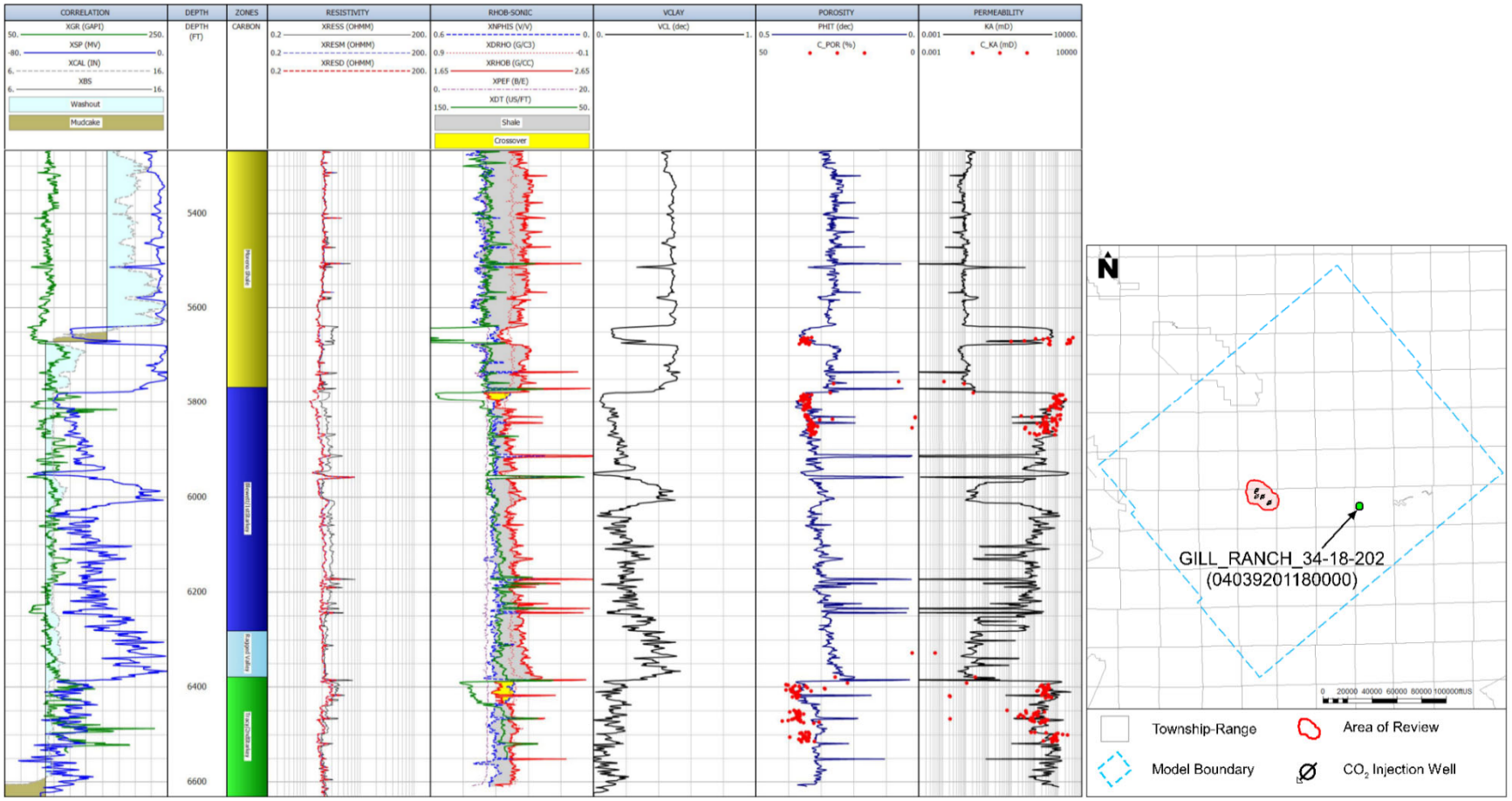

Figure 2.4-4. Example log from the GILL_RANCH_34-18-202 (04039201180000) well in Gill Ranch Gas Field. The last track shows a comparison of the permeability calculated from the transform (black) shown in **Figure 2.4-3** to core permeability (red dots). Track 1: Correlation and caliper logs. Track 2: Measured depth. Track 3: Zones. Track 4: Resistivity. Track 5: Compressional sonic, density, and neutron logs. Track 6: Volume of clay. Track 7: Porosity calculated from density and core porosity (red dots). Track 8: Permeability calculated using permeability transform and core permeability.

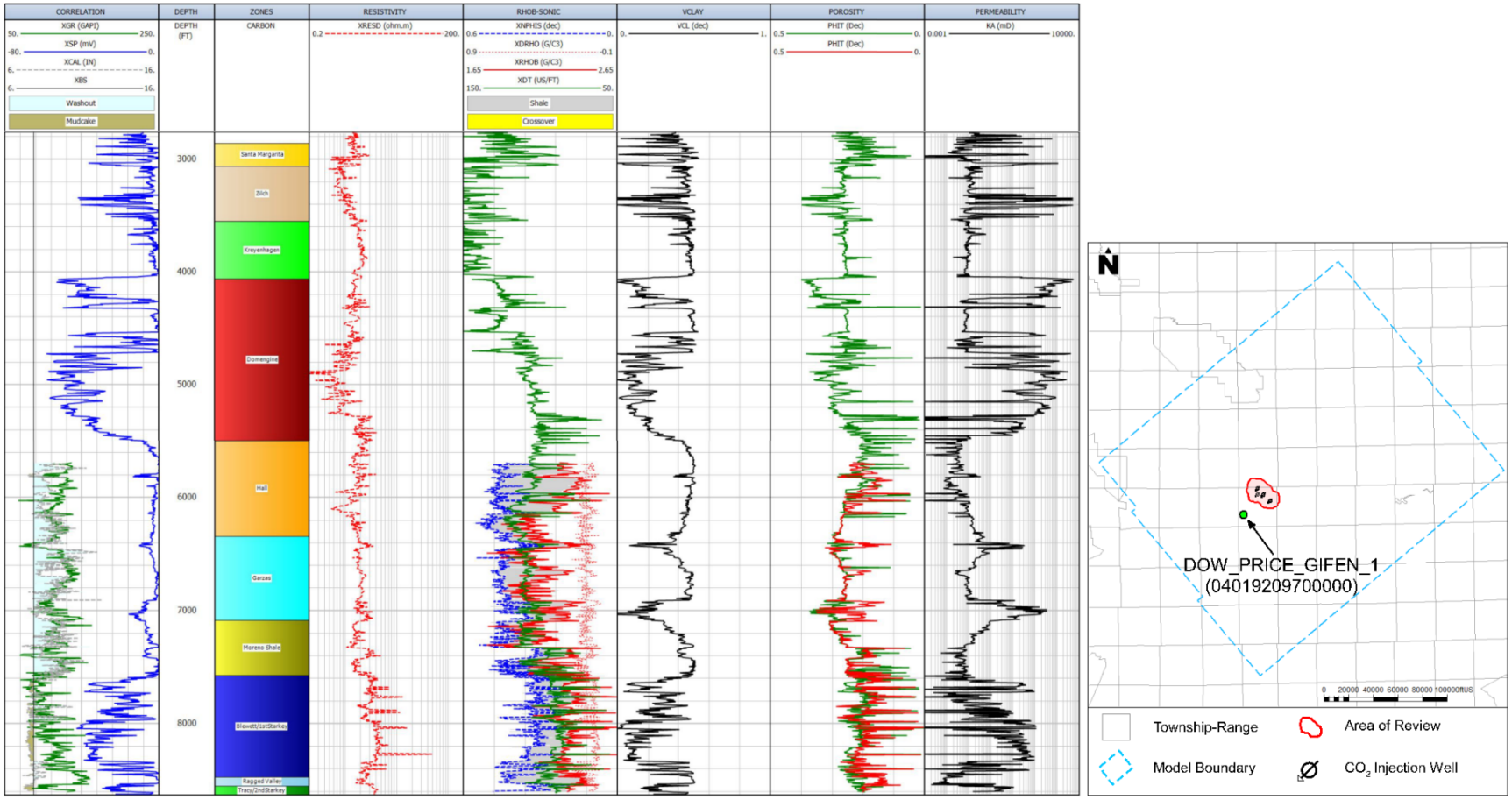

Figure 2.4-5. Log plot for well DOW_PRICE_GIFEN_1 (04019209700000), showing the log curves used as inputs into calculations of clay volume, porosity and permeability, and their outputs. Track 1: Correlation and caliper logs. Track 2: Measured depth. Track 3: Zones. Track 4: Resistivity. Track 5: Compressional sonic, neutron, and density logs. Track 6: Volume of clay. Track 7: Porosity calculated from sonic (green) and density (red). Track 8: Permeability calculated using transform shown in **Figure 2.4-3.**

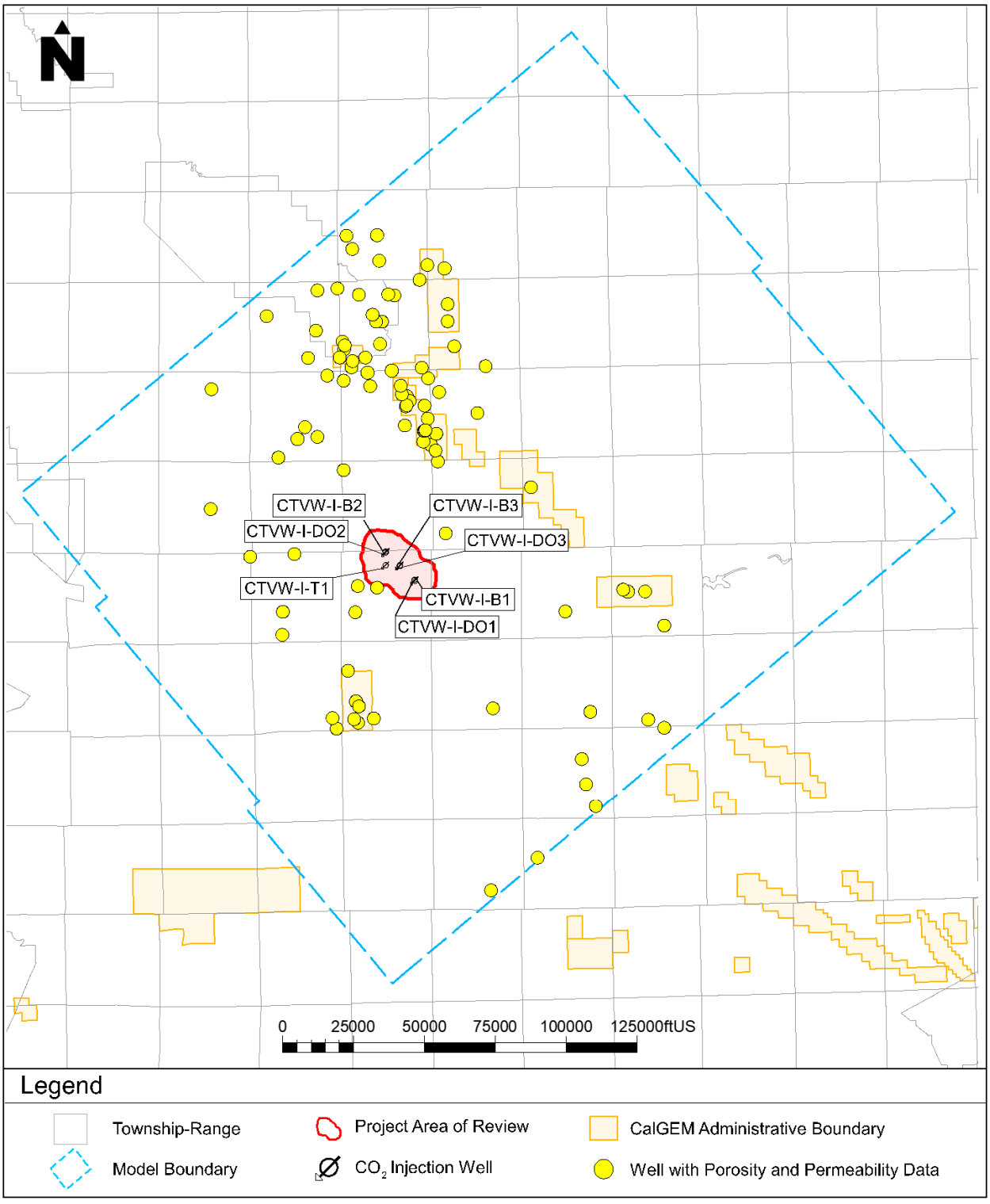

Figure 2.4-6. Map of wells with porosity and permeability data.

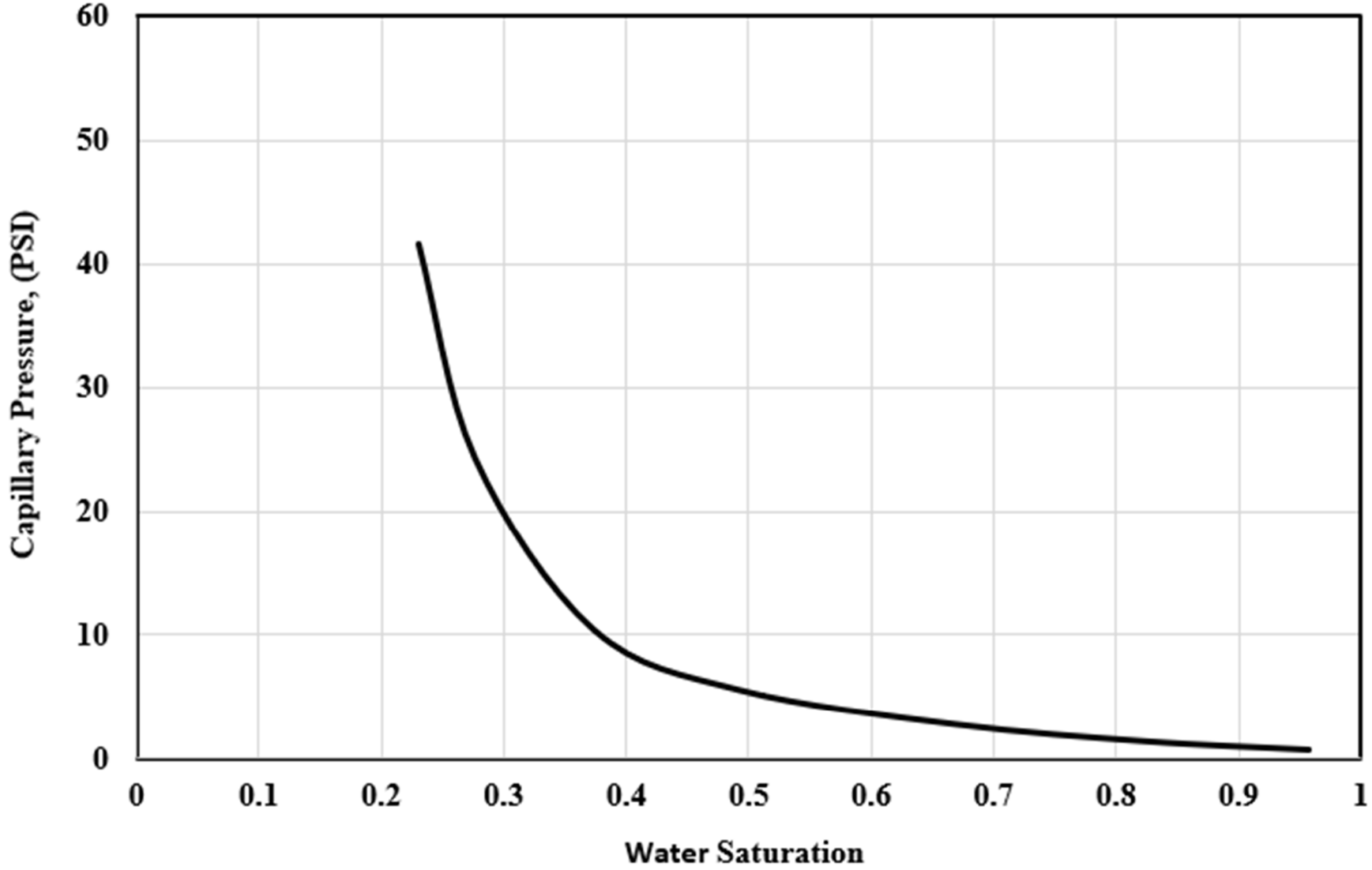

Figure 2.4-7. Injection zone capillary pressure curve used for computational modeling.

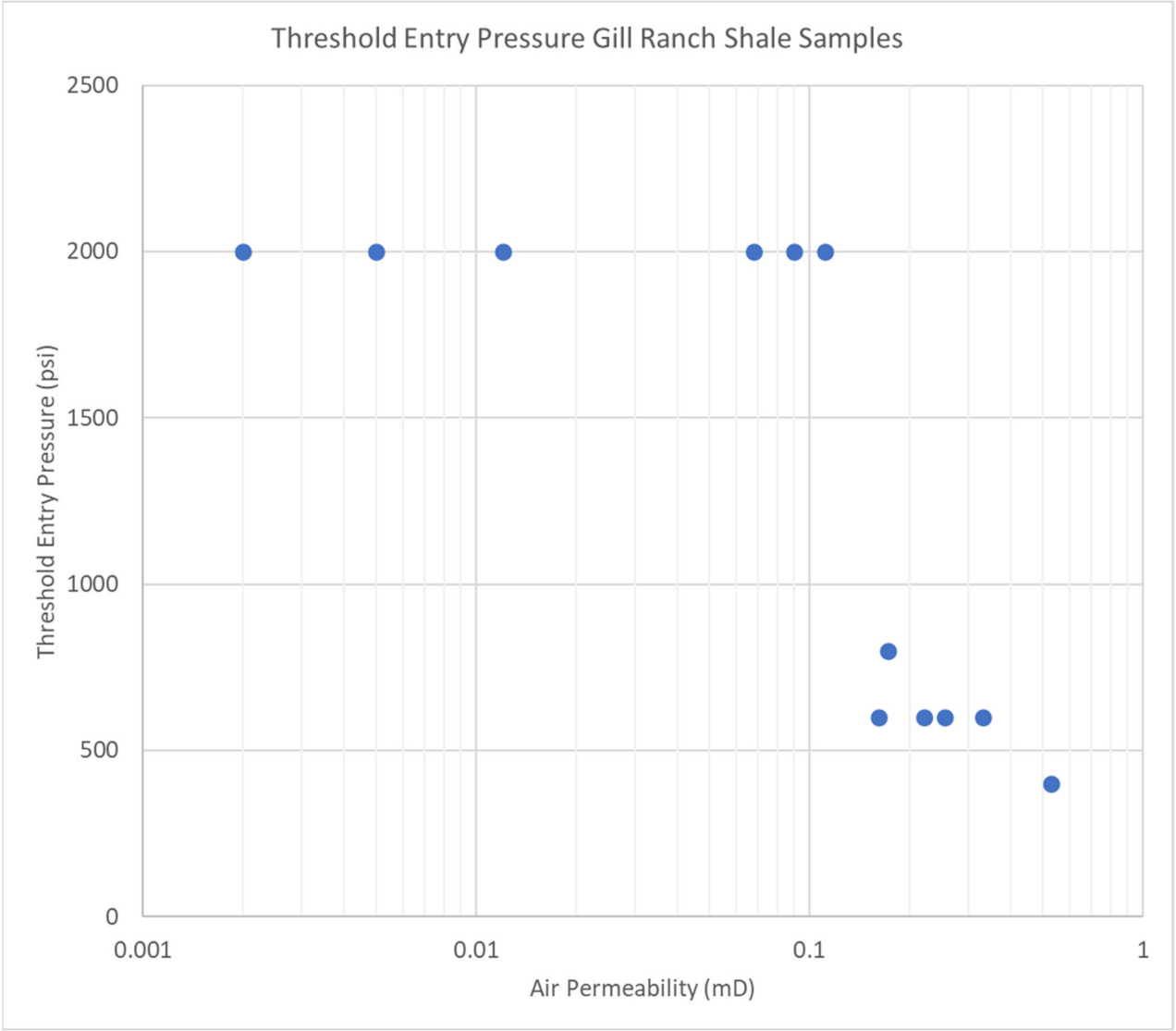

Figure 2.4-8. Threshold entry pressure versus air permeability for samples from Gill Ranch gas field. All the samples with less than 0.1 mD air permeability showed no brine breakthrough even at the maximum tested delta pressure of 2,000 psi.

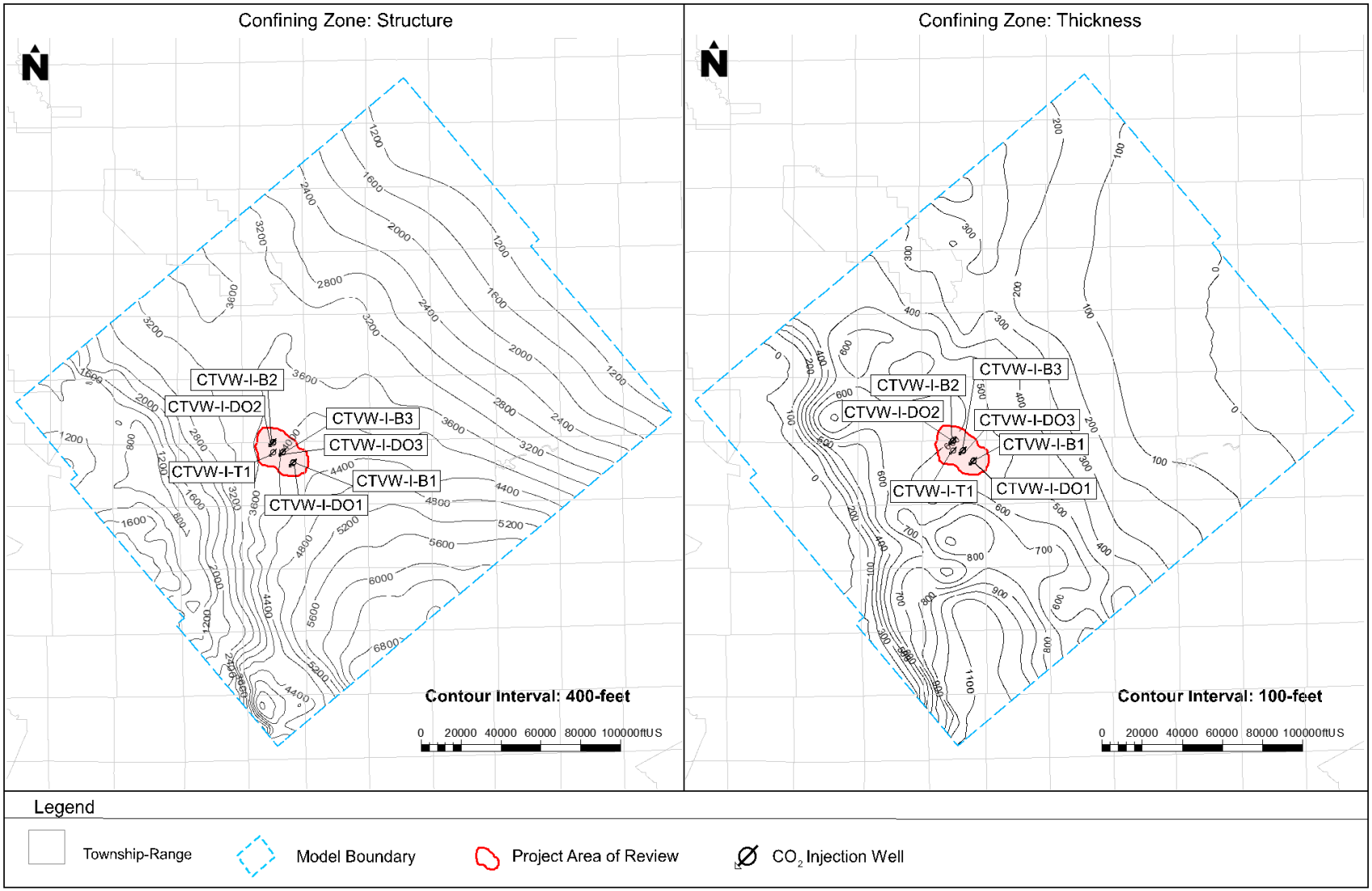

Figure 2.4-9(a). Thickness and structure map for the Confining Zone.

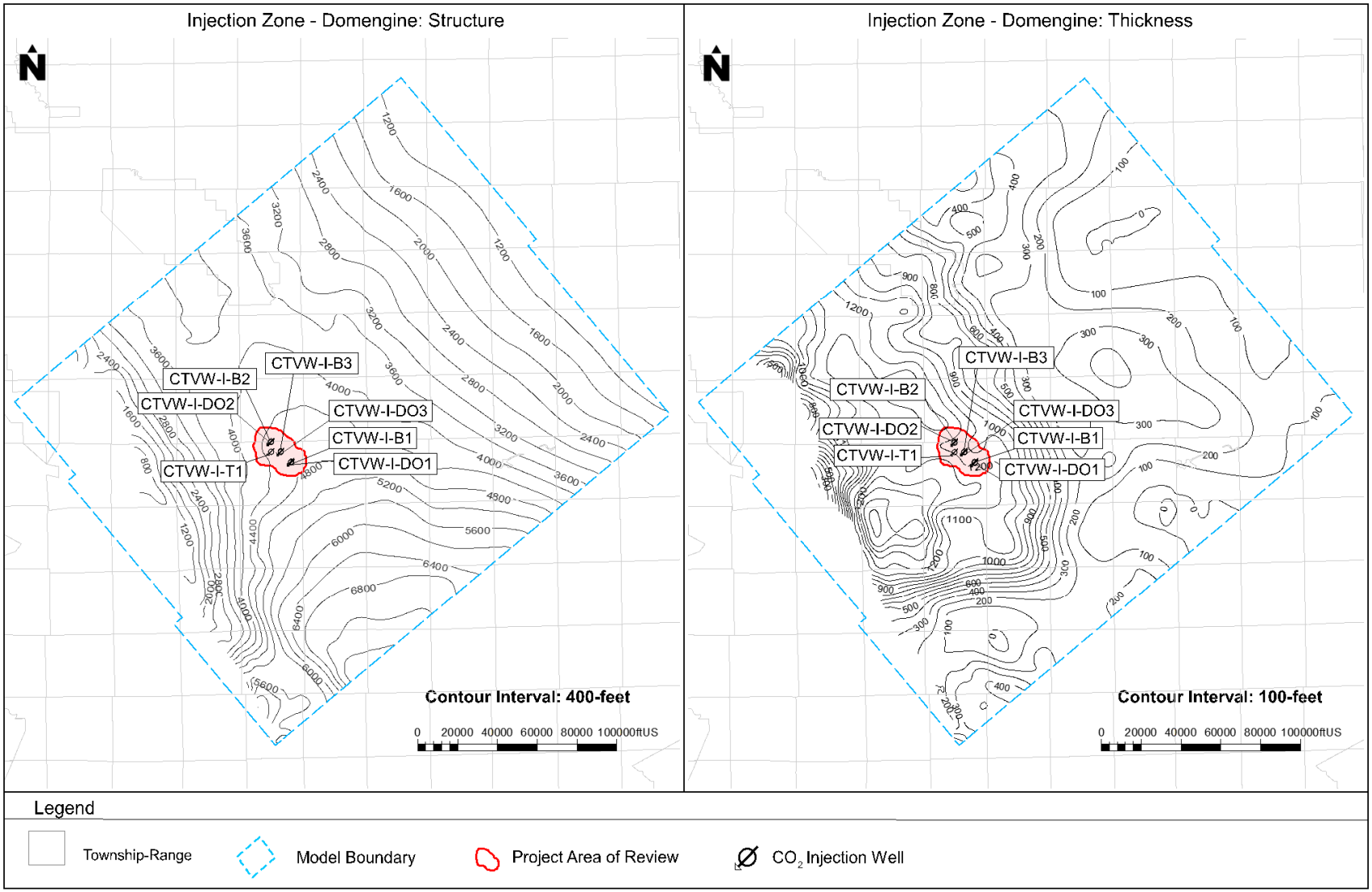

Figure 2.4-9(b). Thickness and structure map for the Domengine Injection Zone.

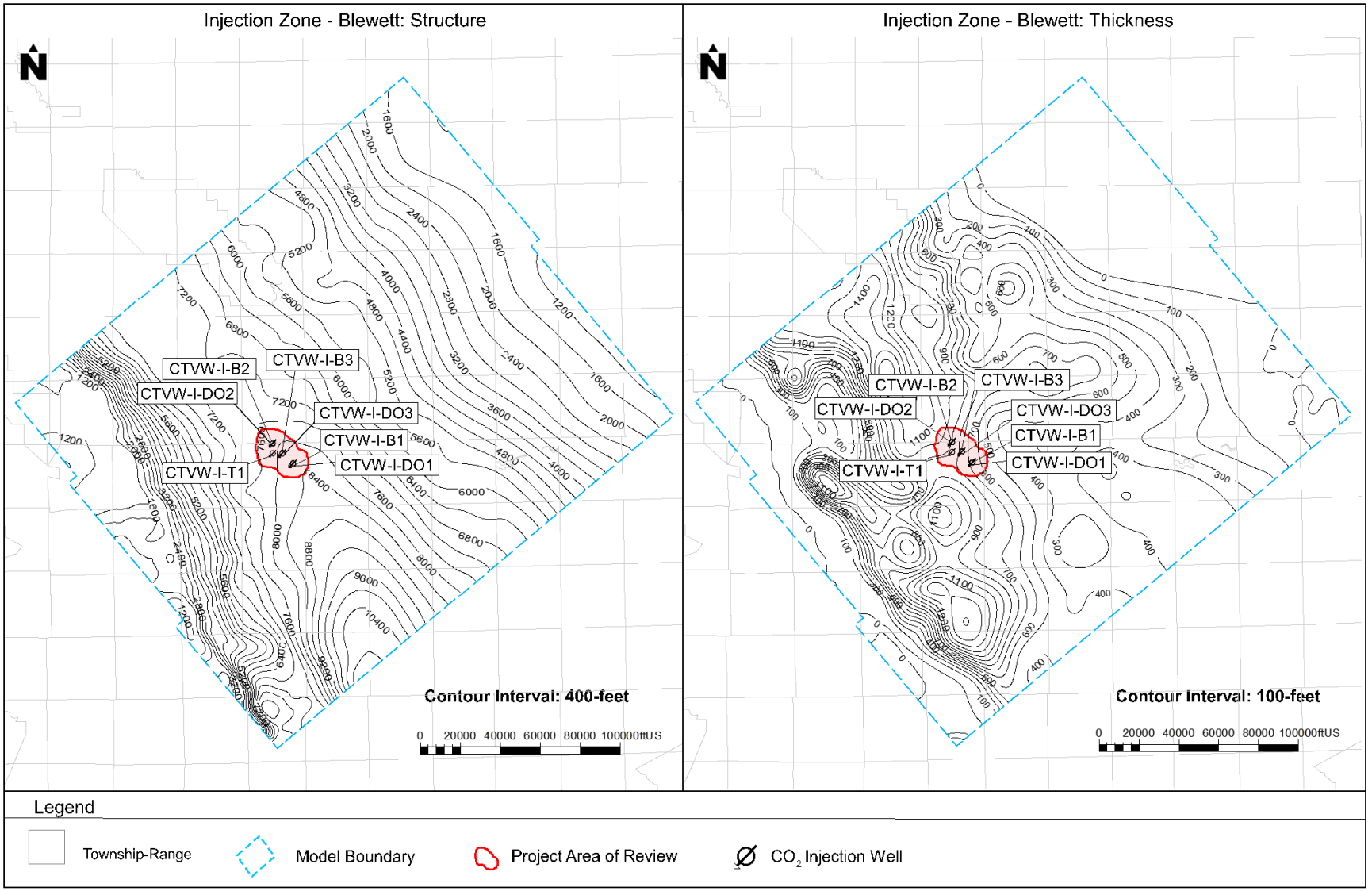

Figure 2.4-9(c). Thickness and structure map for the Blewett Injection Zone.

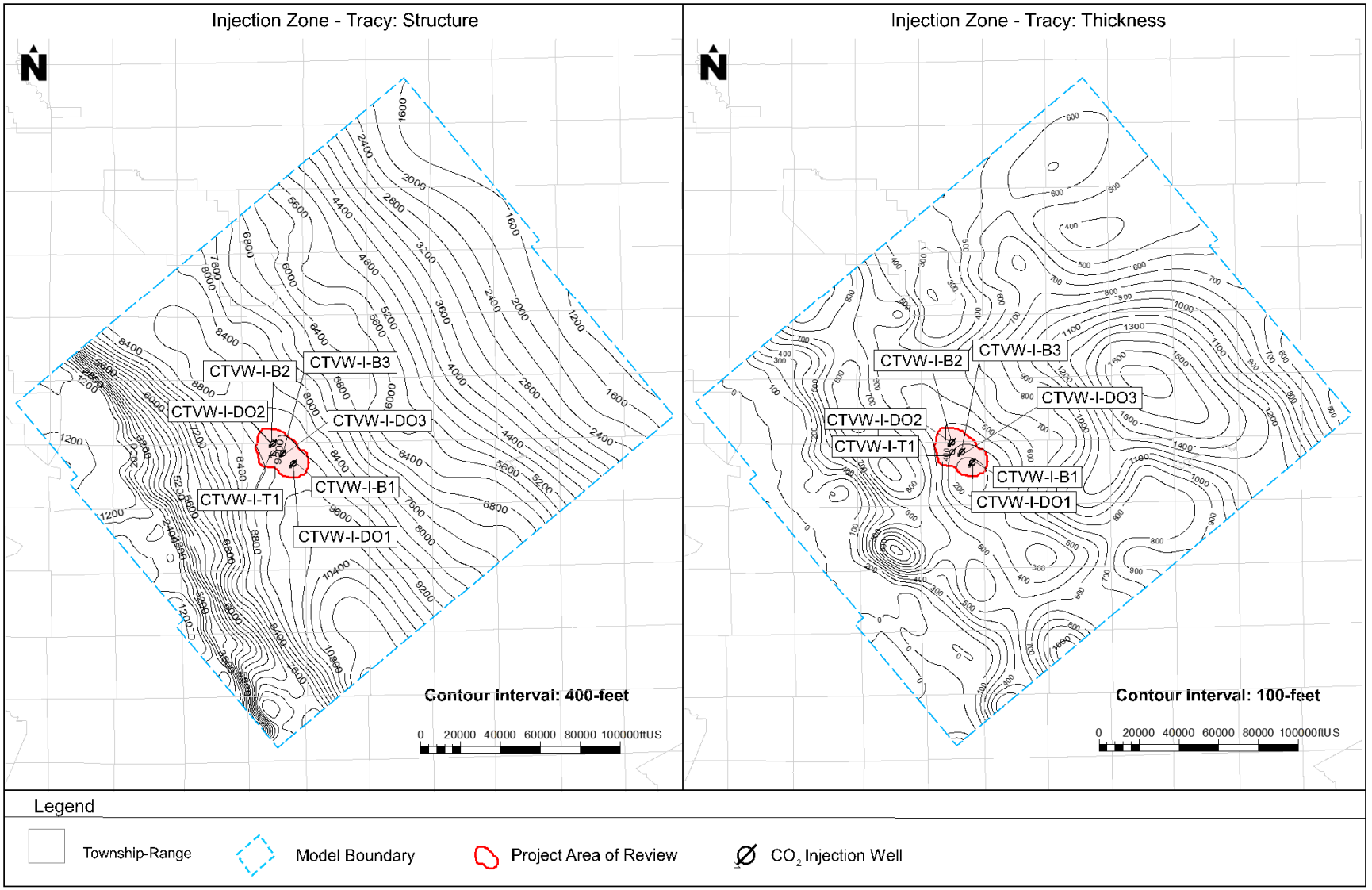

Figure 2.4-9(d). Thickness and structure map for the Tracy Injection Zone.

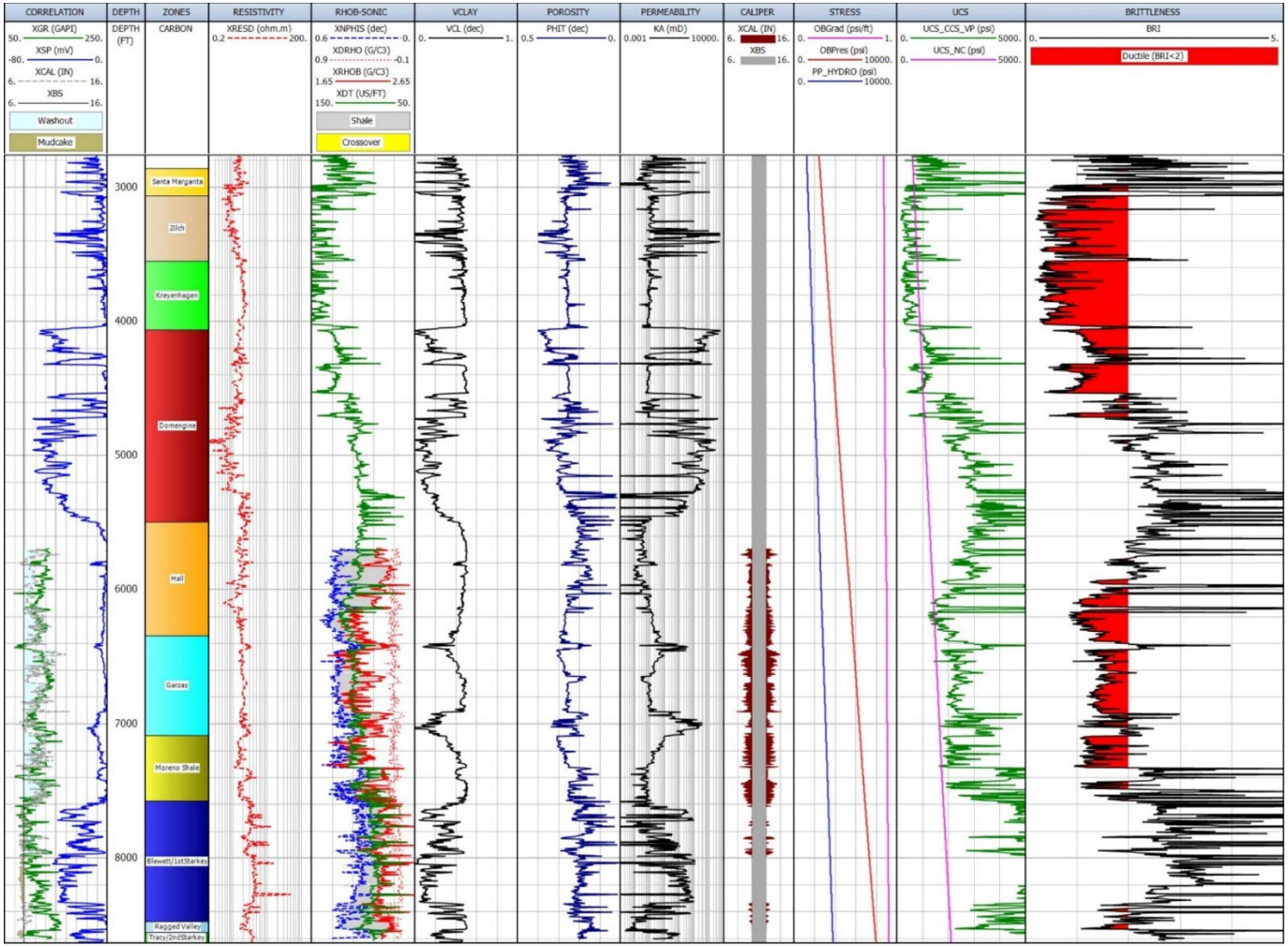

Figure 2.5-1. Unconfined compressive strength and ductility calculations for well DOW_PRICE_GIFEN_1 (04019209700000). The ductility is less than two for all of the upper confining zone as well as most of the internal shale layers. Track 1: Correlation logs. Track 2: Measured depth. Track 3: Zones. Track 4: Resistivity. Track 5: Density, neutron, and sonic logs. Track 6: Volume of clay. Track 7: Porosity calculated from density. Track 8: Permeability. Track 9: Caliper. Track 10: Overburden pressure, overburden pressure gradient, and hydrostatic pore pressure. Track 11: UCS and UCS_NC. Track 12: Brittleness.

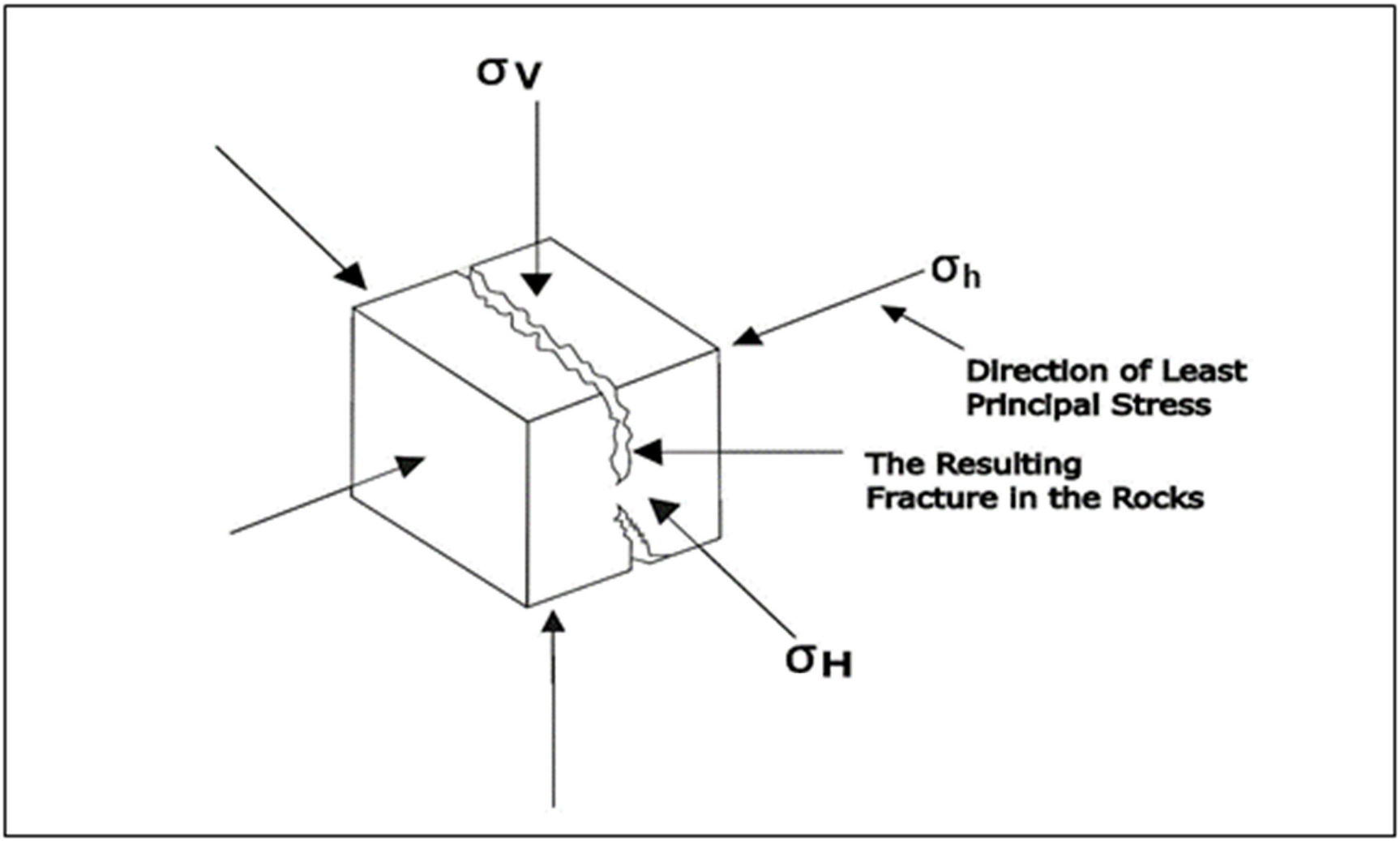

Figure 2.5-2. Stress diagram showing the three principal stresses and the fracturing that will occur perpendicular to the minimum principal stress.

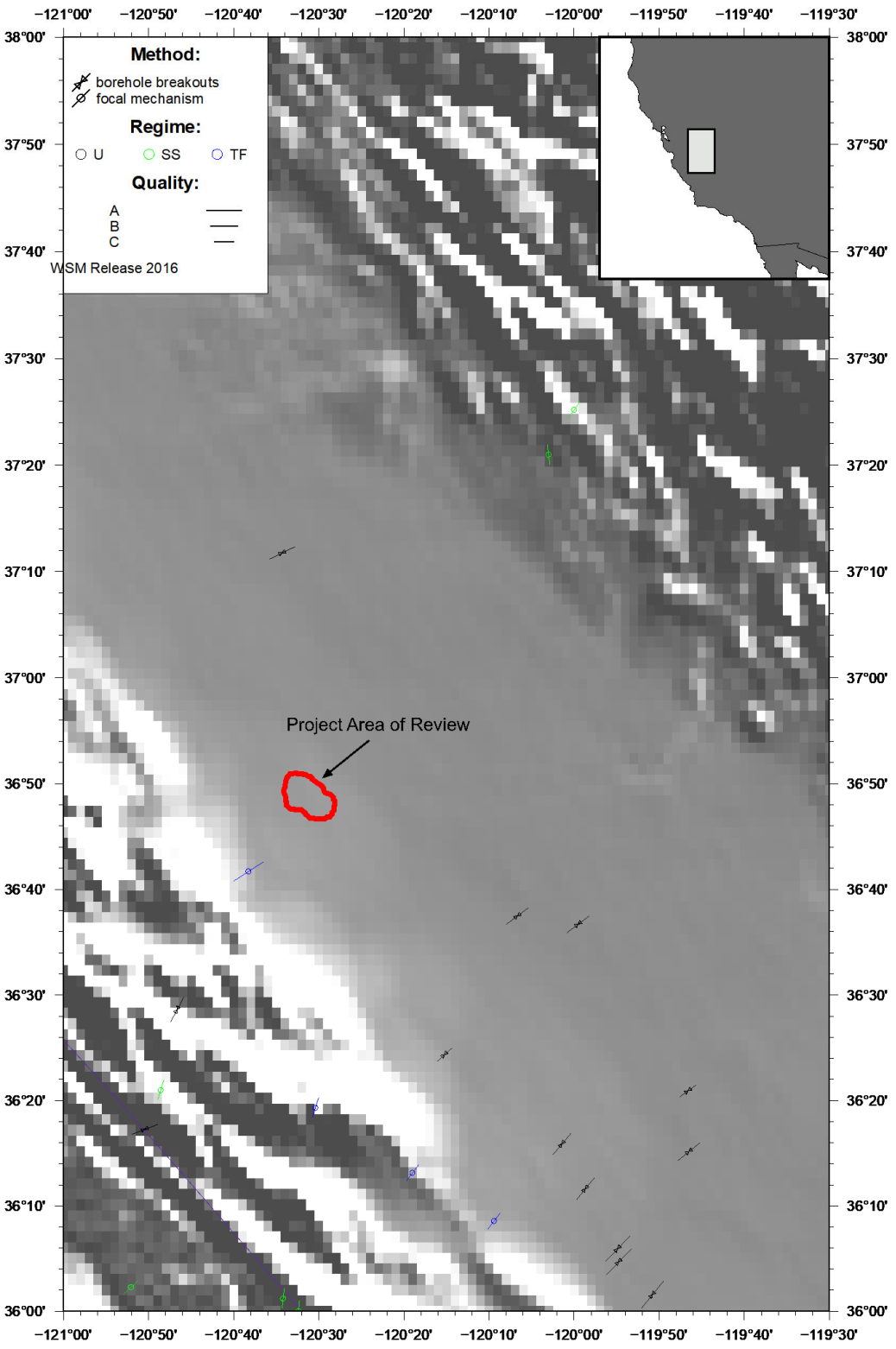

Figure 2.5-3. World Stress Map output showing S_{Hmax} azimuth indicators and earthquake faulting styles in the Sacramento Basin (Heidbach et al., 2016, 2018). In red is the outline of the project AoR. The background coloring represents topography.

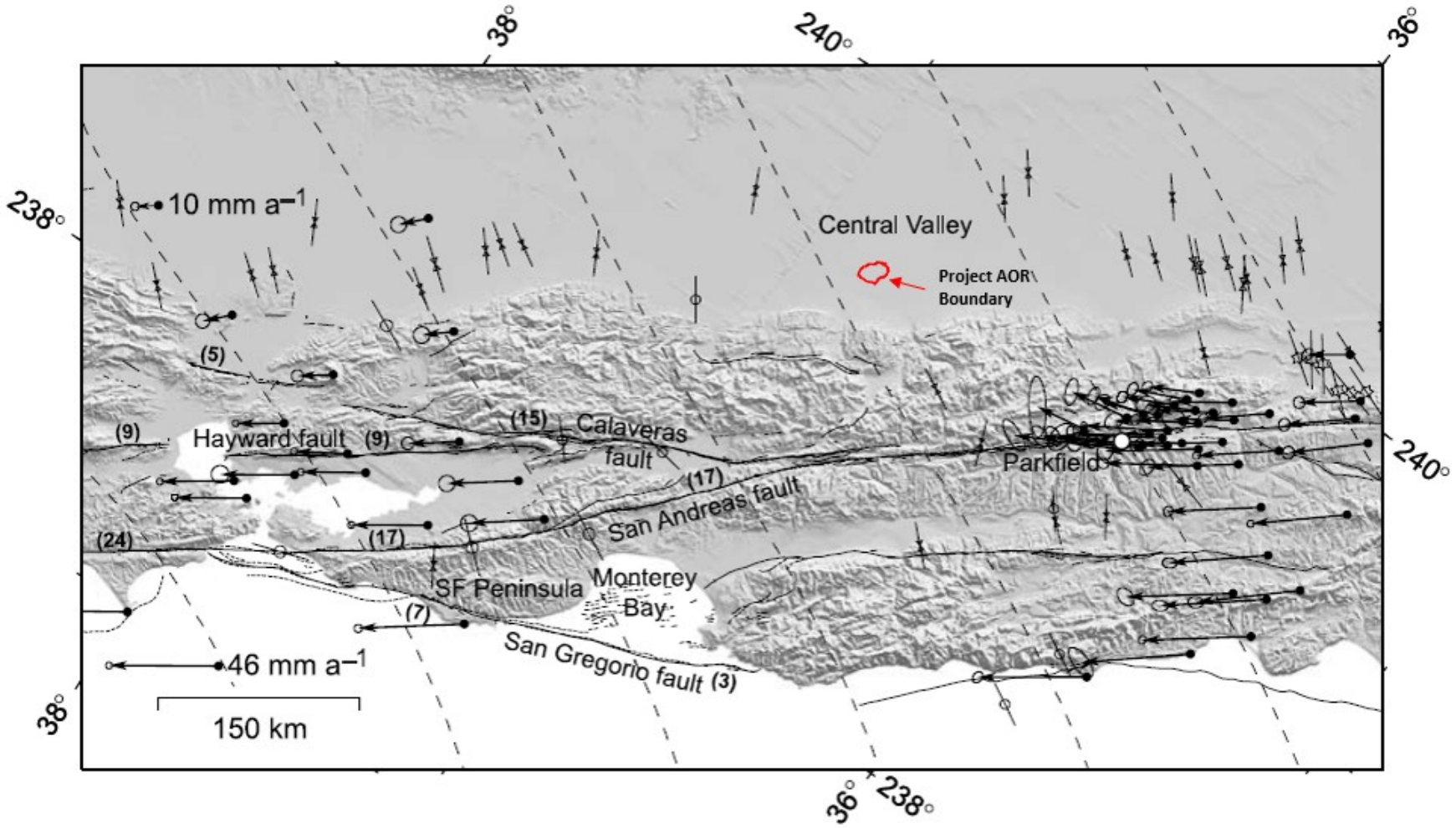

Figure 2.5-4. Figure from Townend & Zoback (2004) showing the location of the project AoR relative to major faults and stress indicators from the world stress map. The dashed lines show regional S_{Hmax} directions calculated from lithospheric buoyancy and plate interaction (Flesch et al., 2000).

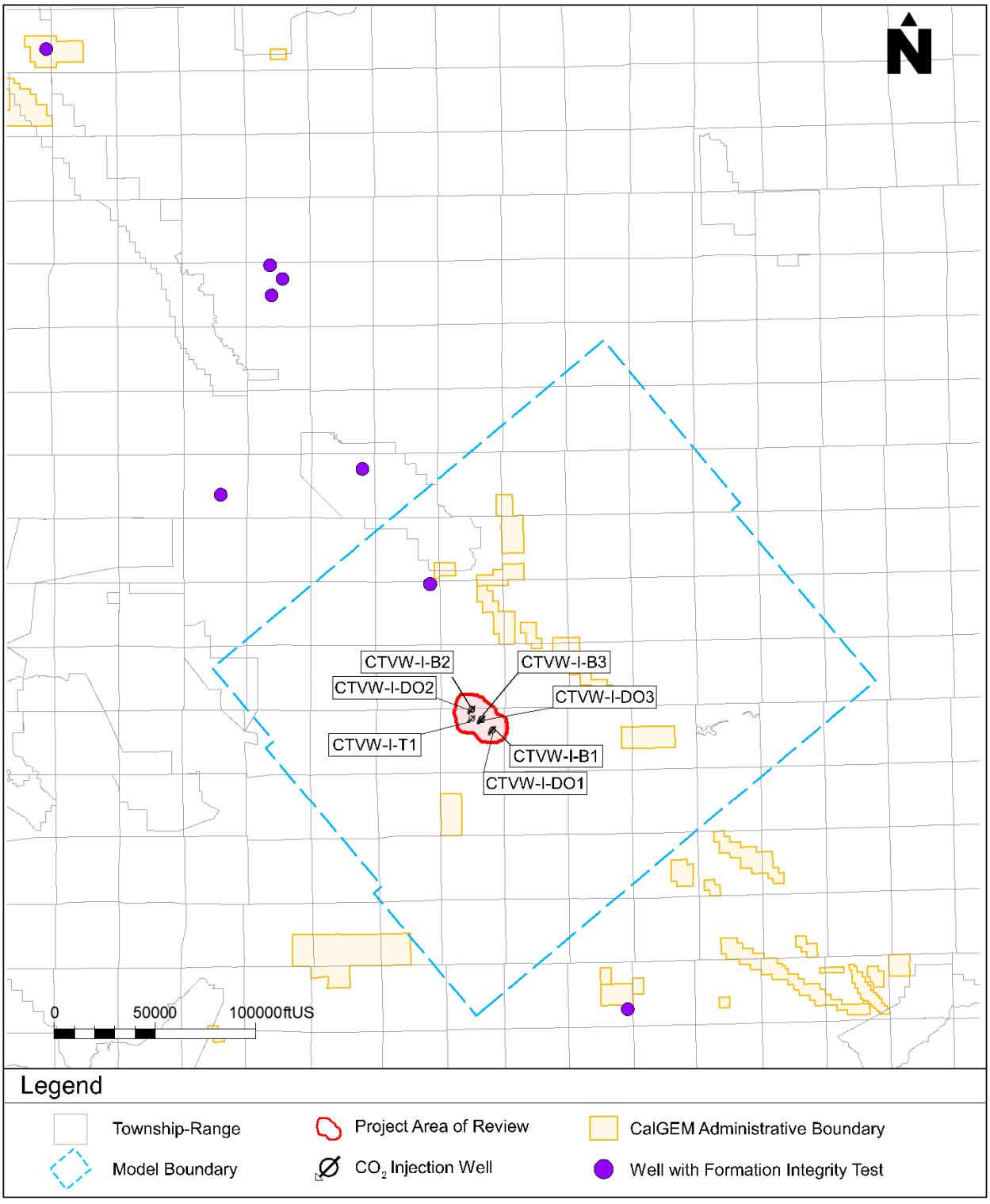

Figure 2.5-5. Map showing the location of wells with formation integrity tests (FIT).

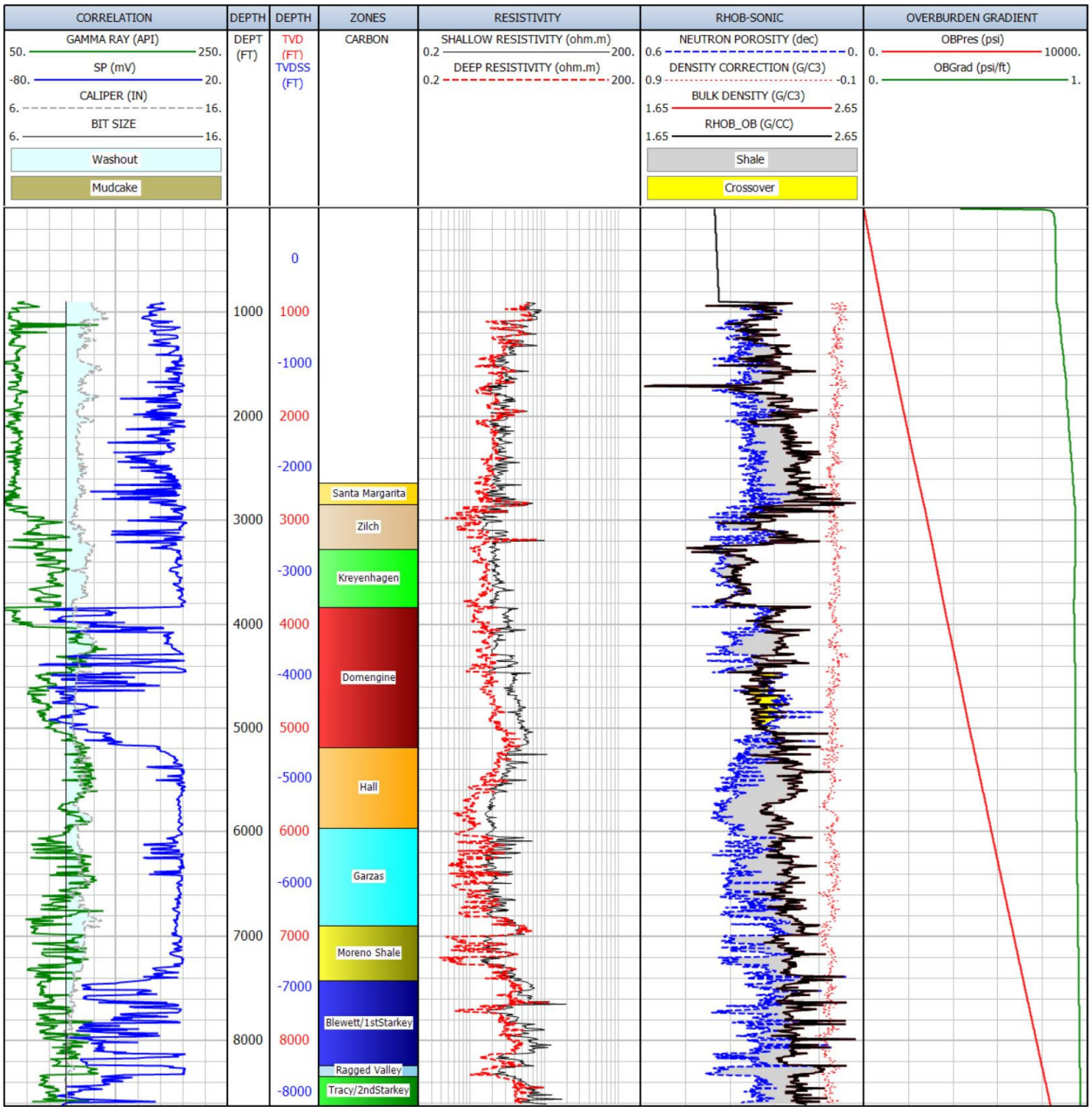

Figure 2.5-6. Overburden gradient calculation for the Hammonds_Ranch_Inc_1 (04019212290000). Track 1: Correlation logs and caliper log. Track 2: Measured depth. Track 3: Vertical depth and vertical subsea depth. Track 4: Zones. Track 5: Resistivity. Track 6: Density, neutron, and compressional sonic logs. The black curve shows the merged density curve with the shallow density trend as determined from nearby shallow density logs that was used for the overburden calculation. Track 7: Overburden pressure (red) and overburden gradient (green).

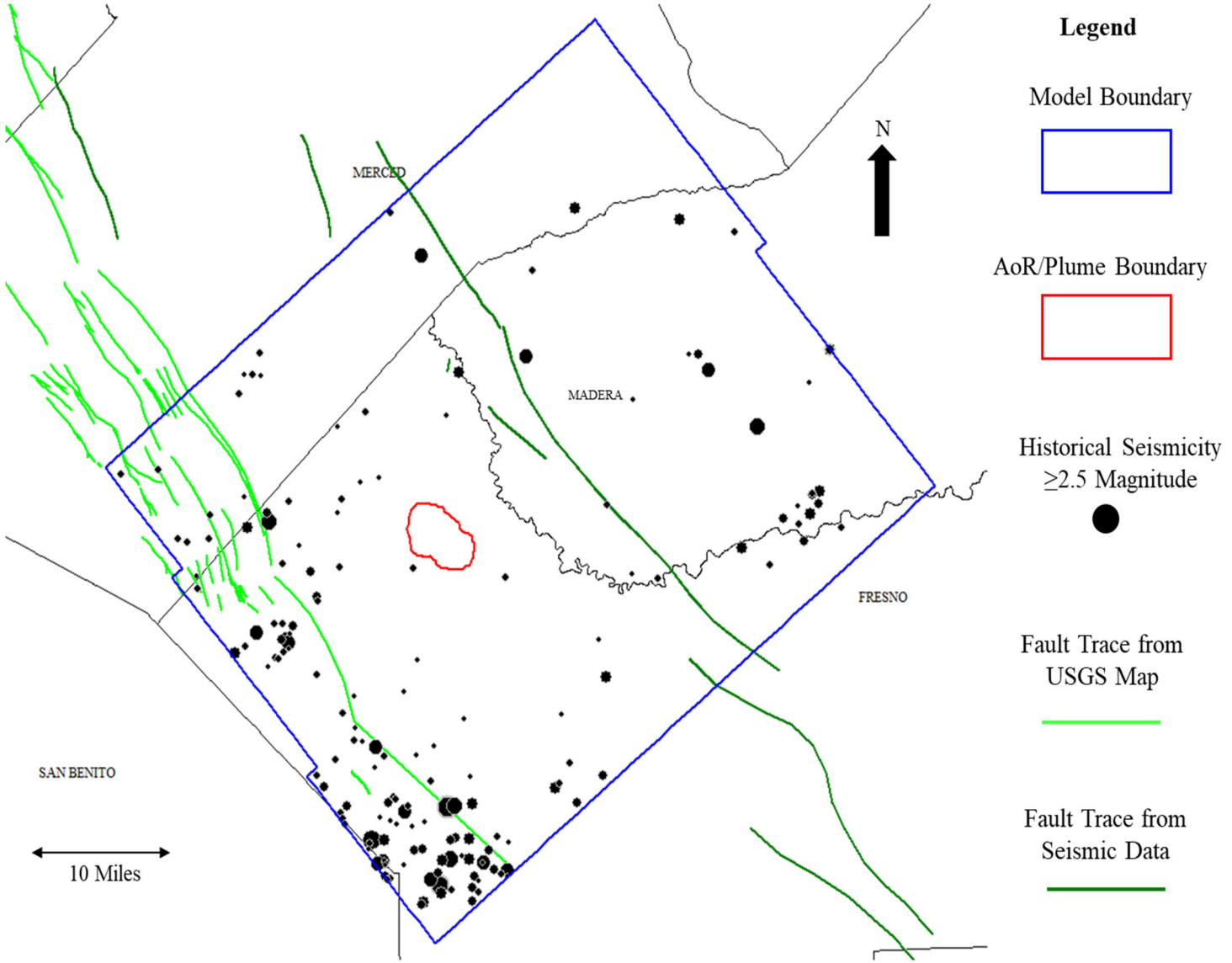

Figure 2.6-1. Historical earthquakes from the USGS catalog tool within the model boundary with magnitudes greater than or equal to 2.5. Events are sized by magnitude ranging from 2.5 to 4.84

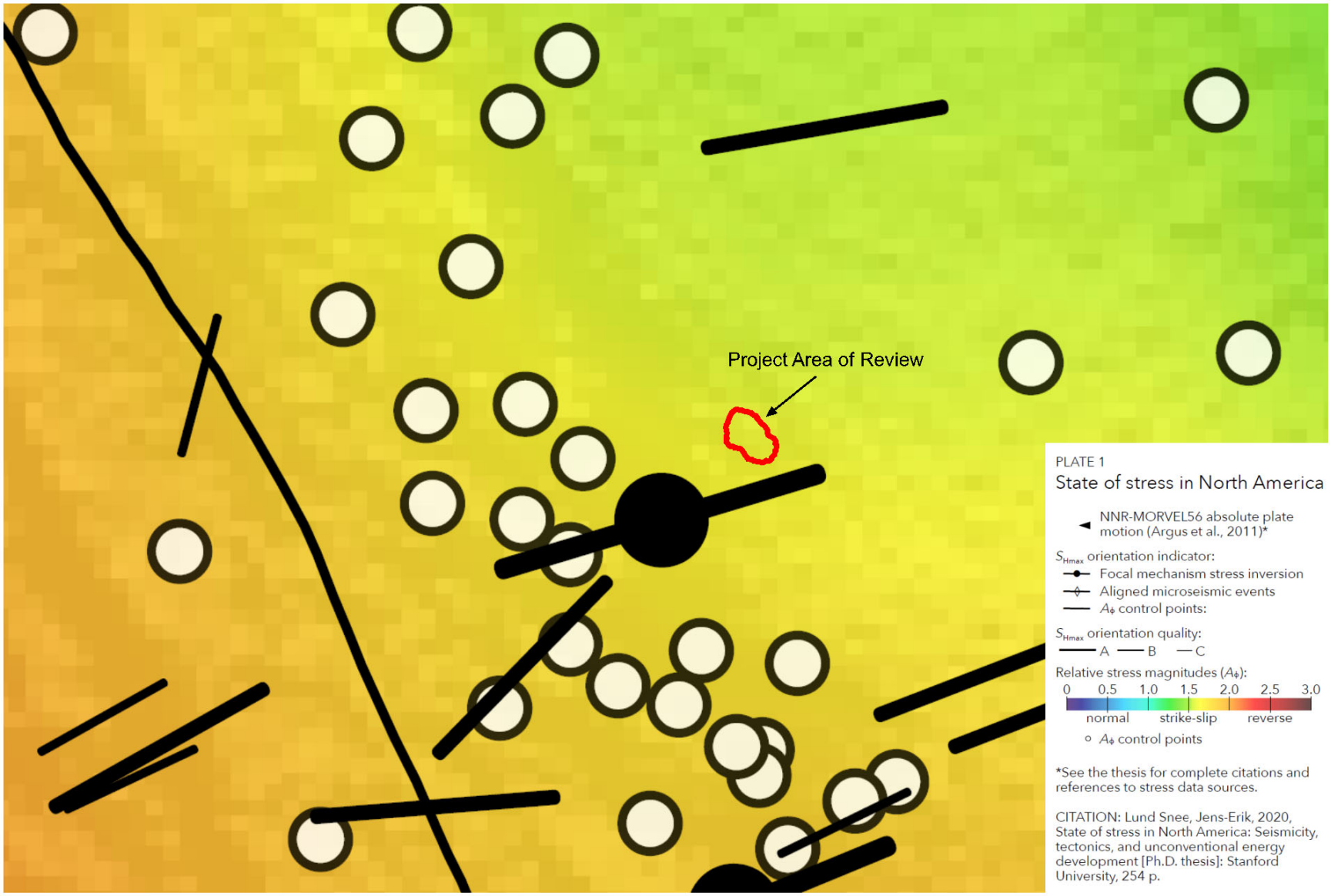

Figure 2.6-2. Image modified from Lundstern (2020) showing relative stress magnitudes across California.

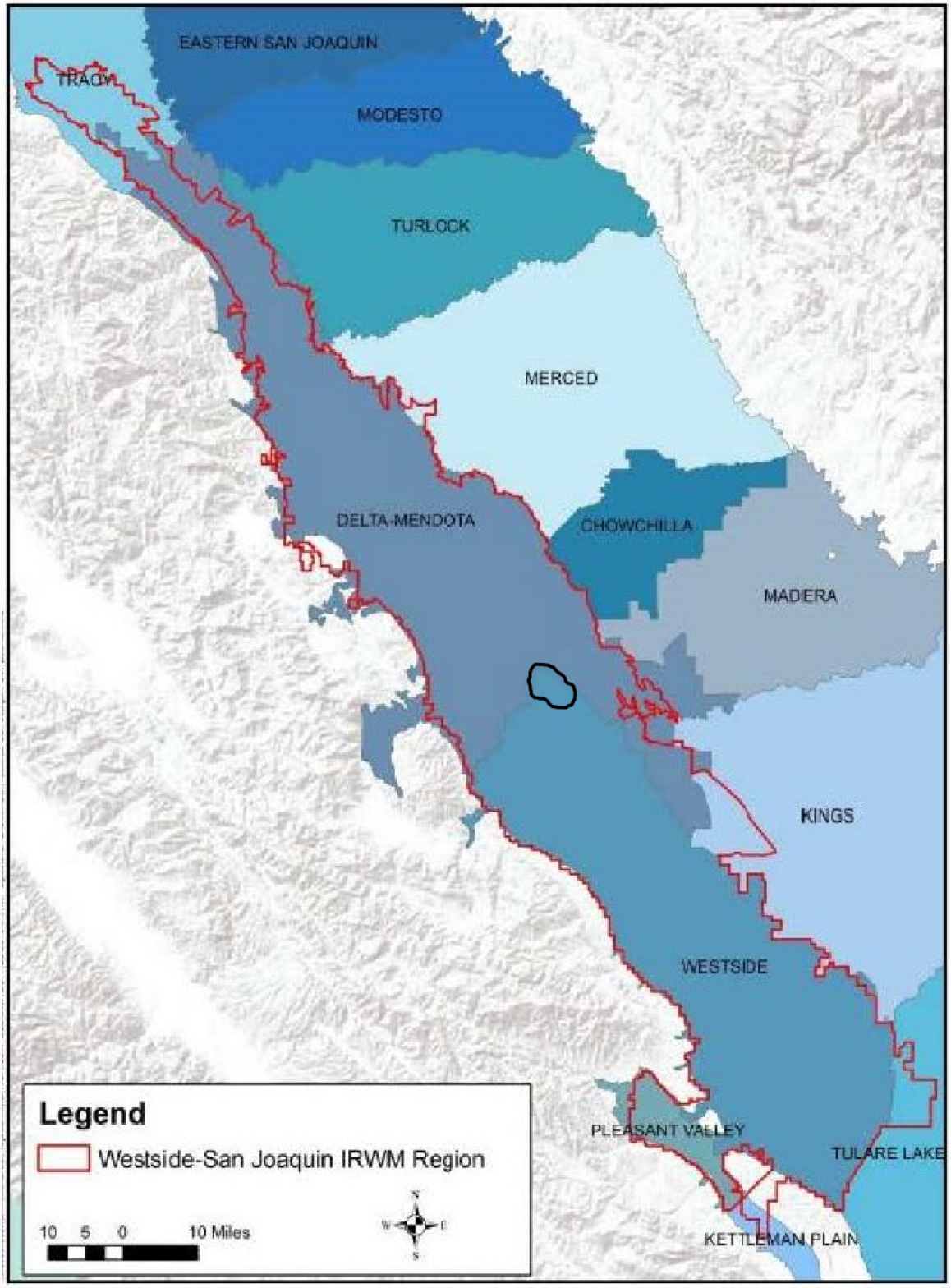

Figure 2.7-1. Map of the project AoR (black boundary) and groundwater subbasins. IRWM = Integrated Regional Water Management. Source: Luhdorff & Scalmanini, 2022.

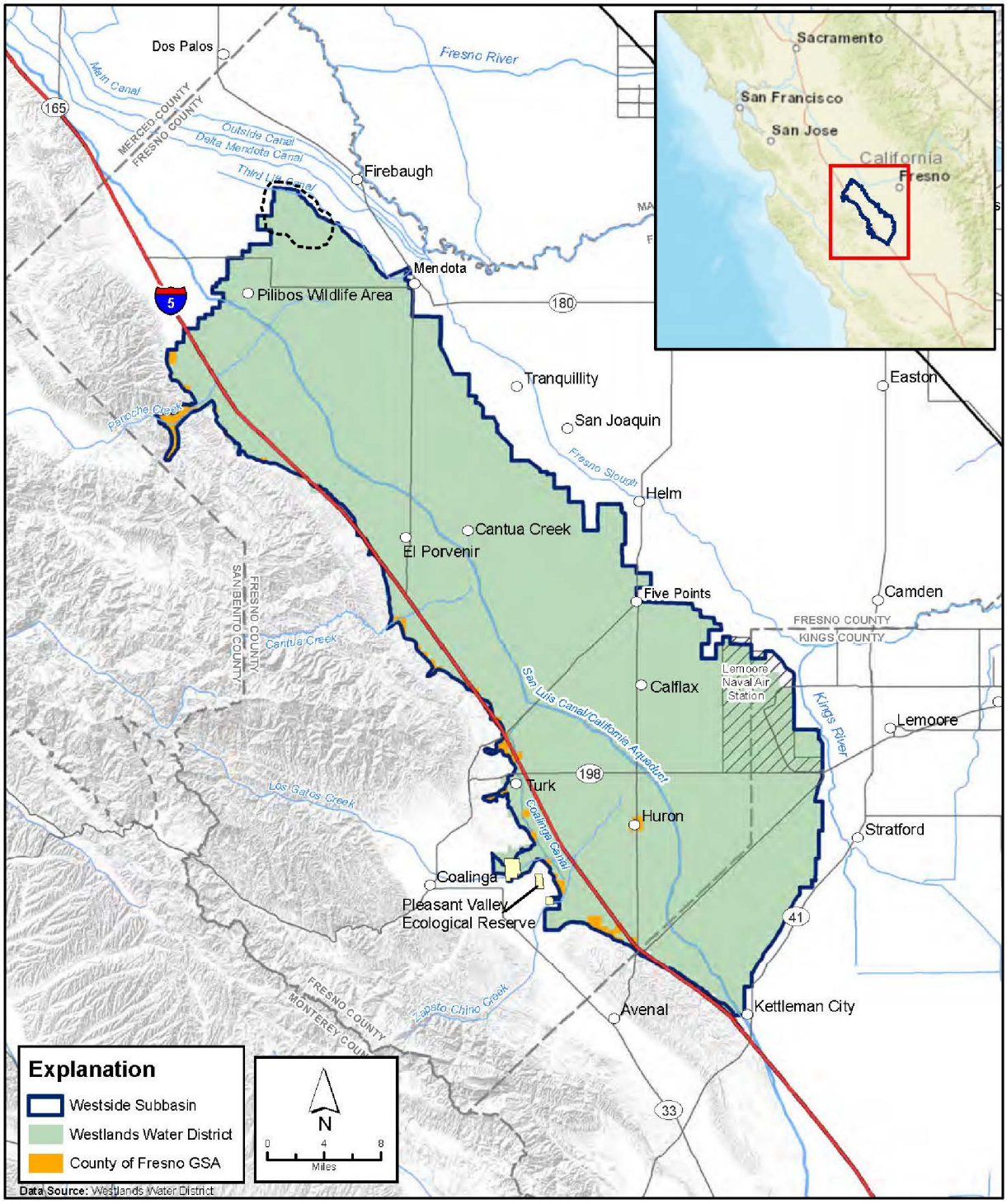

Figure 2.7-2. Map of the project AoR (black dashed boundary) and Westside Subbasin. Source: Luhdorff & Scalmanini, 2022.

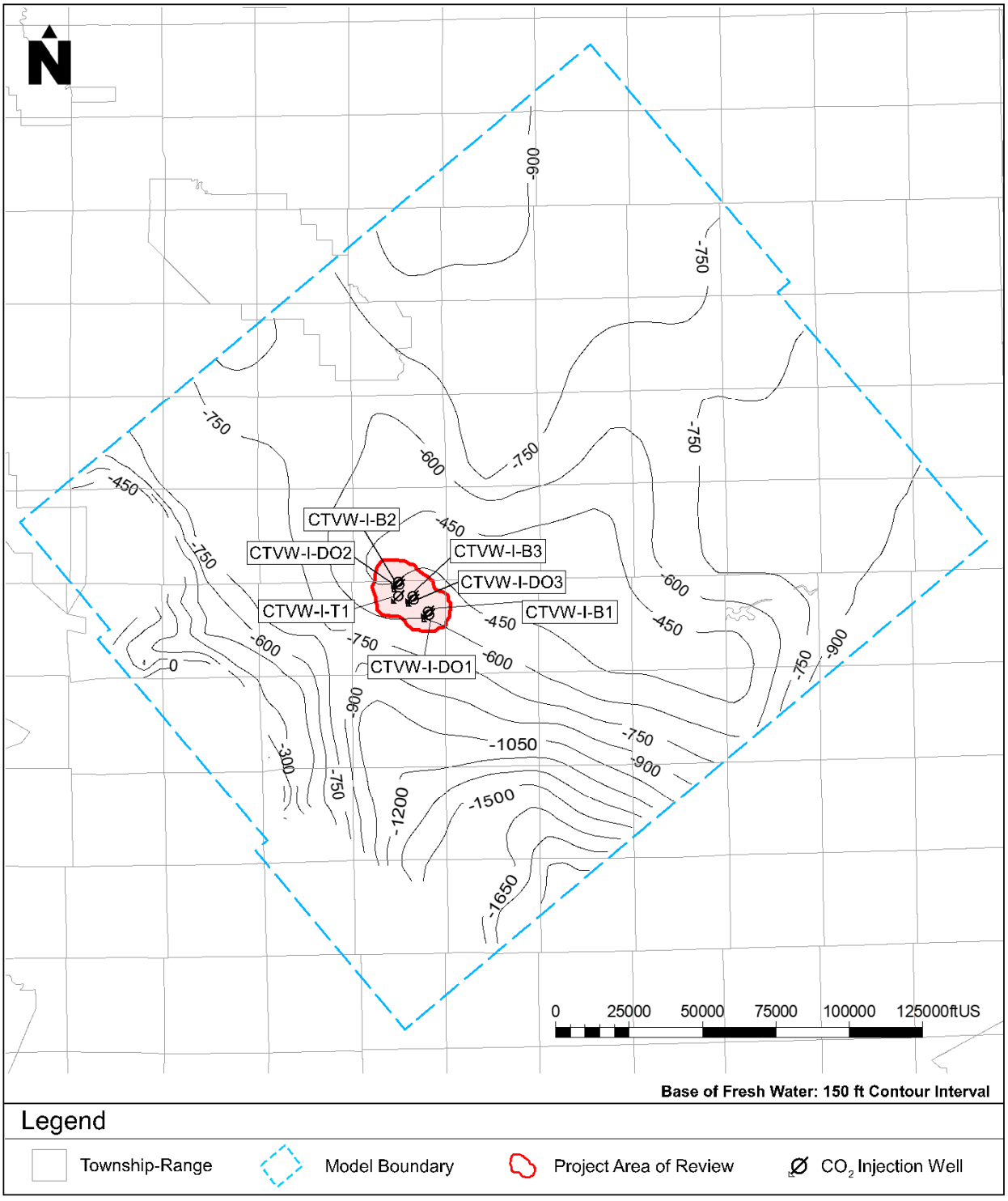

Figure 2.7-3. Base of fresh water map, SSTVD (Kang, 2020).

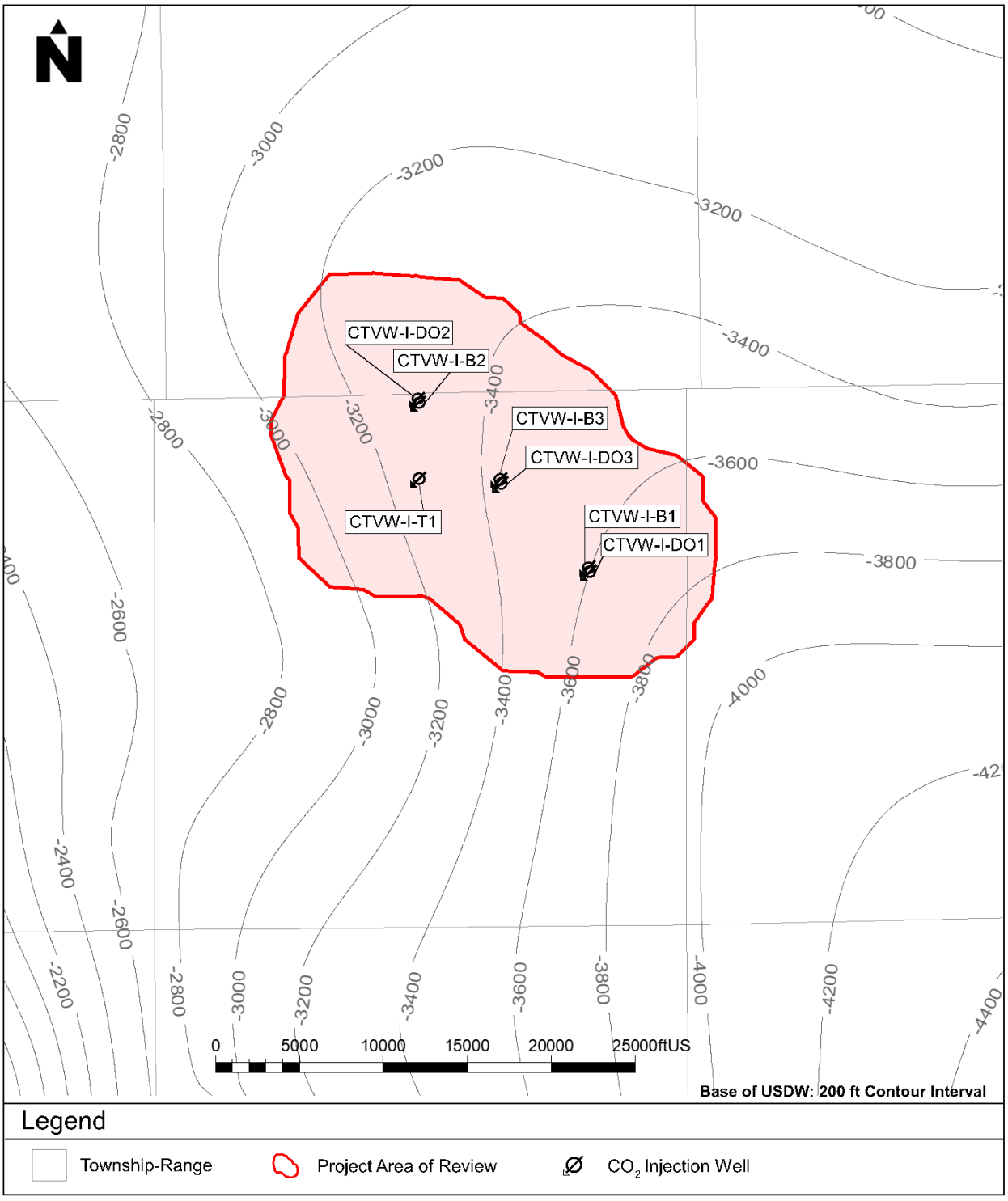

Figure 2.7-4(a). Depth to lower-most USDW (base of Santa Margarita Sandstone), SSTVD

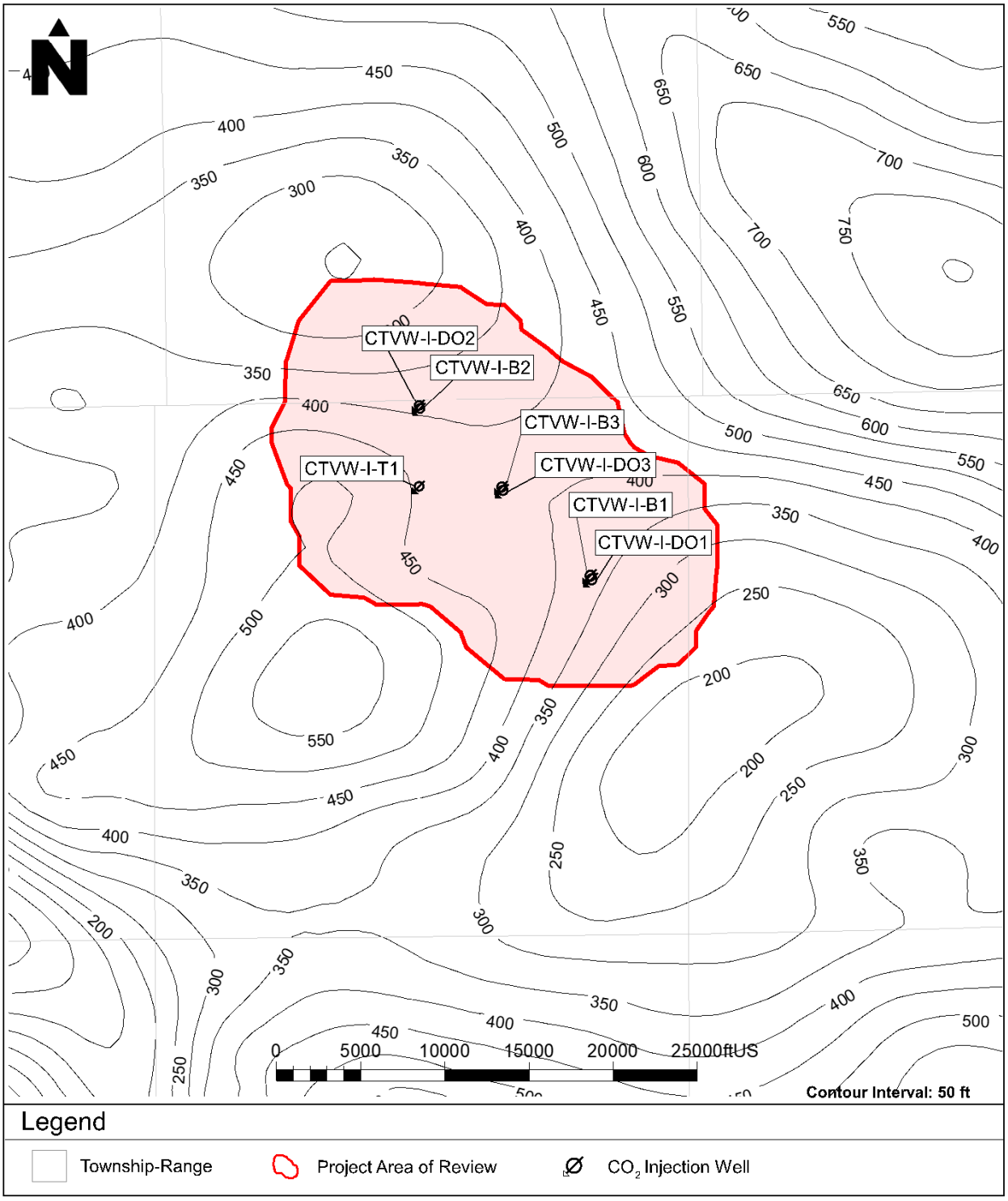

Figure 2.7-4(b). Thickness between the base of the lowermost USDW and the Domengine.

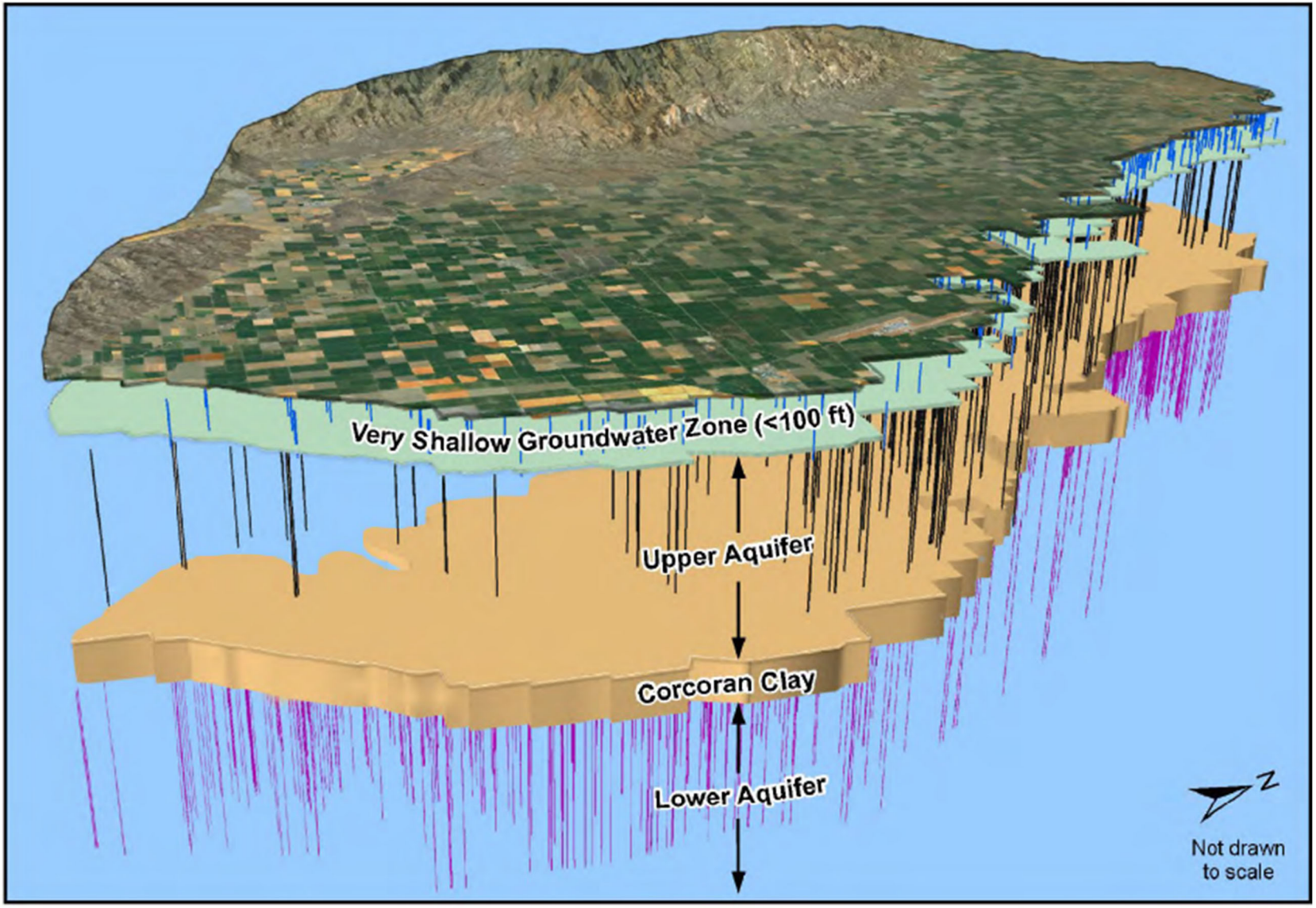

Figure 2.7-5. Westside Subbasin Hydrogeologic Conceptual Model. Source: Luhdorff & Scalmanini, 2022.

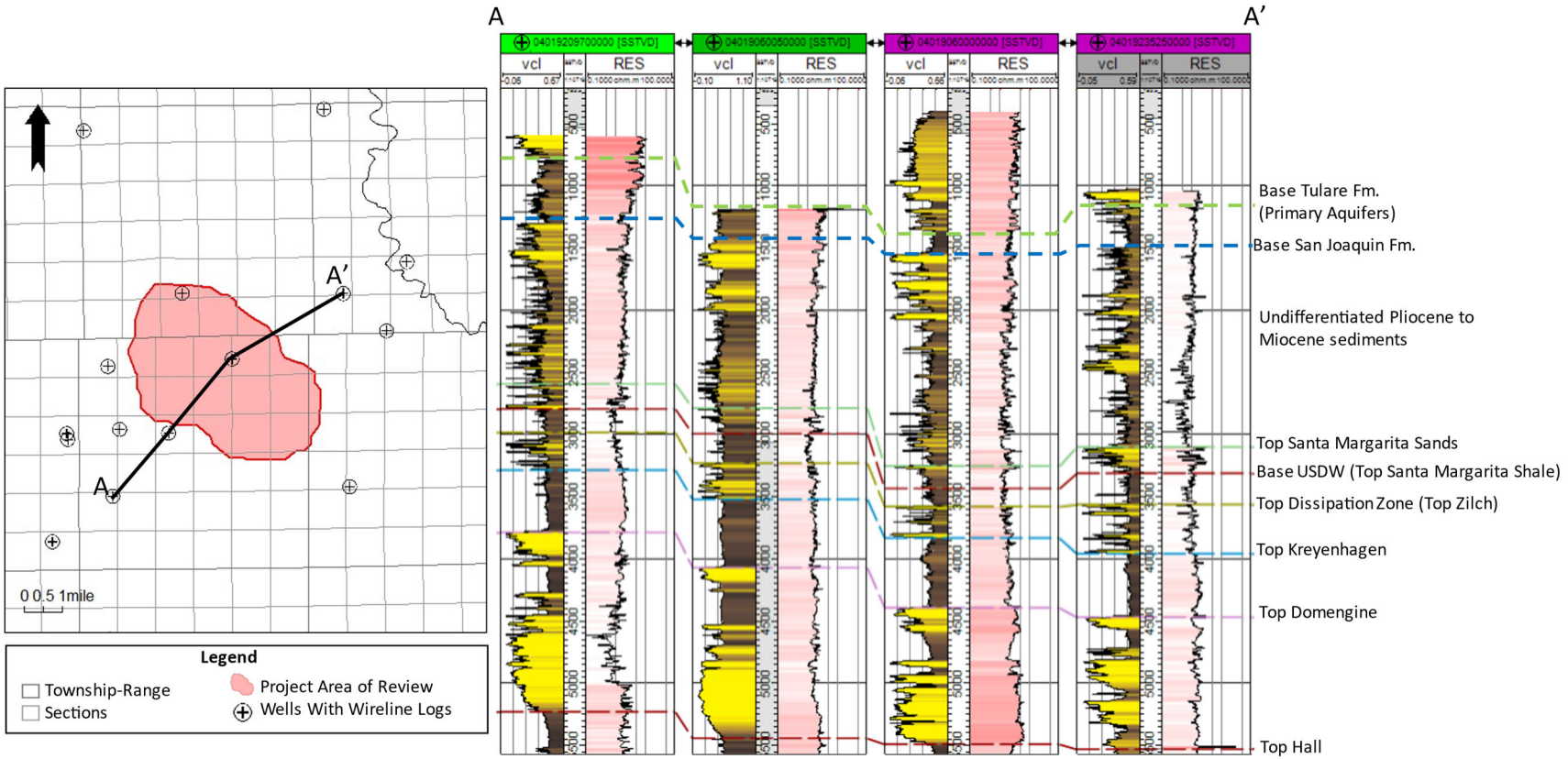

Figure 2.7-6. Cross section of shallow stratigraphy in the project area showing formations containing USDWs.

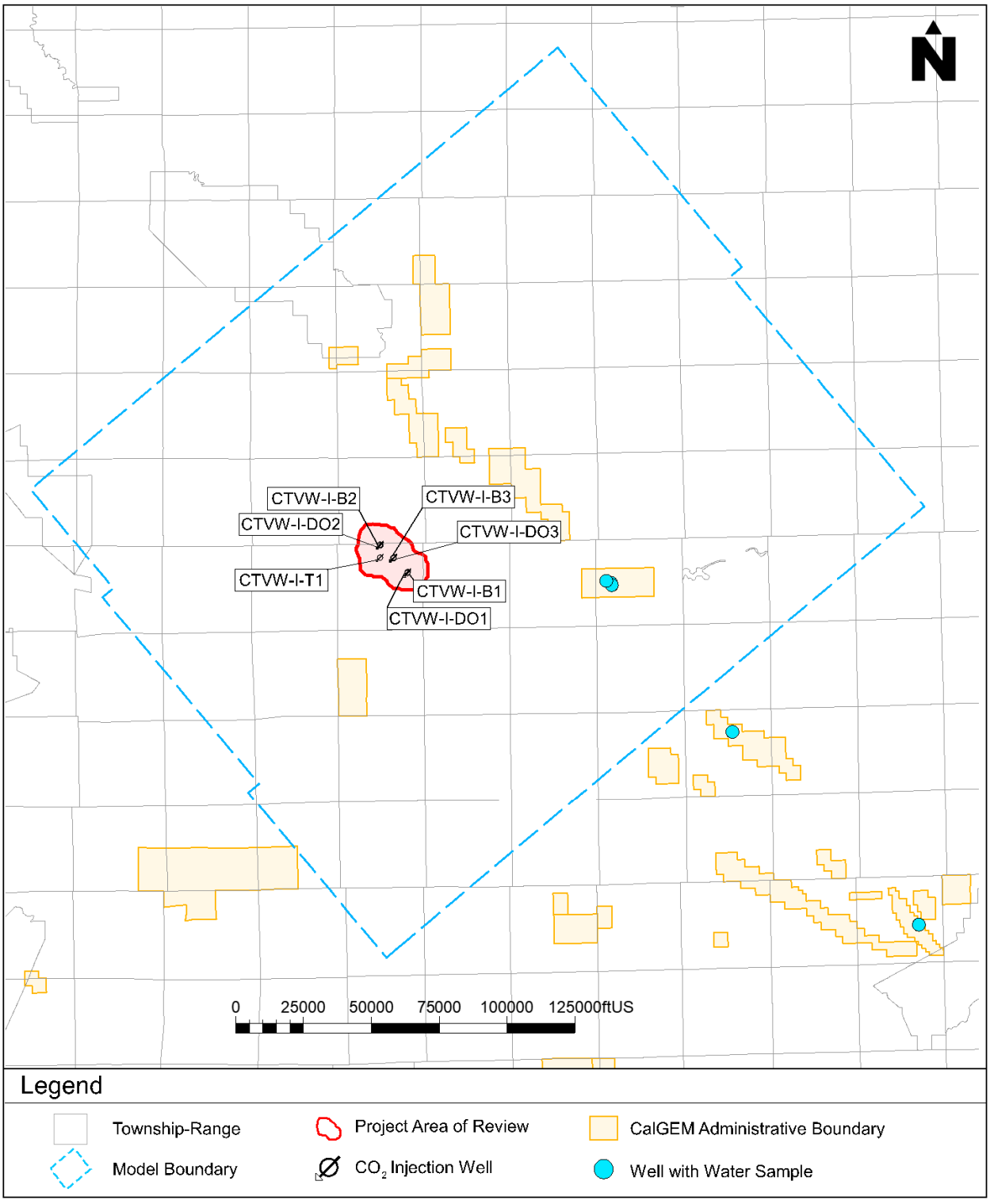

Figure 2.8-1. Map of wells with water samples

ZALCO LABORATORIES, INC.
Analytical & Consulting Services

RECEIVED
FEB 15 1983

BLACKHAWK RESOURCES
STAR ROUTE 4 BOX 6840
BAKERSFIELD CA. 93306
% JON MARSELLOS

DIVISION OF OIL & GAS
COALINGA

LABORATORY NO : 14991
DATE RECEIVED : 2/9/84
DATE REPORTED : 2/10/84

SAMPLE DESCRIPTION : BLACKHAWK NOBLE LEASE W1-1 FORMATION H20

GEOCHEMICAL WATER ANALYSIS

CONSTITUENTS	MG/L	MEQ/L	REACTING PERCENT
CALCIUM, CA	1650.00	82.33	5.85
MAGNESIUM, MG	560.00	46.05	3.27
SODIUM, NA	13129.92	570.94	40.56
POTASSIUM, K	98.00	2.50	0.17
IRON, FE (TOTAL)	34.00	1.82	0.12
CHLORIDE, CL	24750.00	697.67	49.57
SULFATE, S04	57.00	1.18	0.08
SULFIDE, S	0.00		
BICARBONATE, HC03	293.00	4.80	0.34
CARBONATE, C03	0.00	0.00	0.00
HYDROXIDE	0.00	0.00	0.00
TOTALS (SUM)	40422.99	1407.32	100.00
BORON	27.90		
TOTAL DIS SOLIDS (GRAV)	41835.00		
TOTAL HARDNESS AS CAC03	6485.93		
SODIUM CHLORIDE, TOTAL	39362.28		

PH	7.22	PRIMARY SALINITY	81.13
SPECIFIC GRAVITY @ 60 F	1.03	SECONDARY SALINITY	18.17
		TOTAL SALINITY	99.31
ELECTRICAL CONDUCTIVITY, (E.C., MMHO/CM)	62.54	PRIMARY ALKALINITY	0.00
		SECONDARY ALKALINITY	0.68
RESISTIVITY @ 25 C (OHM-METERS)	0.159	TOTAL ALKALINITY	0.68
		LANGELIER SCALE INDEX	1.25

JIM ETHERTON
LABORATORY DIRECTOR

COPY: HALLIBURTON SERVICES

4309 Armour Avenue Bakersfield, California 93308
(805) 395-0539

Figure 2.8-2. Water geochemistry for the Noble_WI_1 (04019209310000) well.

ZALCO LABORATORIES, INC.
Analytical & Consulting Services
4309 Armour Avenue
Bakersfield, California 93308
(805) 395-0539
FAX (805) 395-3069

RECEIVED
JUL 13 1995
DIVISION OF OIL & GAS
COALINGA

Texaco Exploration & Producing, Inc.
3646 W. Reward Road
McKittrick, CA 93251

Laboratory No: 44289-3
Date Received: 6-15-95
Date Reported: 6-21-95

Attention: Kalon Degenhardt

Sample Identification: Gill Ranch Lease, 18X-17 Well Eocene
Sampled by Frank Jimenez on 6-8-95

GEOCHEMICAL ANALYSIS

pH	7.2	Specific Gravity @ 60 F	1.023
Electrical Conductivity, (millimhos/cm @ 25 C)	45.75	Resistivity, (ohm meters @ 25 C)	0.22

Constituents	mg/l	meq/l	Reacting Per Cent
Calcium, Ca	1500	74.85	7.29
Magnesium, Mg	310	25.49	2.48
Sodium, Na (calculated)	9400	410	39.93
Potassium, K	110	2.81	0.27
Iron, Fe (dissolved)	3.8	0.2	0.02
Alkalinity as:			
Hydroxide, OH	0	0	0
Carbonate, CO3	0	0	0
Bicarbonate, HCO3	190	3.06	0.3
Chloride, Cl	18100	510.22	49.69
Sulfate, SO4	< 5.0	0.07	0.01
Sulfide, S	< 5.0	0	0
Totals (Sum)	29500	1026.7	100
Boron, B	28		
Total Dissolved Solids, (Grav)	31200		
Calculated Hardness, CaCO3	5000		
Total Alkalinity, CaCO3	150	Primary Salinity	80.4
Sodium Chloride, (total)	28400	Secondary Salinity	19
		Total Salinity	99.4
Cation/Anion Balance, %	-1.15		
Sodium, Na (determined), mg/l	8900	Primary Alkalinity	0
Langelier Scale Index	1.18	Secondary Alkalinity	0.54
Stiff/Davis Stability Index	0.06	Total Alkalinity	0.54

Jim Etherton
Laboratory Director

Figure 2.8-3. Water geochemistry for the Gill_Ranch_18X-17 (04039200560000) well.

Page 3

WELL NAME LAWTON NO. 1 COUNTY/STATE

AFE NO. PROSPECT NAME PROSPECT NO.:

PROJECTED TD: OBJECTIVE:

HOC INTEREST: WI: BCP ACP:

NRI: BPO: APO:

RIG NAME AND NO.:

DATE	DAILY PROGRESS REPORT
	REGION
1/31	SITP 50. IFL 5600' from surface. Recovered 2 BO + 5 BFW on first run. Released packer & POOH. Set RBP @ 7900'. Perforated 7855'-58' w/2 hpf (7 holes). TIH w/tubing & packer to 7775'. RU swab & recovered 24 BLW w/5% oil cut & 5% sand. SDFN. FFL @ 4000' from surface. DCC $9,115 CCC $336,056
2/1	SITP 350#. IFL 1300' from surface. Recovered 3 bbls of free oil on first swab. Swabbed 3 hrs & recovered 21 BLW + 5 BFW w/20-25% oil cut. FFL 2900' from surface. Shut down 1 hr & fluid rose from 2900'-1900'. Released packer & TIH to 7890'. No fill. POOH. SDFN. Water analysis from Domogene (7910'14'): PH 7.3, Specific gravity 1.022, Chlorides 13,116, Sulfates 750, Calcium 1140, Magnesium 120, Bicarbonates 87, Iron 9. Water analysis from Courtney (7855'-58'): PH 7.95, Specific gravity 1.026, Chlorides 11,699, Sulfates 92, Calcium 512, Magnesium 236, Bicarbonates 295, Iron 1. DCC $3,615 CCC $339,671
2/2	TIH w/tubing, rods & pump. Clamped well off. Built pad for pumping unit. Setting pumping unit. DCC $68,800 CCC $408,471
2/3	Finished setting pumping unit. Hung well on. DCC $3,950 CCC $412,421
2/4	Pumped 14 BO + 177 BLW (28 BLTR). CCC $412,421
2/5	Well sanded up. WO pulling unit. CCC $412,421
2/6	WO pulling unit. Cannot road units in California on weekends. CCC $412,421
2/7	MIRU. Unseated pump & circulated tubing. POOH w/rod & pump. Released TA & tagged fill @ 7834'. Pulled 20 stands. SDFN. DCC $3,115 CCC $415,536

HOC-1012

Figure 2.8-4. Drilling history from the Lawton_1-23 (04019219800000) well showing the partial water geochemistry for the Domengine Formation on February 1, 1984.

ZALCO LABORATORIES, INC.
Analytical & Consulting Services
4309 Armour Avenue
Bakersfield, California 93308
(805) 395-0539
FAX (805) 395-3069

Texaco Exploration & Producing, Inc.
3646 W. Reward Road
McKittrick, CA 93251

Laboratory No: 44289-4
Date Received: 6-15-95
Date Reported: 6-21-95

Attention: Kalon Degenhardt

RECEIVED
JUN 13 1995
DIVISION OF OIL & GAS
COALINGA

Sample Identification: Gill Ranch Lease, 12-20 Well Upper Cretaceous
Sampled by Frank Jimenez on 6-8-95

GEOCHEMICAL ANALYSIS

pH	7.4	Specific Gravity @ 60 F	1.015
Electrical Conductivity, (millimhos/cm @ 25 C)	32.27	Resistivity, (ohm meters @ 25 C)	0.31

Constituents	mg/l	meq/l	Reacting Per Cent
Calcium, Ca	400	19.96	2.94
Magnesium, Mg	67	5.51	0.81
Sodium, Na (calculated)	7200	312.56	46.11
Potassium, K	35	0.9	0.13
Iron, Fe (dissolved)	0.11	0.01	0
Alkalinity as:			
Hydroxide, OH	0	0	0
Carbonate, CO3	0	0	0
Bicarbonate, HCO3	140	2.25	0.33
Chloride, Cl	11900	336.58	49.65
Sulfate, SO4	5.5	0.11	0.02
Sulfide, S	< 5.0	0	0
Totals (Sum)	19700	677.88	100
Boron, B	58		
Total Dissolved Solids, (Grav)	20700		
Calculated Hardness, CaCO3	1300		
Total Alkalinity, CaCO3	110	Primary Salinity	92.48
Sodium Chloride, (total)	19400	Secondary Salinity	6.86
		Total Salinity	99.34
Cation/Anion Balance, %	-0.94		
Sodium, Na (determined), mg/l	6900	Primary Alkalinity	0
Langelier Scale Index	0.68	Secondary Alkalinity	0.64
Stiff/Davis Stability Index	-0.23	Total Alkalinity	0.64

Jim Etherton
Laboratory Director

Figure 2.8-5. Water geochemistry for the Gill_Ranch_12-20 (04039200570000) well.

ZALCO LABORATORIES, INC.
Analytical & Consulting Services
4309 Armour Avenue
Bakersfield, California 93308
(805) 395-0539
FAX (805) 395-3069

Texaco Exploration & Producing, Inc.
3646 W. Reward Road
McKittrick, CA 93251

Laboratory No: 44289-1
Date Received: 6-15-95
Date Reported: 6-21-95

Attention: Kalon Degenhardt

Sample Identification: Gill Ranch Lease, A-3 Well 2nd Panoche
Sampled by Frank Jimenez on 6-8-95

RECEIVED
JUN 13 1995
DIVISION OF OIL & GAS
COALINGA

GEOCHEMICAL ANALYSIS

pH	7.5	Specific Gravity @ 60 F	1.015
Electrical Conductivity, (millimhos/cm @ 25 C)	32.82	Resistivity, (ohm meters @ 25 C)	0.31

Constituents	mg/l	meq/l	Reacting Per Cent
Calcium, Ca	460	22.95	3.28
Magnesium, Mg	29	2.39	0.34
Sodium, Na (calculated)	7450	323.92	46.25
Potassium, K	35	0.9	0.13
Iron, Fe (dissolved)	0.46	0.02	0
Alkalinity as:			
Hydroxide, OH	0	0	0
Carbonate, CO3	0	0	0
Bicarbonate, HCO3	110	1.74	0.25
Chloride, Cl	12400	348.13	49.71
Sulfate, SO4	14	0.3	0.04
Sulfide, S	< 5.0	0	0
Totals (Sum)	20400	700.35	100
Boron, B	72		
Total Dissolved Solids, (Grav)	21100		
Calculated Hardness, CaCO3	1300		
Total Alkalinity, CaCO3	87	Primary Salinity	92.76
Sodium Chloride, (total)	20000	Secondary Salinity	6.74
		Total Salinity	99.5
Cation/Anion Balance, %	-1.11		
Sodium, Na (determined), mg/l	7100	Primary Alkalinity	0
Langelier Scale Index	0.73	Secondary Alkalinity	0.5
Stiff/Davis Stability Index	-0.21	Total Alkalinity	0.5

Jim Etherton
Laboratory Director

Figure 2.8-6. Water geochemistry for the Gill_Ranch_A-3 (04039200510000) well.

Tables

Table 2.2-1. Reference List of Water Supply Wells in the AoR

Well Number	Well ID	Dataset	Type
1	NO3_1027003	UCD_NO3	NA
2	NO3_1026972	UCD_NO3	NA
3	NO3_1026979	UCD_NO3	NA
4	NO3_1026990	UCD_NO3	NA
5	NO3_1026977	UCD_NO3	NA
6	NO3_1026973	UCD_NO3	NA
7	NO3_1026985	UCD_NO3	NA
8	NO3_1026969	UCD_NO3	NA
9	USGS-365018120312602	USGS_NWIS	Monitoring
10	USGS-365018120312610	USGS_NWIS	Monitoring
11	USGS-365018120312607	USGS_NWIS	Monitoring
12	USGS-365018120312643	USGS_NWIS	Monitoring
13	USGS-365018120312628	USGS_NWIS	Monitoring
14	USGS-365018120312615	USGS_NWIS	Monitoring
15	USGS-365018120312630	USGS_NWIS	Monitoring
16	USGS-365018120312611	USGS_NWIS	Monitoring
17	USGS-365018120312622	USGS_NWIS	Monitoring
18	NO3_1027000	UCD_NO3	NA
19	NO3_1026975	UCD_NO3	NA
20	NO3_1026970	UCD_NO3	NA
21	NO3_1026989	UCD_NO3	NA
22	NO3_1026967	UCD_NO3	NA
23	NO3_1026999	UCD_NO3	NA
24	NO3_1026986	UCD_NO3	NA
25	USGS-365018120312637	USGS_NWIS	Monitoring
26	USGS-365018120312640	USGS_NWIS	Monitoring
27	USGS-365018120312632	USGS_NWIS	Monitoring
28	USGS-365018120312642	USGS_NWIS	Monitoring
29	USGS-365018120312624	USGS_NWIS	Water Supply, Other
30	NO3_1027002	UCD_NO3	NA
31	NO3_1026993	UCD_NO3	NA
32	NO3_1026997	UCD_NO3	NA
33	USGS-365018120312616	USGS_NWIS	Monitoring
34	USGS-365018120312618	USGS_NWIS	Monitoring
35	USGS-365018120312638	USGS_NWIS	Monitoring
36	USGS-365018120312601	USGS_NWIS	Water Supply, Other
37	NO3_1026974	UCD_NO3	NA
38	NO3_1026992	UCD_NO3	NA
39	NO3_1026964	UCD_NO3	NA
40	USGS-365018120312644	USGS_NWIS	Monitoring
41	USGS-365018120312604	USGS_NWIS	Monitoring
42	USGS-365018120312614	USGS_NWIS	Monitoring
43	USGS-365018120312629	USGS_NWIS	Monitoring
44	NO3_1026995	UCD_NO3	NA
45	NO3_1026996	UCD_NO3	NA
46	NO3_1026981	UCD_NO3	NA
47	NO3_1027001	UCD_NO3	NA
48	NO3_1026998	UCD_NO3	NA
49	USGS-365018120312609	USGS_NWIS	Monitoring
50	USGS-365018120312620	USGS_NWIS	Monitoring
51	USGS-365018120312612	USGS_NWIS	Monitoring
52	NO3_1026980	UCD_NO3	NA
53	NO3_1026982	UCD_NO3	NA
54	NO3_1026983	UCD_NO3	NA
55	NO3_1026976	UCD_NO3	NA
56	NO3_1026978	UCD_NO3	NA
57	USGS-365018120312633	USGS_NWIS	Monitoring
58	USGS-365018120312613	USGS_NWIS	Monitoring
59	USGS-365018120312636	USGS_NWIS	Monitoring
60	USGS-365018120312626	USGS_NWIS	Water Supply, Other
61	NO3_1026971	UCD_NO3	NA
62	NO3_1026966	UCD_NO3	NA
63	NO3_1026994	UCD_NO3	NA
64	NO3_1026987	UCD_NO3	NA
65	NO3_1026991	UCD_NO3	NA
66	USGS-365018120312619	USGS_NWIS	Monitoring

Well Number	Well ID	Dataset	Type
67	USGS-365018120312621	USGS_NWIS	Monitoring
68	USGS-365018120312631	USGS_NWIS	Monitoring
69	USGS-365018120312641	USGS_NWIS	Monitoring
70	USGS-365018120312605	USGS_NWIS	Monitoring
71	USGS-365018120312617	USGS_NWIS	Monitoring
72	USGS-365018120312635	USGS_NWIS	Monitoring
73	USGS-365018120312625	USGS_NWIS	Water Supply, Other
74	NO3_1026968	UCD_NO3	NA
75	USGS-365018120312606	USGS_NWIS	Monitoring
76	USGS-365018120312645	USGS_NWIS	Monitoring
77	USGS-365018120312634	USGS_NWIS	Monitoring
78	USGS-365018120312608	USGS_NWIS	Monitoring
79	USGS-365018120312623	USGS_NWIS	Water Supply, Other
80	USGS-365012120334401	USGS_NWIS	NA
81	USGS-364832120315901	USGS_NWIS	Water Supply, Other
82	USGS-364904120335301	USGS_NWIS	Water Supply, Other
83	NO3_1010659	UCD_NO3	NA
84	USGS-364916120335401	USGS_NWIS	Monitoring
85	USGS-364827120331101	USGS_NWIS	Water Supply, Other
86	13S13E13N001M	DWR	Water Supply, Other
87	USGS-364826120314901	USGS_NWIS	Domestic
88	T10000010013-MW-5	WB_CLEANUP	Monitoring
89	T10000010013-MW-3	WB_CLEANUP	Monitoring
90	USGS-365103120334701	USGS_NWIS	Monitoring
91	USGS-365031120313001	USGS_NWIS	Water Supply, Other
92	13S14E18M001M	DWR	Water Supply, Other
93	12S13E33N002M	DWR	Water Supply, Other
94	13S13E10R001M	DWR	Water Supply, Other
95	13S13E13P001M	DWR	Water Supply, Other
96	USGS-365008120333201	USGS_NWIS	Water Supply, Other
97	NO3_1026963	UCD_NO3	NA
98	T10000010013-MW-4	WB_CLEANUP	Monitoring
99	USGS-364827120335601	USGS_NWIS	Monitoring
100	USGS-365016120320701	USGS_NWIS	Monitoring
101	93218	DPR	NA
102	USGS-364820120335401	USGS_NWIS	Water Supply, Other
103	13S14E07N001M	DWR	Water Supply, Other
104	12S13E33Q001M	DWR	Water Supply, Other
105	NO3_1027047	UCD_NO3	NA
106	USGS-365012120330501	USGS_NWIS	Monitoring
107	12S13E32A001M	DWR	Water Supply, Other
108	13S13E09Q001M	DWR	Water Supply, Other
109	T10000010013-MW-1	WB_CLEANUP	Monitoring
110	USGS-365012120332701	USGS_NWIS	Water Supply, Other
111	USGS-364734120314401	USGS_NWIS	Water Supply, Other
112	USGS-364914120304401	USGS_NWIS	Water Supply, Other
113	12S13E33N001M	DWR	Water Supply, Other
114	12S13E34P001M	DWR	Water Supply, Other
115	NO3_1026965	UCD_NO3	NA
116	USGS-365013120313301	USGS_NWIS	Monitoring
117	T10000010013-MW-2	WB_CLEANUP	Monitoring
118	13S13E09E003M	DWR	Water Supply, Other
119	USGS-364827120293001	USGS_NWIS	Water Supply, Other
120	WCR0041008	DWR	Unknown
121	WCR0271899	DWR	Unknown
122	WCR0036563	DWR	Unknown
123	WCR0074324	DWR	Unknown
124	WCR0175915	DWR	Unknown
125	WCR0268170	DWR	Water Supply Domestic
126	WCR0077615	DWR	Monitoring
127	WCR0050413	DWR	Unknown
128	WCR0205330	DWR	Monitoring
129	WCR0187767	DWR	Monitoring
130	WCR1990-014072	DWR	Monitoring
131	WCR0108804	DWR	Unknown
132	WCR0108842	DWR	Unknown
133	WCR0138945	DWR	Monitoring
134	WCR1990-014119	DWR	Monitoring

Well Number	Well ID	Dataset	Type
135	WCR0114894	DWR	Unknown
136	WCR0294599	DWR	Unknown

NA= Data are not available or not applicable

Table 2.2-2. Reference List of Oil and Gas Wells in the AoR

Well Number	API	Well Name	Status	Well Type
137	0401920522	Britton 1	Plugged	Dry Hole
138	0401906000	Hotchkiss 15-2	Plugged	Dry Hole

Table 2.4-1. Formation Mineralogy from X-Ray Diffraction (XRD) in Five Wells

UWI	Well	Zone	Depth (ft)	Quartz	Opal A	Opal CT	Feldspar	Plagioclase	K-Feldspar	Ankerite	Calcite	Dolomite	Rhodochrosite	Siderite	Pyrite	Barite	Kaolinite	Chlorite	Illite	Smectite	MXL I/S	Total Clay
0401925323	BRUM_846-15	Kreyenhagen	7581.1	18.5	NM	NM	NM	12.7	5.1	0.0	0.0	0.0	NM	0.0	5	NM	13.4	3.7	16	NM	26.3	59.1
0401925323	BRUM_846-15	Kreyenhagen	7587.1	21.8	NM	NM	NM	15.3	6.3	0.0	0.0	0	NM	0	5.9	NM	9.3	3.4	14.9	NM	23.1	50.7
0401925323	BRUM_846-15	Kreyenhagen	7590.1	17.0	NM	NM	NM	10.6	4.6	0.0	0.0	0	NM	0	7.7	NM	16.6	3.6	15.0	NM	24.8	60
0401925323	BRUM_846-15	Kreyenhagen	7608.2	19.0	NM	NM	NM	10.7	5.4	0.0	0.8	0	NM	0	7.1	NM	23.4	3.4	11.0	NM	19.2	57
0401925328	RIPPERDAN_544-13	Kreyenhagen	6011.35	19.1	0.0	5.5	NM	16.1	5.1	NM	4.6	1	NM	0	4.3	NM	2.3	2.1	21.2	NM	18.7	44.3
0401925328	RIPPERDAN_544-13	Kreyenhagen	6014.1	10.7	0.0	10.4	NM	13.1	4.5	NM	0.0	0.4	NM	0	5.5	NM	3	3	23.2	NM	26.3	55.5
0401925328	RIPPERDAN_544-13	Kreyenhagen	6023.75	23.2	0.0	3.9	NM	18.7	7.3	NM	0.3	0.7	NM	0	4	NM	2.9	1.8	14.9	NM	22.2	41.8
0401925328	RIPPERDAN_544-13	Kreyenhagen	6030.35	9.1	0.0	20.9	NM	11.7	4.8	NM	0.0	0	NM	0	4.6	NM	1.6	1.6	14.9	NM	30.9	49
0401925328	RIPPERDAN_544-13	Kreyenhagen	6036.1	29.1	0.0	6.1	NM	20.6	7.3	NM	0.0	1.2	NM	0	4.7	NM	2.1	1.1	11.2	NM	16.7	31.1
0401925328	RIPPERDAN_544-13	Kreyenhagen	6039.15	45.1	0.0	5.3	NM	20.1	9.9	NM	0	0	NM	1.3	5.9	NM	1.6	0.2	4.1	NM	6.5	12.4
0401925328	RIPPERDAN_544-13	Kreyenhagen	6048.10	20.6	0.0	3.1	NM	16.6	5.9	NM	0.0	0.8	NM	0	4.3	NM	8.2	1.1	15.4	NM	24.1	48.8
0401922538	NAPA_AVE_A1	Lathrop	8200.00	32.0	NM	NM	NM	35.0	22.0	NM	NM	NM	NM	NM	4.0	NM	2.5	0.8	2.7	0	1.1	7
0401922538	NAPA_AVE_A1	Lathrop	8612.00	36.0	NM	NM	NM	33.0	20.0	NM	NM	NM	NM	NM	2.0	NM	3.5	0.9	4.2	0	0.4	9
0401922538	NAPA_AVE_A1	Lathrop	8618.00	20.0	NM	NM	NM	16.0	12.0	3	25.0	NM	4	11	NM	NM	1.8	2.1	3.8	0	1.4	9
0401922538	NAPA_AVE_A1	Lathrop	8751.00	36.0	NM	NM	NM	33.0	20.0	NM	NM	NM	NM	NM	NM	1.0	3.4	0.7	3.9	0	2.0	10
0401922538	NAPA_AVE_A1	Lathrop	8208.00	15.0	NM	NM	NM	22.0	10.0	NM	1.0	NM	NM	NM	7.0	NM	7.7	6.3	27.0	0	4.1	45
0401922538	NAPA_AVE_A1	Lathrop	8222.00	19.0	NM	NM	NM	20.0	13.0	NM	NM	NM	7	NM	5.0	3.0	6.6	6.6	16.2	0	3.6	33
0406720514	Wilcox_20	Domengine	4304.00	42.9	NM	NM	NM	14.1	11.9	NM	0.0	0.0	NM	NM	5.8	NM	20.2	2.4	1.9	NM	0.8	25.3
0401921930	PACLAND_THREE_36-4	Zilch	5034.00	20-30	NM	NM	40-50	NM	NM	NM	0.0	0.0	NM	0.5-2	NM	NM	2-5	0.0	2-5	NM	10-20	NM
0401921930	PACLAND_THREE_36-4	Zilch	5039.00	25-35	NM	NM	50-60	NM	NM	NM	0.0	0.0	NM	0.5-2	NM	NM	0.5-2	0.0	2-5	NM	5-10	NM

NM = No measure

Table 2.4-2. Core Samples from Three Wells in the Monitoring Zone

Well	UWI	Formation	Depth (feet)	KA (mD)	PHIT (%)	SOC (%)	SWC (%)	GD (G/CC)
BOWLES_1	04039200340000	Zilch	2453	4.5	43.4	NM	NM	NM
BOWLES_1	04039200340000	Zilch	2457	4	40.8	NM	NM	NM
BOWLES_1	04039200340000	Zilch	2499	1320	36.3	NM	NM	NM
BOWLES_1	04039200340000	Zilch	2501	1990	26.1	NM	NM	NM
BOWLES_1	04039200340000	Zilch	2503	2410	32.1	NM	NM	NM
BOWLES_1	04039200340000	Zilch	2540	55	46	NM	NM	NM
BOWLES_1	04039200340000	Zilch	2546	40	41.4	NM	NM	NM
BOWLES_1	04039200340000	Zilch	2548	100	43.2	NM	NM	NM
BOWLES_1	04039200340000	Zilch	2565	6.5	34.5	NM	NM	NM
BOWLES_1	04039200340000	Zilch	2567	6	35.7	NM	NM	NM
BOWLES_1	04039200340000	Zilch	2581	12	37.9	NM	NM	NM
BOWLES_1	04039200340000	Zilch	2600	45	28.4	NM	NM	NM
BOWLES_1	04039200340000	Zilch	2613	50	30.1	NM	NM	NM
BOWLES_1	04039200340000	Zilch	2619	650	32.7	NM	NM	NM
BOWLES_1	04039200340000	Zilch	2724	15	43.3	NM	NM	NM
BOWLES_1	04039200340000	Zilch	2745	25	26.9	NM	NM	NM
NAPA_AVE_A1	04019225380000	Zilch	4027	10	28.7	0	89.9	2.55
NAPA_AVE_A1	04019225380000	Zilch	4179	151	29.5	0	81	2.61
NAPA_AVE_A1	04019225380000	Zilch	4590	464	30.3	0	81.5	2.6
NAPA_AVE_A1	04019225380000	Zilch	4603	322	30.3	0	82.9	2.64
RODUNER_1-32	04039200780000	Zilch	2794	0.8	28.5	0	99.4	2.67
RODUNER_1-32	04039200780000	Zilch	2822	10.2	31.9	0	99.2	2.68
RODUNER_1-32	04039200780000	Zilch	3101	46.8	31.9	0	94.6	2.65
RODUNER_1-32	04039200780000	Zilch	3110	661.7	29.2	0	95.8	2.65
RODUNER_1-32	04039200780000	Zilch	3116	183.9	29.5	0	99.6	2.65
RODUNER_1-32	04039200780000	Zilch	3120	114.7	41.8	0	80.6	2.41

Well	UWI	Formation	Depth (feet)	KA (mD)	PHIT (%)	SOC (%)	SWC (%)	GD (G/CC)
RODUNER_1-32	04039200780000	Zilch	3124	1033	33.5	0	99.4	2.67
RODUNER_1-32	04039200780000	Zilch	3142	236.4	28.7	0	89.2	2.64
RODUNER_1-32	04039200780000	Zilch	3156	779.3	33	0	98.5	2.68
RODUNER_1-32	04039200780000	Zilch	3160	292.4	28.9	0	99.6	2.67

NM = No measure

Table 2.4-3. Core Samples from Three Wells in the Confining Zone

Well	UWI	Formation	Depth (feet)	KA (mD)	PHIT (%)	SOC (%)	SWC (%)	GD (G/CC)
BRUM_846-15	04019253230000	Kreyenhagen	7575	4.57E-07	27.82521	0.0017236	93.90917	2.558103
BRUM_846-15	04019253230000	Kreyenhagen	7578	1.44E-07	27.13091	-0.000533	95.15664	2.601545
BRUM_846-15	04019253230000	Kreyenhagen	7581	2.14E-05	24.1123	-0.002861	85.15693	2.532091
BRUM_846-15	04019253230000	Kreyenhagen	7584	3.24E-06	22.4604	0.0021166	90.72861	2.532279
BRUM_846-15	04019253230000	Kreyenhagen	7587	1.27E-06	23.32498	0.0038271	92.24212	2.569717
BRUM_846-15	04019253230000	Kreyenhagen	7590	5.2E-07	22.89844	-0.000519	92.57377	2.583976
BRUM_846-15	04019253230000	Kreyenhagen	7593	6.77E-05	22.85641	0.0008232	84.67971	2.510312
BRUM_846-15	04019253230000	Kreyenhagen	7596	2.01E-06	22.88157	-0.002575	91.51079	2.612066
BRUM_846-15	04019253230000	Kreyenhagen	7597	2.97E-06	22.637	1.4784165	89.85053	2.540947
BRUM_846-15	04019253230000	Kreyenhagen	7605	3.22E-06	23.00727	-0.003551	92.47386	2.536035
BRUM_846-15	04019253230000	Kreyenhagen	7608	3.81E-05	22.22626	4.4667814	79.16643	2.489799
BRUM_846-15	04019253230000	Kreyenhagen	7611	3.72E-09	22.4501	-0.000839	97.30009	2.62268
BRUM_846-15	04019253230000	Kreyenhagen	7614	2.08E-11	26.80448	3.1160209	96.23727	2.699329
BRUM_846-15	04019253230000	Kreyenhagen	7617	4.16E-06	25.59347	2.709405	90.06168	2.684389
NAPA_AVE_A1	04019225380000	Kreyenhagen	4788	1	35.6	0	99	2.57
RIPPERDAN_544-13	04019253280000	Kreyenhagen	6008	4.11E-07	25.64342	0.0004426	85.26365	2.497028
RIPPERDAN_544-13	04019253280000	Kreyenhagen	6011	8.09E-07	25.507	-0.003438	84.67012	2.558176
RIPPERDAN_544-13	04019253280000	Kreyenhagen	6014.6	1.74E-07	23.65808	0.0004564	92.84647	2.503873
RIPPERDAN_544-13	04019253280000	Kreyenhagen	6017	4.84E-06	27.00153	-0.001493	87.59128	2.426195
RIPPERDAN_544-13	04019253280000	Kreyenhagen	6021	1.97E-07	27.1255	-0.002164	95.1866	2.503971
RIPPERDAN_544-13	04019253280000	Kreyenhagen	6023	2.89E-06	24.9614	-0.000561	88.30426	2.560567
RIPPERDAN_544-13	04019253280000	Kreyenhagen	6027.3	9.1E-05	26.94047	-0.000334	81.43355	2.70172
RIPPERDAN_544-13	04019253280000	Kreyenhagen	6030.3	2.3E-07	25.91489	0.0005368	90.16842	2.500844
RIPPERDAN_544-13	04019253280000	Kreyenhagen	6033.3	8.08E-06	25.7877	-0.002259	84.18736	2.564044
RIPPERDAN_544-13	04019253280000	Kreyenhagen	6036	6.28E-08	22.42081	-0.001905	94.60923	2.579773
RIPPERDAN_544-13	04019253280000	Kreyenhagen	6039	2.07E-07	28.16935	0.0029693	97.45758	2.973044

Well	UWI	Formation	Depth (feet)	KA (mD)	PHIT (%)	SOC (%)	SWC (%)	GD (G/CC)
RIPPERDAN_544-13	04019253280000	Kreyenhagen	6042	0.000118	26.81613	-0.000695	80.56322	2.572497
RIPPERDAN_544-13	04019253280000	Kreyenhagen	6045	5.9E-07	25.0593	-5.94E-05	91.92891	2.69879
RIPPERDAN_544-13	04019253280000	Kreyenhagen	6048	5.28E-05	28.21283	-0.002147	73.74189	2.546275
RIPPERDAN_544-13	04019253280000	Kreyenhagen	6051	2.61E-06	25.02698	-0.001859	90.18902	2.517669
RIPPERDAN_544-13	04019253280000	Kreyenhagen	6054.3	8.45E-06	26.90825	0.0048684	88.42809	2.555224
RIPPERDAN_544-13	04019253280000	Kreyenhagen	6058	3.21E-05	28.2857	0.0047662	78.52368	2.528988
RIPPERDAN_544-13	04019253280000	Kreyenhagen	6060.2	0.000108	26.13522	0.0010965	79.5151	2.496567

NM = No measure

Table 2.4-4. Core Samples from Three Wells in the Domengine Formation

Well	UWI	Formation	Depth (feet)	KA (mD)	PHIT (%)	SOC (%)	SWC (%)	GD (G/CC)
GILL_32-21	04039200580000	Domengine	4557	31.9	32	9.8	81.1	NM
GILL_32-21	04039200580000	Domengine	4745	21.2	31.1	0	83.5	NM
GILL_32-21	04039200580000	Domengine	4759	65.5	33.8	0	97.7	NM
NAPA_AVE_A1	04019225380000	Domengine	4863	61	32.2	0	99.7	2.65
NAPA_AVE_A1	04019225380000	Domengine	4883	742	36.9	0	81.6	2.62
NAPA_AVE_A1	04019225380000	Domengine	4907	13	27.8	0	99.3	2.7
NLF_POTTER_19-1	04047200700000	Domengine	3685	240	32.4	0	81.6	NM
NLF_POTTER_19-1	04047200700000	Domengine	3687	200	32.5	0	81.5	NM
NLF_POTTER_19-1	04047200700000	Domengine	3690	100	33.3	0	87	NM
NLF_POTTER_19-1	04047200700000	Domengine	3711	430	34.1	0	84.6	NM
NLF_POTTER_19-1	04047200700000	Domengine	3713	390	29.4	0	86.3	NM

NM = No measure

Table 2.4-5. Core Samples from Five Wells in the Garzas Formation

Well	UWI	Formation	Depth (feet)	Pressure	KA (mD)	Vertical Perm (mD)	PHIT (%)	SOC (%)	SWC (%)	GD (G/CC)
ADAMS_1_WESTLANDS	04019231020000	Garzas	7028	NM	NM	14.7	NM	NM	NM	NM
ADAMS_1_WESTLANDS	04019231020000	Garzas	7037	NM	NM	0.2	NM	NM	NM	NM
ADAMS_1_WESTLANDS	04019231020000	Garzas	7040	NM	NM	0.1	NM	NM	NM	NM
ADAMS_1_WESTLANDS	04019231020000	Garzas	7515	300	405	NM	27.8	NM	NM	NM
ADAMS_1_WESTLANDS	04019231020000	Garzas	7515	3758	484	NM	NM	NM	NM	NM
ADAMS_1_WESTLANDS	04019231020000	Garzas	7517	300	7.4	NM	26.5	NM	NM	NM
ADAMS_1_WESTLANDS	04019231020000	Garzas	7518	300	8.3	NM	26.2	0	76.9	2.67
ADAMS_1_WESTLANDS	04019231020000	Garzas	7518	300	46	NM	24.4	NM	NM	NM
ADAMS_1_WESTLANDS	04019231020000	Garzas	7520	300	91	NM	26.2	NM	NM	NM
ADAMS_1_WESTLANDS	04019231020000	Garzas	7520	3760	40	NM	NM	NM	NM	NM
ADAMS_1_WESTLANDS	04019231020000	Garzas	7522	300	36	NM	23.9	NM	NM	NM
ADAMS_1_WESTLANDS	04019231020000	Garzas	7523	300	339	NM	28.5	NM	NM	NM
ADAMS_1_WESTLANDS	04019231020000	Garzas	7525	3762	3.35	NM	NM	NM	NM	NM
ADAMS_1_WESTLANDS	04019231020000	Garzas	7527	300	224	NM	28.9	NM	NM	NM
ADAMS_1_WESTLANDS	04019231020000	Garzas	7527	3763	91	NM	NM	NM	NM	NM
ADAMS_1_WESTLANDS	04019231020000	Garzas	7529	300	19	NM	26.7	0	80.8	2.66
ADAMS_1_WESTLANDS	04019231020000	Garzas	7639	3820	50	NM	NM	NM	NM	NM
ADAMS_1_WESTLANDS	04019231020000	Garzas	7639	300	128	NM	26.4	NM	NM	NM
ADAMS_1_WESTLANDS	04019231020000	Garzas	7642	300	18	NM	27.2	0	73.6	2.66
ADAMS_1_WESTLANDS	04019231020000	Garzas	7645	3822	29.8	NM	NM	NM	NM	NM
ADAMS_1_WESTLANDS	04019231020000	Garzas	7645	300	678	NM	26.6	NM	NM	NM
ADAMS_1_WESTLANDS	04019231020000	Garzas	7647	300	47	NM	23.6	NM	NM	NM
ADAMS_1_WESTLANDS	04019231020000	Garzas	7650	300	203	NM	25.5	NM	NM	NM
ADAMS_1_WESTLANDS	04019231020000	Garzas	7650	3825	129	NM	NM	NM	NM	NM
ADAMS_1_WESTLANDS	04019231020000	Garzas	7651	3825	40.1	NM	NM	NM	NM	NM

Well	UWI	Formation	Depth (feet)	Pressure	KA (mD)	Vertical Perm (mD)	PHIT (%)	SOC (%)	SWC (%)	GD (G/CC)
ADAMS_1_WESTLANDS	04019231020000	Garzas	7653	300	188	NM	25.7	NM	NM	NM
ADAMS_1_WESTLANDS	04019231020000	Garzas	7654	300	100	NM	25.4	NM	NM	NM
ADAMS_1_WESTLANDS	04019231020000	Garzas	7657	300	50	NM	25.8	NM	NM	NM
ADAMS_1_WESTLANDS	04019231020000	Garzas	7659	3830	18	NM	NM	NM	NM	NM
ADAMS_1_WESTLANDS	04019231020000	Garzas	7659	300	111	NM	25.5	NM	NM	NM
ADAMS_1_WESTLANDS	04019231020000	Garzas	7660	300	23	NM	22.8	NM	NM	NM
ADAMS_1_WESTLANDS	04019231020000	Garzas	7663	300	11	NM	24.8	0	74.5	2.66
CHOWCHILLA_FARMS_74-9	04039001240000	Garzas	4717	NM	NM	NM	27.6	NM	NM	NM
LE_COMPTE_1	04019231840000	Garzas	5428	NM	18	NM	33.6	0	84.3	2.65
NAPA_AVE_A1	04019225380000	Garzas	4921	NM	644	NM	37.3	0	93.3	2.72
NAPA_AVE_A1	04019225380000	Garzas	4983	NM	27	NM	33.6	0	99.4	2.62
NAPA_AVE_A1	04019225380000	Garzas	5145	NM	100	NM	37.3	0	91	2.6
NAPA_AVE_A1	04019225380000	Garzas	5255	NM	21	NM	33.6	0	94	2.62
TRIANGLE_A_1	04039200520000	Garzas	4491	NM	NM	NM	NM	NM	NM	2.63
TRIANGLE_A_1	04039200520000	Garzas	4914	NM	NM	NM	NM	NM	NM	2.64
TRIANGLE_A_1	04039200520000	Garzas	4936	NM	NM	NM	NM	NM	NM	2.66
TRIANGLE_A_1	04039200520000	Garzas	4956	NM	NM	NM	NM	NM	NM	2.64

NM = No measure

Table 2.4-6. Core Samples from 14 Wells in the Blewett Formation

Well	UWI	Formation	Depth (feet)	Pressure	KA (mD)	Vertical Perm (mD)	PHIT (%)	SOC (%)	SWC (%)	GD (G/CC)
B&N_1	04019231910000	Blewett	6658	NM	40.8	NM	28	0	27.2	NM
B&N_1	04019231910000	Blewett	6668	NM	137.4	NM	27.9	0	65	NM
B&N_1	04019231910000	Blewett	6678	NM	0.2	NM	21.7	0	47.1	NM
B&N_1	04019231910000	Blewett	6686	NM	86.4	NM	28	0	79.9	NM
B&N_1	04019231910000	Blewett	6704	NM	77	NM	29.9	0	57.8	NM
B&N_1	04019231910000	Blewett	6713	NM	190.2	NM	30.4	0	60.1	NM
B&N_1	04019231910000	Blewett	6748	NM	197.9	NM	30.5	0	76.9	NM
B&N_1	04019231910000	Blewett	6764	NM	104.9	NM	30.1	0	82.9	NM
B&N_1	04019231910000	Blewett	6815	NM	160.6	NM	26.3	0	72.6	NM
B&N_1	04019231910000	Blewett	6826	NM	130.9	NM	28.3	0	75.1	NM
B&N_1	04019231910000	Blewett	6886	NM	<1.0	NM	31.6	9.8	56	NM
B&N_1	04019231910000	Blewett	6898	NM	137.1	NM	28.8	0	20.4	NM
B&N_1	04019231910000	Blewett	6930	NM	96.5	NM	28	0	48.2	NM
B&N_1	04019231910000	Blewett	6946	NM	105.9	NM	28.6	0	16.1	NM
B&N_1	04019231910000	Blewett	6967	NM	22.7	NM	22	0	73.5	NM
B&N_1_RD1	04019231910010	Blewett	6785	NM	60.6	NM	27.1	0	68.2	NM
B&N_1_RD1	04019231910010	Blewett	6791	NM	6.3	NM	25.5	0	25.4	NM
B&N_1_RD1	04019231910010	Blewett	6829	NM	172.1	NM	35.5	0	96.6	NM
B&N_1_RD1	04019231910010	Blewett	6844	NM	155	NM	28.8	0	89.9	NM
B&N_1_RD1	04019231910010	Blewett	6868	NM	151.7	NM	28.8	0	95.3	NM
B&N_1_RD1	04019231910010	Blewett	6876	NM	127.9	NM	29.8	0	94.4	NM
B&N_1_RD1	04019231910010	Blewett	6969	NM	1871.2	NM	35.7	0	78.5	NM
B&N_1_RD1	04019231910010	Blewett	7032	NM	2.4	NM	23.5	0	88.7	NM
B&N_1_RD1	04019231910010	Blewett	7048	NM	1746.3	NM	30	0	79.6	NM
B&N_1_RD1	04019231910010	Blewett	7144	NM	2097.4	NM	34.1	0	77.3	NM

Well	UWI	Formation	Depth (feet)	Pressure	KA (mD)	Vertical Perm (mD)	PHIT (%)	SOC (%)	SWC (%)	GD (G/CC)
CHENEY_RANCH_1_NAHAMA	04019216700000	Blewett	7186	NM	350	NM	21.9	0	73.4	NM
CHENEY_RANCH_1_NAHAMA	04019216700000	Blewett	7188	NM	290	NM	22.1	0	76.9	NM
CHENEY_RANCH_1_NAHAMA	04019216700000	Blewett	7191	NM	11	NM	8	0	55.6	NM
CHENEY_RANCH_1_NAHAMA	04019216700000	Blewett	7194	NM	200	NM	25.6	0	67.1	NM
CHENEY_RANCH_1_NAHAMA	04019216700000	Blewett	7196	NM	130	NM	22.6	0	72	NM
CHENEY_RANCH_1_NAHAMA	04019216700000	Blewett	7197	NM	270	NM	22.9	0	79.9	NM
CHENEY_RANCH_1_NAHAMA	04019216700000	Blewett	7199	NM	160	NM	24.6	0	66.9	NM
CHENEY_RANCH_1_NAHAMA	04019216700000	Blewett	7200	NM	290	NM	25	0	76.9	NM
CHENEY_RANCH_1_NAHAMA	04019216700000	Blewett	7202	NM	240	NM	22.3	0	74.5	NM
CHENEY_RANCH_1_NAHAMA	04019216700000	Blewett	7204	NM	310	NM	26.2	0	71.3	NM
CHENEY_RANCH_1_NAHAMA	04019216700000	Blewett	7206	NM	75	NM	24.6	0	72.5	NM
CHENEY_RANCH_1_NAHAMA	04019216700000	Blewett	7208	NM	150	NM	24.4	0	75.3	NM
CHENEY_RANCH_1_NAHAMA	04019216700000	Blewett	7218	NM	180	NM	26.8	0.6	67.5	NM
CHENEY_RANCH_1_NAHAMA	04019216700000	Blewett	7220	NM	260	NM	25.1	0	71.5	NM
CHENEY_RANCH_1_NAHAMA	04019216700000	Blewett	7222	NM	210	NM	24.3	0	66.7	NM
CHENEY_RANCH_1_NAHAMA	04019216700000	Blewett	7226	NM	170	NM	23.2	0	70.4	NM
CHENEY_RANCH_1_NAHAMA	04019216700000	Blewett	7228	NM	95	NM	25	0	75.2	NM
CHENEY_RANCH_1_NAHAMA	04019216700000	Blewett	7235	NM	5.9	NM	25	3.1	73.6	NM
CHENEY_RANCH_1_NAHAMA	04019216700000	Blewett	7237	NM	3.5	NM	23	0	81.5	NM
CHENEY_RANCH_1_NAHAMA	04019216700000	Blewett	7238	NM	6.4	NM	24.2	0	72.6	NM
CHENEY_RANCH_1_NAHAMA	04019216700000	Blewett	7239	NM	16	NM	22.9	0	80	NM
CHENEY_RANCH_1_NAHAMA	04019216700000	Blewett	7246	NM	45	NM	26.6	0	86.8	NM
CHENEY_RANCH_1_NAHAMA	04019216700000	Blewett	7248	NM	0.8	NM	22.8	4.6	75.7	NM
CHENEY_RANCH_1_NAHAMA	04019216700000	Blewett	7249	NM	0.4	NM	15.5	0	81.1	NM
CHENEY_RANCH_1_NAHAMA	04019216700000	Blewett	7250	NM	0.7	NM	21.9	8.2	77.9	NM
CHENEY_RANCH_1_NAHAMA	04019216700000	Blewett	7251	NM	1.5	NM	26.6	1.2	74.1	NM
CHENEY_RANCH_1_NAHAMA	04019216700000	Blewett	7252	NM	270	NM	28.3	0	80.6	NM

Well	UWI	Formation	Depth (feet)	Pressure	KA (mD)	Vertical Perm (mD)	PHIT (%)	SOC (%)	SWC (%)	GD (G/CC)
CHENEY_RANCH_1_NAHAMA	04019216700000	Blewett	7253	NM	190	NM	25.5	0	79.4	NM
CHENEY_RANCH_1_NAHAMA	04019216700000	Blewett	7254	NM	350	NM	26.2	0	77.4	NM
CHENEY_RANCH_1_NAHAMA	04019216700000	Blewett	7255	NM	230	NM	24.4	0	76.4	NM
CHENEY_RANCH_1_NAHAMA	04019216700000	Blewett	7256	NM	400	NM	24.7	0	63.8	NM
CHENEY_RANCH_1_NAHAMA	04019216700000	Blewett	7259	NM	130	NM	24.6	0	61	NM
CHENEY_RANCH_1_NAHAMA	04019216700000	Blewett	7261	NM	180	NM	26.2	0	69.3	NM
CHENEY_RANCH_1_NAHAMA	04019216700000	Blewett	7264	NM	310	NM	26.7	0	75.5	NM
CHENEY_RANCH_1_NAHAMA	04019216700000	Blewett	7272	NM	250	NM	25.3	0	77.1	NM
CHENEY_RANCH_1_NAHAMA	04019216700000	Blewett	7273	NM	98	NM	25.7	0	77.5	NM
CHENEY_RANCH_1_NAHAMA	04019216700000	Blewett	7274	NM	110	NM	25.7	0	85.3	NM
CHENEY_RANCH_1_NAHAMA	04019216700000	Blewett	7276	NM	280	NM	26.6	0	72.4	NM
CHENEY_RANCH_1_NAHAMA	04019216700000	Blewett	7278	NM	200	NM	25.7	0	82.4	NM
CHENEY_RANCH_1_NAHAMA	04019216700000	Blewett	7295	NM	73	NM	24.3	0	63.5	NM
GILL_32-21	04039200580000	Blewett	5780	NM	0.2	NM	0.1	NM	NM	NM
GILL_32-21	04039200580000	Blewett	5780	NM	13.8	NM	33	0	96.5	NM
GILL_32-21	04039200580000	Blewett	6002	NM	0.73	NM	7.3	NM	NM	NM
GILL_32-21	04039200580000	Blewett	6002	NM	5.9	NM	24.4	0	73.5	NM
GILL_RANCH_34-18-202	04039201180000	Blewett	5781	250	1149.4	NM	35.4	0	74.4	2.66
GILL_RANCH_34-18-202	04039201180000	Blewett	5782	250	NM	1042.7	NM	NM	NM	NM
GILL_RANCH_34-18-202	04039201180000	Blewett	5782	250	1608.3	NM	33	0	72.1	2.66
GILL_RANCH_34-18-202	04039201180000	Blewett	5783	250	NM	1457.9	NM	NM	NM	NM
GILL_RANCH_34-18-202	04039201180000	Blewett	5783	250	1397.4	NM	34.1	0	88.2	2.67
GILL_RANCH_34-18-202	04039201180000	Blewett	5784	250	NM	1190.6	NM	NM	NM	NM
GILL_RANCH_34-18-202	04039201180000	Blewett	5784	250	1218	NM	35	0	81.1	2.74
GILL_RANCH_34-18-202	04039201180000	Blewett	5785	250	NM	788	NM	NM	NM	NM
GILL_RANCH_34-18-202	04039201180000	Blewett	5785	250	838.8	NM	35.5	0	77.8	2.68
GILL_RANCH_34-18-202	04039201180000	Blewett	5786	250	NM	612.8	NM	NM	NM	NM

Well	UWI	Formation	Depth (feet)	Pressure	KA (mD)	Vertical Perm (mD)	PHIT (%)	SOC (%)	SWC (%)	GD (G/CC)
GILL_RANCH_34-18-202	04039201180000	Blewett	5786	250	896.7	NM	36.2	0	65	2.67
GILL_RANCH_34-18-202	04039201180000	Blewett	5787	250	NM	663.8	NM	NM	NM	NM
GILL_RANCH_34-18-202	04039201180000	Blewett	5787	250	633.7	NM	34.5	0	80.6	2.66
GILL_RANCH_34-18-202	04039201180000	Blewett	5788	250	NM	777.4	NM	NM	NM	NM
GILL_RANCH_34-18-202	04039201180000	Blewett	5788	250	671.3	NM	34.9	0	81.9	2.66
GILL_RANCH_34-18-202	04039201180000	Blewett	5789	250	NM	1159.3	NM	NM	NM	NM
GILL_RANCH_34-18-202	04039201180000	Blewett	5789	250	631.3	NM	35.3	0	81.3	2.66
GILL_RANCH_34-18-202	04039201180000	Blewett	5790	250	NM	1138.1	NM	NM	NM	NM
GILL_RANCH_34-18-202	04039201180000	Blewett	5790	250	805.6	NM	35.5	0	76	2.66
GILL_RANCH_34-18-202	04039201180000	Blewett	5791	250	NM	1212.2	NM	NM	NM	NM
GILL_RANCH_34-18-202	04039201180000	Blewett	5791	250	849.5	NM	36	0	84.6	2.66
GILL_RANCH_34-18-202	04039201180000	Blewett	5792	250	NM	1043.1	NM	NM	NM	NM
GILL_RANCH_34-18-202	04039201180000	Blewett	5792	250	868.9	NM	33.4	0	86.5	2.67
GILL_RANCH_34-18-202	04039201180000	Blewett	5793	250	NM	761	NM	NM	NM	NM
GILL_RANCH_34-18-202	04039201180000	Blewett	5793	250	2027.4	NM	33.7	0	88.8	2.67
GILL_RANCH_34-18-202	04039201180000	Blewett	5794	250	NM	1144	NM	NM	NM	NM
GILL_RANCH_34-18-202	04039201180000	Blewett	5794	250	1099.9	NM	34.7	0	94.7	2.67
GILL_RANCH_34-18-202	04039201180000	Blewett	5795	250	NM	1532.5	NM	NM	NM	NM
GILL_RANCH_34-18-202	04039201180000	Blewett	5796	250	967.8	NM	36.8	0	78.7	2.67
GILL_RANCH_34-18-202	04039201180000	Blewett	5796	250	NM	882	NM	NM	NM	NM
GILL_RANCH_34-18-202	04039201180000	Blewett	5797	250	846.7	NM	33.8	0	87.3	2.67
GILL_RANCH_34-18-202	04039201180000	Blewett	5797	250	NM	635	NM	NM	NM	NM
GILL_RANCH_34-18-202	04039201180000	Blewett	5798	250	947.5	NM	35.6	0	54	2.71
GILL_RANCH_34-18-202	04039201180000	Blewett	5798	250	NM	1246.2	NM	NM	NM	NM
GILL_RANCH_34-18-202	04039201180000	Blewett	5799	250	1204.5	NM	33.9	0	62	2.71
GILL_RANCH_34-18-202	04039201180000	Blewett	5800	250	NM	1271.8	NM	NM	NM	NM
GILL_RANCH_34-18-202	04039201180000	Blewett	5800	250	1332.5	NM	33.6	0	58.8	2.7

Well	UWI	Formation	Depth (feet)	Pressure	KA (mD)	Vertical Perm (mD)	PHIT (%)	SOC (%)	SWC (%)	GD (G/CC)
GILL_RANCH_34-18-202	04039201180000	Blewett	5801	250	NM	1319.9	NM	NM	NM	NM
GILL_RANCH_34-18-202	04039201180000	Blewett	5801	250	1028	NM	33.6	0	62.5	2.71
GILL_RANCH_34-18-202	04039201180000	Blewett	5802	250	NM	224	NM	NM	NM	NM
GILL_RANCH_34-18-202	04039201180000	Blewett	5802	250	1018.6	NM	33.8	0	62.9	2.68
GILL_RANCH_34-18-202	04039201180000	Blewett	5803	250	NM	1117.2	NM	NM	NM	NM
GILL_RANCH_34-18-202	04039201180000	Blewett	5803	250	1132.7	NM	33.9	0	61.6	2.71
GILL_RANCH_34-18-202	04039201180000	Blewett	5804	250	NM	850.4	NM	NM	NM	NM
GILL_RANCH_34-18-202	04039201180000	Blewett	5804	250	692.5	NM	34.8	0	61.3	2.69
GILL_RANCH_34-18-202	04039201180000	Blewett	5805	250	NM	498.1	NM	NM	NM	NM
GILL_RANCH_34-18-202	04039201180000	Blewett	5805	250	810.4	NM	34.6	0	64.5	2.68
GILL_RANCH_34-18-202	04039201180000	Blewett	5806	250	NM	595.3	NM	NM	NM	NM
GILL_RANCH_34-18-202	04039201180000	Blewett	5806	250	694	NM	34.5	0	57.3	2.7
GILL_RANCH_34-18-202	04039201180000	Blewett	5807	250	NM	393.3	NM	NM	NM	NM
GILL_RANCH_34-18-202	04039201180000	Blewett	5807	250	664.9	NM	35.4	0	57.7	2.72
GILL_RANCH_34-18-202	04039201180000	Blewett	5808	250	NM	374.3	NM	NM	NM	NM
GILL_RANCH_34-18-202	04039201180000	Blewett	5808	250	466.1	NM	34	0	63.8	2.71
GILL_RANCH_34-18-202	04039201180000	Blewett	5809	250	NM	356.5	NM	NM	NM	NM
GILL_RANCH_34-18-202	04039201180000	Blewett	5809	250	529.4	NM	33.8	0	59.5	2.73
GILL_RANCH_34-18-202	04039201180000	Blewett	5810	250	NM	383.6	NM	NM	NM	NM
GILL_RANCH_34-18-202	04039201180000	Blewett	5810	250	776.2	NM	34.4	0	61.2	2.71
GILL_RANCH_34-18-202	04039201180000	Blewett	5811	250	NM	718.5	NM	NM	NM	NM
GILL_RANCH_34-18-202	04039201180000	Blewett	5811	250	889.3	NM	33.4	0	64.3	2.69
GILL_RANCH_34-18-202	04039201180000	Blewett	5812	250	NM	713.4	NM	NM	NM	NM
GILL_RANCH_34-18-202	04039201180000	Blewett	5812	250	806.4	NM	34.2	0	65.2	2.69
GILL_RANCH_34-18-202	04039201180000	Blewett	5813	250	NM	698.5	NM	NM	NM	NM
GILL_RANCH_34-18-202	04039201180000	Blewett	5813	250	1051.6	NM	34.8	0	62.9	2.69
GILL_RANCH_34-18-202	04039201180000	Blewett	5814	250	NM	720.3	NM	NM	NM	NM

Well	UWI	Formation	Depth (feet)	Pressure	KA (mD)	Vertical Perm (mD)	PHIT (%)	SOC (%)	SWC (%)	GD (G/CC)
GILL_RANCH_34-18-202	04039201180000	Blewett	5814	250	1281.6	NM	34.8	0	62.9	2.69
GILL_RANCH_34-18-202	04039201180000	Blewett	5815	250	NM	192.8	NM	NM	NM	NM
GILL_RANCH_34-18-202	04039201180000	Blewett	5815	250	385.9	NM	35.6	0	63.1	2.69
GILL_RANCH_34-18-202	04039201180000	Blewett	5816	250	NM	288.2	NM	NM	NM	NM
GILL_RANCH_34-18-202	04039201180000	Blewett	5816	250	406.9	NM	35.3	0	63.4	2.68
GILL_RANCH_34-18-202	04039201180000	Blewett	5817	250	NM	27.8	NM	NM	NM	NM
GILL_RANCH_34-18-202	04039201180000	Blewett	5826	250	1257.2	NM	34.7	0	64.5	2.69
GILL_RANCH_34-18-202	04039201180000	Blewett	5827	250	NM	480	NM	NM	NM	NM
GILL_RANCH_34-18-202	04039201180000	Blewett	5827	250	1178.2	NM	35	0	63.6	2.69
GILL_RANCH_34-18-202	04039201180000	Blewett	5828	250	NM	483.3	NM	NM	NM	NM
GILL_RANCH_34-18-202	04039201180000	Blewett	5828	250	945.5	NM	34.6	0	62.4	2.69
GILL_RANCH_34-18-202	04039201180000	Blewett	5829	250	NM	709.6	NM	NM	NM	NM
GILL_RANCH_34-18-202	04039201180000	Blewett	5829	250	25.8	NM	34.1	0	59.7	2.69
GILL_RANCH_34-18-202	04039201180000	Blewett	5830	250	NM	70.5	NM	NM	NM	NM
GILL_RANCH_34-18-202	04039201180000	Blewett	5830	250	287.7	NM	35	0	63	2.69
GILL_RANCH_34-18-202	04039201180000	Blewett	5831	250	NM	295.7	NM	NM	NM	NM
GILL_RANCH_34-18-202	04039201180000	Blewett	5831	250	73	NM	1.2	0	83.3	2.73
GILL_RANCH_34-18-202	04039201180000	Blewett	5832	250	NM	0.004	NM	NM	NM	NM
GILL_RANCH_34-18-202	04039201180000	Blewett	5832	250	325.1	NM	1.1	0	99.4	2.73
GILL_RANCH_34-18-202	04039201180000	Blewett	5833	250	NM	144.4	NM	NM	NM	NM
GILL_RANCH_34-18-202	04039201180000	Blewett	5833	250	550.3	NM	34	0	57.7	2.68
GILL_RANCH_34-18-202	04039201180000	Blewett	5834	250	NM	396.1	NM	NM	NM	NM
GILL_RANCH_34-18-202	04039201180000	Blewett	5834	250	753.7	NM	34.3	0	56.5	2.69
GILL_RANCH_34-18-202	04039201180000	Blewett	5835	250	NM	876.8	NM	NM	NM	NM
GILL_RANCH_34-18-202	04039201180000	Blewett	5835	250	1214.5	NM	34	0	64.7	2.71
GILL_RANCH_34-18-202	04039201180000	Blewett	5836	250	NM	475.3	NM	NM	NM	NM
GILL_RANCH_34-18-202	04039201180000	Blewett	5836	250	222.4	NM	26.5	0	84.7	2.7

Well	UWI	Formation	Depth (feet)	Pressure	KA (mD)	Vertical Perm (mD)	PHIT (%)	SOC (%)	SWC (%)	GD (G/CC)
GILL_RANCH_34-18-202	04039201180000	Blewett	5837	250	NM	97.1	NM	NM	NM	NM
GILL_RANCH_34-18-202	04039201180000	Blewett	5837	250	684.6	NM	30.5	0	80.1	2.68
GILL_RANCH_34-18-202	04039201180000	Blewett	5838	250	NM	599.4	NM	NM	NM	NM
GILL_RANCH_34-18-202	04039201180000	Blewett	5838	250	768.6	NM	33.2	0	79.8	2.7
GILL_RANCH_34-18-202	04039201180000	Blewett	5839	250	NM	391.6	NM	NM	NM	NM
GILL_RANCH_34-18-202	04039201180000	Blewett	5839	250	584.2	NM	33.1	0	79.6	2.69
GILL_RANCH_34-18-202	04039201180000	Blewett	5840	250	NM	547.8	NM	NM	NM	NM
GILL_RANCH_34-18-202	04039201180000	Blewett	5840	250	554.1	NM	33.1	0	76.9	2.69
GILL_RANCH_34-18-202	04039201180000	Blewett	5841	250	NM	274.4	NM	NM	NM	NM
GILL_RANCH_34-18-202	04039201180000	Blewett	5841	250	301	NM	32.9	0	81.3	2.69
GILL_RANCH_34-18-202	04039201180000	Blewett	5842	250	NM	280	NM	NM	NM	NM
GILL_RANCH_34-18-202	04039201180000	Blewett	5842	250	251.6	NM	33.3	0	78.7	2.68
GILL_RANCH_34-18-202	04039201180000	Blewett	5843	250	NM	116.2	NM	NM	NM	NM
GILL_RANCH_34-18-202	04039201180000	Blewett	5843	250	898.3	NM	32.6	0	87.9	2.68
GILL_RANCH_34-18-202	04039201180000	Blewett	5844	250	NM	175.1	NM	NM	NM	NM
GILL_RANCH_34-18-202	04039201180000	Blewett	5844	250	125.8	NM	33.3	0	81.1	2.68
GILL_RANCH_34-18-202	04039201180000	Blewett	5845	250	NM	446.4	NM	NM	NM	NM
GILL_RANCH_34-18-202	04039201180000	Blewett	5845	250	291.2	NM	32.5	0	84.2	2.68
GILL_RANCH_34-18-202	04039201180000	Blewett	5846	250	NM	142	NM	NM	NM	NM
GILL_RANCH_34-18-202	04039201180000	Blewett	5846	250	342.2	NM	33.1	0	80.7	2.68
GILL_RANCH_34-18-202	04039201180000	Blewett	5847	250	NM	285.8	NM	NM	NM	NM
GILL_RANCH_34-18-202	04039201180000	Blewett	5847	250	197.9	NM	34	0	81.4	2.67
GILL_RANCH_34-18-202	04039201180000	Blewett	5848	250	NM	148.5	NM	NM	NM	NM
GILL_RANCH_34-18-202	04039201180000	Blewett	5848	250	300.8	NM	33.3	0	79.6	2.68
GILL_RANCH_34-18-202	04039201180000	Blewett	5849	250	NM	482.5	NM	NM	NM	NM
GILL_RANCH_34-18-202	04039201180000	Blewett	5849	250	884.1	NM	32	0	80.4	2.68
GILL_RANCH_34-18-202	04039201180000	Blewett	5850	250	NM	419.4	NM	NM	NM	NM

Well	UWI	Formation	Depth (feet)	Pressure	KA (mD)	Vertical Perm (mD)	PHIT (%)	SOC (%)	SWC (%)	GD (G/CC)
GILL_RANCH_34-18-202	04039201180000	Blewett	5850	250	254.2	NM	31.2	0	85.8	2.68
GILL_RANCH_34-18-202	04039201180000	Blewett	5851	250	NM	145.8	NM	NM	NM	NM
GILL_RANCH_34-18-202	04039201180000	Blewett	5851	250	169.1	NM	31.2	0	85.5	2.68
GILL_RANCH_34-18-202	04039201180000	Blewett	5852	250	NM	139.7	NM	NM	NM	NM
GILL_RANCH_34-18-202	04039201180000	Blewett	5852	250	39.9	NM	32.4	0	76.4	2.68
GILL_RANCH_34-18-202	04039201180000	Blewett	5853	250	NM	263.3	NM	NM	NM	NM
GILL_RANCH_34-18-202	04039201180000	Blewett	5853	250	331.8	NM	32.4	0	78.2	2.69
GILL_RANCH_34-18-202	04039201180000	Blewett	5853	250	NM	263.4	NM	NM	NM	NM
GILL_RANCH_34-18-202	04039201180000	Blewett	5854	250	256.3	NM	2.1	0	86.7	2.71
GILL_RANCH_34-18-202	04039201180000	Blewett	5855	250	NM	80.6	NM	NM	NM	NM
GILL_RANCH_34-18-202	04039201180000	Blewett	5855	250	615.4	NM	33.6	0	78	2.68
GILL_RANCH_34-18-202	04039201180000	Blewett	5856	250	NM	190.7	NM	NM	NM	NM
GILL_RANCH_34-18-202	04039201180000	Blewett	5856	250	37.2	NM	32.9	0	86.2	2.67
GILL_RANCH_34-18-202	04039201180000	Blewett	5857	250	NM	173	NM	NM	NM	NM
GILL_RANCH_34-18-202	04039201180000	Blewett	5857	250	285.4	NM	33.8	0	79.3	2.69
GILL_RANCH_34-18-202	04039201180000	Blewett	5858	250	NM	183.4	NM	NM	NM	NM
GILL_RANCH_34-18-202	04039201180000	Blewett	5858	250	258.7	NM	34	0	87.5	2.73
GILL_RANCH_34-18-202	04039201180000	Blewett	5859	250	NM	325.9	NM	NM	NM	NM
GILL_RANCH_34-18-202	04039201180000	Blewett	5859	250	779.5	NM	33.4	0	89.6	2.68
GILL_RANCH_34-18-202	04039201180000	Blewett	5860	250	NM	216.5	NM	NM	NM	NM
GILL_RANCH_34-18-202	04039201180000	Blewett	5860	250	244.3	NM	32.9	0	85.1	2.67
GILL_RANCH_34-18-202	04039201180000	Blewett	5861	250	NM	144.1	NM	NM	NM	NM
GILL_RANCH_34-18-202	04039201180000	Blewett	5861	250	336	NM	33.3	0	84.2	2.72
GILL_RANCH_34-18-202	04039201180000	Blewett	5862	250	NM	176.6	NM	NM	NM	NM
GILL_RANCH_34-18-202	04039201180000	Blewett	5862	250	326.8	NM	32.4	0	80.3	2.73
GILL_RANCH_34-18-202	04039201180000	Blewett	5863	250	NM	154.4	NM	NM	NM	NM
GILL_RANCH_34-18-202	04039201180000	Blewett	5863	250	391.4	NM	31.6	0	82	2.73

Well	UWI	Formation	Depth (feet)	Pressure	KA (mD)	Vertical Perm (mD)	PHIT (%)	SOC (%)	SWC (%)	GD (G/CC)
GILL_RANCH_34-18-202	04039201180000	Blewett	5864	250	NM	235.9	NM	NM	NM	NM
GILL_RANCH_34-18-202	04039201180000	Blewett	5864	250	235.9	NM	32.6	0	80.4	2.71
GILL_RANCH_34-18-202	04039201180000	Blewett	5865	250	NM	278.4	NM	NM	NM	NM
GILL_RANCH_34-18-202	04039201180000	Blewett	5865	250	59.6	NM	32.3	0	87.7	2.67
GILL_RANCH_34-18-202	04039201180000	Blewett	5866	250	NM	798.8	NM	NM	NM	NM
GILL_RANCH_34-18-202	04039201180000	Blewett	5866	250	93.3	NM	32.2	0	70.9	2.66
GILL_RANCH_34-18-202	04039201180000	Blewett	5867	250	NM	61.1	NM	NM	NM	NM
GILL_RANCH_34-18-202	04039201180000	Blewett	5867	250	150.1	NM	32.1	0	63.9	2.68
GILL_RANCH_34-18-202	04039201180000	Blewett	5868	250	NM	1152.1	NM	NM	NM	NM
GILL_RANCH_34-18-202	04039201180000	Blewett	5868	250	701.5	NM	32.9	0	83.7	2.83
GILL_RANCH_34-18-202	04039201180000	Blewett	5869	250	NM	221.2	NM	NM	NM	NM
GILL_RANCH_34-18-202	04039201180000	Blewett	5869	250	117	NM	33.2	0	63.2	2.67
LE_COMPTE_1	04019231840000	Blewett	6566	NM	130	NM	32	0	58.4	2.64
LE_COMPTE_1	04019231840000	Blewett	6568	NM	89	NM	31.8	0	48.2	2.65
LE_COMPTE_1	04019231840000	Blewett	6574	NM	95	NM	32.9	0	57.2	2.63
LE_COMPTE_1	04019231840000	Blewett	6578	NM	102	NM	31.1	0	57.6	2.64
LE_COMPTE_1	04019231840000	Blewett	6591	NM	111	NM	32.4	0	71.2	2.64
LE_COMPTE_1	04019231840000	Blewett	6606	NM	359	NM	31.1	0	84.2	2.49
LE_COMPTE_1	04019231840000	Blewett	6608	NM	126	NM	32.3	0	54.2	2.63
LE_COMPTE_1	04019231840000	Blewett	6622	NM	360	NM	26.8	0	76.7	2.51
LE_COMPTE_1	04019231840000	Blewett	6628	NM	90	NM	31.1	0	66.2	2.65
LE_COMPTE_1	04019231840000	Blewett	6640	NM	28	NM	32.2	0	61.7	2.48
LE_COMPTE_1	04019231840000	Blewett	6645	NM	224	NM	31.5	0	71.8	2.46
LE_COMPTE_1	04019231840000	Blewett	6649	NM	47	NM	31.1	0	62.1	2.66
LE_COMPTE_1	04019231840000	Blewett	6760	NM	77	NM	27.5	0	55.5	2.53
NAPA_AVE_A1	04019225380000	Blewett	6052	NM	682	NM	37.7	0	93.4	2.6
NAPA_AVE_A1	04019225380000	Blewett	6196	NM	98	NM	36.2	0	87.8	2.63

Well	UWI	Formation	Depth (feet)	Pressure	KA (mD)	Vertical Perm (mD)	PHIT (%)	SOC (%)	SWC (%)	GD (G/CC)
NLF_POTTER_19-1	04047200700000	Blewett	5602	NM	360	NM	33.3	0	87	NM
NLF_POTTER_19-1	04047200700000	Blewett	5613	NM	210	NM	33.8	0	84.6	NM
NLF_POTTER_19-1	04047200700000	Blewett	5640	NM	840	NM	32.5	0	79.6	NM
NLF_POTTER_19-1	04047200700000	Blewett	5644	NM	1530	NM	30.9	0	90.8	NM
NLF_POTTER_19-1	04047200700000	Blewett	5667	NM	330	NM	37.3	0	82.7	NM
NLF_POTTER_19-1	04047200700000	Blewett	5684	NM	120	NM	35.1	0	75.1	NM
NLF_POTTER_19-1	04047200700000	Blewett	5698	NM	390	NM	32.1	0	93.3	NM
NLF_POTTER_19-1	04047200700000	Blewett	5726	NM	390	NM	33.8	0	88.9	NM
NLF_POTTER_19-1	04047200700000	Blewett	5746	NM	530	NM	28.3	0	89.4	NM
O'BANION_1	04019231180000	Blewett	6543	NM	516	NM	31.9	0	60.5	2.64
O'BANION_1	04019231180000	Blewett	6545	NM	608	NM	31.7	0	45.6	2.65
O'BANION_1	04019231180000	Blewett	6546	NM	780	NM	31.6	0	45.3	2.64
O'BANION_1	04019231180000	Blewett	6547	NM	554	NM	31.8	0	47.9	2.65
O'BANION_1	04019231180000	Blewett	6548	NM	236	NM	30.5	0	45.3	2.65
O'BANION_1	04019231180000	Blewett	6549	NM	453	NM	28.7	0	54.4	2.63
O'BANION_1	04019231180000	Blewett	6550	NM	563	NM	30.5	0	51.6	2.65
O'BANION_1	04019231180000	Blewett	6551	NM	549	NM	30.6	0	54.6	2.64
O'BANION_1	04019231180000	Blewett	6552	NM	319	NM	31.4	0	55.1	2.64
O'BANION_1	04019231180000	Blewett	6552	NM	379	NM	31.1	0	63.6	2.63
O'BANION_1	04019231180000	Blewett	6554	NM	448	NM	30.3	0	60.2	2.64
O'BANION_1	04019231180000	Blewett	6555	NM	378	NM	29.3	0	54.3	2.65
O'BANION_1	04019231180000	Blewett	6556	NM	471	NM	30.2	0	54.4	2.64
O'BANION_1	04019231180000	Blewett	6557	NM	378	NM	29.8	0	57.9	2.64
O'BANION_1	04019231180000	Blewett	6558	NM	438	NM	30.7	0	50.8	2.64
O'BANION_1	04019231180000	Blewett	6559	NM	384	NM	30	0	55.2	2.63
O'BANION_1	04019231180000	Blewett	6560	NM	504	NM	31.6	0	53.7	2.62
O'BANION_1	04019231180000	Blewett	6560	NM	636	NM	30.9	0	47	2.63

Well	UWI	Formation	Depth (feet)	Pressure	KA (mD)	Vertical Perm (mD)	PHIT (%)	SOC (%)	SWC (%)	GD (G/CC)
O'BANION_1	04019231180000	Blewett	6562	NM	270	NM	34.8	0	57.8	2.62
O'BANION_1	04019231180000	Blewett	6565	NM	150	NM	28.7	0	47	2.64
O'BANION_1	04019231180000	Blewett	6570	NM	837	NM	32.2	0	51.1	2.64
O'BANION_1	04019231180000	Blewett	6571	NM	741	NM	32.5	0	61.5	2.64
O'BANION_1	04019231180000	Blewett	6571	NM	1100	NM	33.4	0	63.1	2.64
O'BANION_1	04019231180000	Blewett	6572	NM	687	NM	32.5	0	55	2.65
O'BANION_1	04019231180000	Blewett	6574	NM	719	NM	31.4	0	58.1	2.64
O'BANION_1	04019231180000	Blewett	6575	NM	667	NM	30.3	0	58.7	2.64
O'BANION_1	04019231180000	Blewett	6576	NM	608	NM	30.8	0	54.3	2.64
O'BANION_1	04019231180000	Blewett	6577	NM	721	NM	30.6	0	51.3	2.64
O'BANION_1	04019231180000	Blewett	6578	NM	700	NM	31.4	0	53	2.65
O'BANION_1	04019231180000	Blewett	6579	NM	795	NM	30	0	53.6	2.66
O'BANION_1	04019231180000	Blewett	6580	NM	859	NM	31.7	0	53.5	2.65
O'BANION_1	04019231180000	Blewett	6580	NM	867	NM	31.1	0	49.4	2.62
O'BANION_1	04019231180000	Blewett	6582	NM	1550	NM	33.6	0	47.5	2.63
O'BANION_1	04019231180000	Blewett	6583	NM	1700	NM	31.8	0	48.4	2.64
O'BANION_1	04019231180000	Blewett	6584	NM	1450	NM	30.9	0	53.3	2.64
O'BANION_1	04019231180000	Blewett	6585	NM	865	NM	31.1	0	53.4	2.65
O'BANION_1	04019231180000	Blewett	6586	NM	1615	NM	32.6	0	49.1	2.65
O'BANION_1	04019231180000	Blewett	6587	NM	50	NM	27.2	0	40.1	3.07
O'BANION_1	04019231180000	Blewett	6588	NM	1200	NM	32.3	0	52.2	2.64
O'BANION_1	04019231180000	Blewett	6589	NM	1180	NM	31.8	0	49.9	2.64
O'BANION_1	04019231180000	Blewett	6590	NM	1409	NM	31.7	0	51.4	2.65
O'BANION_1	04019231180000	Blewett	6591	NM	999	NM	31.3	0	52	2.63
O'BANION_1	04019231180000	Blewett	6592	NM	225	NM	28.6	0	57.7	2.65
O'BANION_1	04019231180000	Blewett	6593	NM	682	NM	31.3	0	45.1	2.65
O'BANION_1	04019231180000	Blewett	6594	NM	1190	NM	32.2	0	49	2.64

Well	UWI	Formation	Depth (feet)	Pressure	KA (mD)	Vertical Perm (mD)	PHIT (%)	SOC (%)	SWC (%)	GD (G/CC)
O'BANION_1	04019231180000	Blewett	6595	NM	2910	NM	32.7	0	48.2	2.64
O'BANION_1	04019231180000	Blewett	6596	NM	1040	NM	31.2	0	51.7	2.64
O'BANION_1	04019231180000	Blewett	6597	NM	1360	NM	32.5	0	48	2.64
O'BANION_1	04019231180000	Blewett	6598	NM	1430	NM	31.5	0	49.2	2.65
O'BANION_1	04019231180000	Blewett	6599	NM	1080	NM	30.3	0	53.5	2.64
O'BANION_1	04019231180000	Blewett	6599	NM	1150	NM	31.9	0	51.3	2.65
O'BANION_1	04019231180000	Blewett	6601	NM	874	NM	30.7	0	55.5	2.65
O'BANION_1	04019231180000	Blewett	6602	NM	975	NM	31.6	0	51.9	2.65
O'BANION_1	04019231180000	Blewett	6603	NM	984	NM	31.6	0	50.5	2.65
O'BANION_1	04019231180000	Blewett	6604	NM	374	NM	30.2	0	63.4	2.65
O'BANION_1	04019231180000	Blewett	6605	NM	304	NM	31.5	0	55.1	2.64
O'BANION_1	04019231180000	Blewett	6609	NM	47	NM	27.8	0	82.2	2.64
O'BANION_1	04019231180000	Blewett	6610	NM	38	NM	27.5	0	69.7	2.6
O'BANION_1	04019231180000	Blewett	6610	NM	100	NM	25.5	0	84.4	2.63
O'BANION_1	04019231180000	Blewett	6611	NM	101	NM	29.6	0	83.7	2.65
O'BANION_1	04019231180000	Blewett	6612	NM	32	NM	27.2	0	89.1	2.67
O'BANION_1	04019231180000	Blewett	6614	NM	476	NM	30.9	0	67.4	2.64
O'BANION_1	04019231180000	Blewett	6615	NM	1220	NM	32.3	0	61.6	2.65
O'BANION_1	04019231180000	Blewett	6616	NM	1730	NM	34.1	0	54.8	2.64
O'BANION_1	04019231180000	Blewett	6616	NM	175	NM	31.4	0	73.1	2.67
O'BANION_1	04019231180000	Blewett	6620	NM	1246	NM	33.8	0	60.1	2.65
O'BANION_1	04019231180000	Blewett	6621	NM	776	NM	32.3	0	66.3	2.65
O'BANION_1	04019231180000	Blewett	6622	NM	596	NM	32.4	0	68.4	2.65
O'BANION_1	04019231180000	Blewett	6623	NM	1200	NM	32.7	0	66.5	2.64
O'BANION_1	04019231180000	Blewett	6624	NM	1010	NM	32.5	0	73.1	2.64
O'BANION_1	04019231180000	Blewett	6624	NM	908	NM	32.7	0	71.6	2.64
O'BANION_1	04019231180000	Blewett	6626	NM	263	NM	31.6	0	80.6	2.64

Well	UWI	Formation	Depth (feet)	Pressure	KA (mD)	Vertical Perm (mD)	PHIT (%)	SOC (%)	SWC (%)	GD (G/CC)
O'BANION_1	04019231180000	Blewett	6627	NM	170	NM	29.7	0	80.3	2.64
O'BANION_1	04019231180000	Blewett	6628	NM	279	NM	31.6	0	79.6	2.64
O'BANION_1	04019231180000	Blewett	6629	NM	458	NM	31.3	0	71.6	2.65
O'BANION_1	04019231180000	Blewett	6630	NM	334	NM	31.5	0	76.3	2.65
O'BANION_1	04019231180000	Blewett	6630	NM	50	NM	29	0	77.6	2.73
O'BANION_1	04019231180000	Blewett	6631	NM	121	NM	30.7	0	73.9	2.65
O'BANION_2_RD1	04019231850100	Blewett	7162	250	64.8	NM	23.3	0	95.2	NM
O'BANION_2_RD1	04019231850100	Blewett	7163	250	254.9	NM	24.7	0	99.6	NM
O'BANION_2_RD1	04019231850100	Blewett	7195	250	5	NM	23.9	0	85.2	NM
O'BANION_2_RD1	04019231850100	Blewett	7312	250	42.5	NM	29.1	0	97.5	NM
O'BANION_3	04019232040000	Blewett	7135	250	37.9	NM	28.1	0	90.6	NM
O'BANION_3	04019232040000	Blewett	7147	250	16.2	NM	26.3	0	66	NM
O'BANION_3	04019232040000	Blewett	7155	250	41.2	NM	27.4	0	75.3	NM
O'BANION_3	04019232040000	Blewett	7164	250	48.4	NM	27.5	0	60.3	NM
O'BANION_3	04019232040000	Blewett	7172	250	19.1	NM	26.4	0	68.3	NM
O'BANION_3	04019232040000	Blewett	7178	250	20.1	NM	26.4	0	76.7	NM
O'BANION_3	04019232040000	Blewett	7182	250	14.5	NM	25.6	0	74.6	NM
O'BANION_3	04019232040000	Blewett	7185	250	25.4	NM	27.7	0	76.7	NM
O'BANION_3	04019232040000	Blewett	7194	250	21.7	NM	26.4	0	83.8	NM
O'BANION_4	04019232700000	Blewett	6784	NM	0.4	NM	25	0	81.4	2.68
O'BANION_4	04019232700000	Blewett	6790	NM	22.1	NM	25.8	0	99.3	2.67
O'BANION_4	04019232700000	Blewett	6798	NM	18.8	NM	21.8	0	98.2	2.65
O'BANION_4	04019232700000	Blewett	6807	NM	6	NM	24.3	0	97.5	2.64
O'BANION_4	04019232700000	Blewett	6814	NM	1.4	NM	19	0	99.8	2.63
O'BANION_4	04019232700000	Blewett	6855	NM	107.2	NM	26.6	0	95	2.65
O'BANION_4	04019232700000	Blewett	6857	NM	12.7	NM	26.7	0	99.6	2.68
O'BANION_4	04019232700000	Blewett	6870	NM	1067.3	NM	31.8	0	77.8	2.68

Well	UWI	Formation	Depth (feet)	Pressure	KA (mD)	Vertical Perm (mD)	PHIT (%)	SOC (%)	SWC (%)	GD (G/CC)
O'BANION_4	04019232700000	Blewett	6872	NM	20.4	NM	25.8	0	86.6	2.69
O'BANION_4	04019232700000	Blewett	6876	NM	182.6	NM	30.9	0	85.2	2.67
O'BANION_4	04019232700000	Blewett	6890	NM	103.6	NM	28.5	0	95.2	2.66
O'BANION_4	04019232700000	Blewett	6910	NM	103.7	NM	33	0	99.1	2.6
O'BANION_4	04019232700000	Blewett	6930	NM	305.5	NM	28.2	0	90	2.69
O'BANION_4	04019232700000	Blewett	6968	NM	58.9	NM	25.7	0	97.2	2.67
O'BANION_4	04019232700000	Blewett	6980	NM	105.2	NM	28.3	0	96.5	2.68
O'BANION_4	04019232700000	Blewett	6983	NM	197	NM	28.4	0	84.5	2.73
O'BANION_4	04019232700000	Blewett	6985	NM	116.6	NM	28.3	0	98.2	2.69
O'BANION_4	04019232700000	Blewett	6989	NM	965.4	NM	34.2	0	96.8	2.67
O'BANION_4	04019232700000	Blewett	7072	NM	64.3	NM	26.7	0	99.9	2.64
O'BANION_4	04019232700000	Blewett	7080	NM	42.6	NM	27.6	0	88.6	2.67
O'BANION_4	04019232700000	Blewett	7085	NM	32.5	NM	26.7	0	98.6	2.69
O'BANION_4	04019232700000	Blewett	7128	NM	95.8	NM	28	0	93.1	2.66
O'BANION_4	04019232700000	Blewett	7149	NM	594.3	NM	31.4	0	99.4	2.6
O'BANION_4	04019232700000	Blewett	7171	NM	14.2	NM	23.7	0	98.9	2.69
O'BANION_4	04019232700000	Blewett	7196	NM	17	NM	21.4	0	99.4	2.69
O'BANION_4	04019232700000	Blewett	7205	NM	120.1	NM	26.8	0	99.3	2.67
O'BANION_4	04019232700000	Blewett	7212	NM	80.3	NM	26.7	0	99	2.67
RODUNER_1-32	04039200780000	Blewett	5850	NM	2727	NM	33.1	0	97.6	2.68
RODUNER_1-32	04039200780000	Blewett	5851	NM	1728.9	NM	34.4	0	87.2	2.66
SILVER_CREEK_73X	04019207110000	Blewett	7248	NM	19	NM	22.5	NM	NM	NM
SILVER_CREEK_73X	04019207110000	Blewett	7254	NM	59	NM	28.9	NM	NM	NM
SILVER_CREEK_73X	04019207110000	Blewett	7260	NM	53	NM	27.9	NM	NM	NM
SILVER_CREEK_73X	04019207110000	Blewett	7290	NM	81	NM	30.8	NM	NM	NM
SILVER_CREEK_73X	04019207110000	Blewett	7296	NM	126	NM	25.8	NM	NM	NM

NM = No measure

Table 2.4-7. Core Samples from Seven Wells in the Tracy Formation

Well	UWI	Formation	Depth (feet)	Pressure	KA (mD)	Vertical Perm (mD)	PHIT (%)	SOC (%)	SWC (%)	GD (G/CC)
B&N_1	04019231910000	Tracy	7301		132.8	NM	27.3	0	43	NM
B&N_1	04019231910000	Tracy	7318		63.1	NM	32	0	15.2	NM
CHOWCHILLA_FARMS_74-9	04039001240000	Tracy	5972		16.3	NM	NM	NM	NM	NM
GILL_32-21	04039200580000	Tracy	6203		16	NM	31.3	0	94.7	NM
GILL_32-21	04039200580000	Tracy	6253		51.7	NM	32.2	0	93.4	NM
GILL_RANCH_34-18-202	04039201180000	Tracy	6394	250	373.2	NM	40.9	0	76.1	2.67
GILL_RANCH_34-18-202	04039201180000	Tracy	6395	250	NM	141.2	NM	NM	NM	NM
GILL_RANCH_34-18-202	04039201180000	Tracy	6395	250	198.7	NM	40.1	0	68.8	2.67
GILL_RANCH_34-18-202	04039201180000	Tracy	6396	250	NM	257.9	NM	NM	NM	NM
GILL_RANCH_34-18-202	04039201180000	Tracy	6396	250	375.6	NM	38.1	0	75.6	2.69
GILL_RANCH_34-18-202	04039201180000	Tracy	6397	250	NM	19	NM	NM	NM	NM
GILL_RANCH_34-18-202	04039201180000	Tracy	6397	250	177.7	NM	36.7	0	70.6	2.67
GILL_RANCH_34-18-202	04039201180000	Tracy	6398	250	NM	144.7	NM	NM	NM	NM
GILL_RANCH_34-18-202	04039201180000	Tracy	6398	250	182.9	NM	34.8	0	81.4	2.68
GILL_RANCH_34-18-202	04039201180000	Tracy	6399	250	NM	115	NM	NM	NM	NM
GILL_RANCH_34-18-202	04039201180000	Tracy	6399	250	228.7	NM	36.8	0	56.7	2.66
GILL_RANCH_34-18-202	04039201180000	Tracy	6400	250	NM	107.3	NM	NM	NM	NM
GILL_RANCH_34-18-202	04039201180000	Tracy	6400	250	279.4	NM	38.7	0	59.8	2.67
GILL_RANCH_34-18-202	04039201180000	Tracy	6401	250	NM	126.5	NM	NM	NM	NM
GILL_RANCH_34-18-202	04039201180000	Tracy	6401	250	229.1	NM	34.2	0	79.8	2.67
GILL_RANCH_34-18-202	04039201180000	Tracy	6402	250	NM	221.2	NM	NM	NM	NM
GILL_RANCH_34-18-202	04039201180000	Tracy	6402	250	411.7	NM	29	0	99.3	2.69
GILL_RANCH_34-18-202	04039201180000	Tracy	6403	250	NM	269.3	NM	NM	NM	NM
GILL_RANCH_34-18-202	04039201180000	Tracy	6403	250	346.5	NM	28.9	0	101.5	2.68
GILL_RANCH_34-18-202	04039201180000	Tracy	6404	250	NM	126	NM	NM	NM	NM

Well	UWI	Formation	Depth (feet)	Pressure	KA (mD)	Vertical Perm (mD)	PHIT (%)	SOC (%)	SWC (%)	GD (G/CC)
GILL_RANCH_34-18-202	04039201180000	Tracy	6404	250	246.8	NM	39.5	0	59.1	2.66
GILL_RANCH_34-18-202	04039201180000	Tracy	6405	250	NM	220.5	NM	NM	NM	NM
GILL_RANCH_34-18-202	04039201180000	Tracy	6405	250	342	NM	40.8	0	56.9	2.66
GILL_RANCH_34-18-202	04039201180000	Tracy	6406	250	NM	246.8	NM	NM	NM	NM
GILL_RANCH_34-18-202	04039201180000	Tracy	6406	250	292.2	NM	38.7	0	71.7	2.66
GILL_RANCH_34-18-202	04039201180000	Tracy	6407	250	NM	140.4	NM	NM	NM	NM
GILL_RANCH_34-18-202	04039201180000	Tracy	6407	250	138.5	NM	36.6	0	82.3	2.66
GILL_RANCH_34-18-202	04039201180000	Tracy	6408	250	NM	2.4	NM	NM	NM	NM
GILL_RANCH_34-18-202	04039201180000	Tracy	6408	250	127.4	NM	33.1	0	85	2.66
GILL_RANCH_34-18-202	04039201180000	Tracy	6409	250	NM	133.3	NM	NM	NM	NM
GILL_RANCH_34-18-202	04039201180000	Tracy	6409	250	286.6	NM	39.2	0	76.9	2.67
GILL_RANCH_34-18-202	04039201180000	Tracy	6410	250	NM	43.1	NM	NM	NM	NM
GILL_RANCH_34-18-202	04039201180000	Tracy	6410	250	242.1	NM	37.2	0	60.3	2.66
GILL_RANCH_34-18-202	04039201180000	Tracy	6411	250	NM	53.6	NM	NM	NM	NM
GILL_RANCH_34-18-202	04039201180000	Tracy	6411	250	228.2	NM	38.5	0	50	2.66
GILL_RANCH_34-18-202	04039201180000	Tracy	6412	250	NM	98.2	NM	NM	NM	NM
GILL_RANCH_34-18-202	04039201180000	Tracy	6412	250	283.6	NM	37.8	0	56	2.67
GILL_RANCH_34-18-202	04039201180000	Tracy	6413	250	NM	264.4	NM	NM	NM	NM
GILL_RANCH_34-18-202	04039201180000	Tracy	6413	250	234.7	NM	37.8	0	50.1	2.66
GILL_RANCH_34-18-202	04039201180000	Tracy	6413	250	NM	142	NM	NM	NM	NM
GILL_RANCH_34-18-202	04039201180000	Tracy	6414	250	233	NM	37.2	0	62.7	2.66
GILL_RANCH_34-18-202	04039201180000	Tracy	6415	250	NM	345	NM	NM	NM	NM
GILL_RANCH_34-18-202	04039201180000	Tracy	6415	250	201.9	NM	37.2	0	57	2.66
GILL_RANCH_34-18-202	04039201180000	Tracy	6415	250	NM	189.4	NM	NM	NM	NM
GILL_RANCH_34-18-202	04039201180000	Tracy	6416	250	383.7	NM	37.3	0	65.4	2.68
GILL_RANCH_34-18-202	04039201180000	Tracy	6417	250	NM	65.7	NM	NM	NM	NM
GILL_RANCH_34-18-202	04039201180000	Tracy	6417	250	202.1	NM	37.8	0	63.6	2.67

Well	UWI	Formation	Depth (feet)	Pressure	KA (mD)	Vertical Perm (mD)	PHIT (%)	SOC (%)	SWC (%)	GD (G/CC)
GILL_RANCH_34-18-202	04039201180000	Tracy	6418	250	NM	171	NM	NM	NM	NM
GILL_RANCH_34-18-202	04039201180000	Tracy	6418	250	0.02	NM	36.8	0	65.3	2.67
GILL_RANCH_34-18-202	04039201180000	Tracy	6419	250	NM	0.024	NM	NM	NM	NM
GILL_RANCH_34-18-202	04039201180000	Tracy	6419	250	0.022	NM	37.7	0	56.6	2.66
GILL_RANCH_34-18-202	04039201180000	Tracy	6420	250	NM	79.3	NM	NM	NM	NM
GILL_RANCH_34-18-202	04039201180000	Tracy	6420	250	400	NM	38.8	0	62.9	2.66
GILL_RANCH_34-18-202	04039201180000	Tracy	6421	250	NM	202	NM	NM	NM	NM
GILL_RANCH_34-18-202	04039201180000	Tracy	6421	250	517.3	NM	37.2	0	56.6	2.66
GILL_RANCH_34-18-202	04039201180000	Tracy	6422	250	NM	331.8	NM	NM	NM	NM
GILL_RANCH_34-18-202	04039201180000	Tracy	6422	250	294.2	NM	37.5	0	64.4	2.65
GILL_RANCH_34-18-202	04039201180000	Tracy	6448	250	6.4	NM	38.3	0	60.2	2.66
GILL_RANCH_34-18-202	04039201180000	Tracy	6448	250	NM	109.1	NM	NM	NM	NM
GILL_RANCH_34-18-202	04039201180000	Tracy	6449	250	41.3	NM	36.9	0	67.2	2.67
GILL_RANCH_34-18-202	04039201180000	Tracy	6449	250	NM	82	NM	NM	NM	NM
GILL_RANCH_34-18-202	04039201180000	Tracy	6450	250	138.1	NM	37.8	0	77.9	2.68
GILL_RANCH_34-18-202	04039201180000	Tracy	6451	250	NM	42.7	NM	NM	NM	NM
GILL_RANCH_34-18-202	04039201180000	Tracy	6451	250	143.8	NM	37	0	62.5	2.66
GILL_RANCH_34-18-202	04039201180000	Tracy	6452	250	NM	153.7	NM	NM	NM	NM
GILL_RANCH_34-18-202	04039201180000	Tracy	6452	250	263.6	NM	39.6	0	56.4	2.66
GILL_RANCH_34-18-202	04039201180000	Tracy	6452	250	NM	212.4	NM	NM	NM	NM
GILL_RANCH_34-18-202	04039201180000	Tracy	6453	250	113.9	NM	36.6	0	64.8	2.66
GILL_RANCH_34-18-202	04039201180000	Tracy	6454	250	NM	13.8	NM	NM	NM	NM
GILL_RANCH_34-18-202	04039201180000	Tracy	6454	250	43.7	NM	37.3	0	64.3	2.66
GILL_RANCH_34-18-202	04039201180000	Tracy	6455	250	NM	57.6	NM	NM	NM	NM
GILL_RANCH_34-18-202	04039201180000	Tracy	6455	250	90.4	NM	37.7	0	63.2	2.65
GILL_RANCH_34-18-202	04039201180000	Tracy	6456	250	NM	36.3	NM	NM	NM	NM
GILL_RANCH_34-18-202	04039201180000	Tracy	6456	250	111.5	NM	35.4	0	63.3	2.65

Well	UWI	Formation	Depth (feet)	Pressure	KA (mD)	Vertical Perm (mD)	PHIT (%)	SOC (%)	SWC (%)	GD (G/CC)
GILL_RANCH_34-18-202	04039201180000	Tracy	6457	250	NM	182.1	NM	NM	NM	NM
GILL_RANCH_34-18-202	04039201180000	Tracy	6457	250	24.1	NM	36.6	0	66.6	2.66
GILL_RANCH_34-18-202	04039201180000	Tracy	6458	250	NM	96.9	NM	NM	NM	NM
GILL_RANCH_34-18-202	04039201180000	Tracy	6458	250	90.4	NM	37.3	0	72.2	2.66
GILL_RANCH_34-18-202	04039201180000	Tracy	6459	250	NM	187.5	NM	NM	NM	NM
GILL_RANCH_34-18-202	04039201180000	Tracy	6459	250	127.5	NM	37.4	0	67.5	2.66
GILL_RANCH_34-18-202	04039201180000	Tracy	6460	250	NM	141.5	NM	NM	NM	NM
GILL_RANCH_34-18-202	04039201180000	Tracy	6460	250	136.7	NM	37	0	73.6	2.66
GILL_RANCH_34-18-202	04039201180000	Tracy	6460	250	NM	40	NM	NM	NM	NM
GILL_RANCH_34-18-202	04039201180000	Tracy	6461	250	31.9	NM	36.6	0	70.3	2.65
GILL_RANCH_34-18-202	04039201180000	Tracy	6462	250	NM	21.5	NM	NM	NM	NM
GILL_RANCH_34-18-202	04039201180000	Tracy	6462	250	19.3	NM	36.7	0	66	2.66
GILL_RANCH_34-18-202	04039201180000	Tracy	6463	250	NM	33.7	NM	NM	NM	NM
GILL_RANCH_34-18-202	04039201180000	Tracy	6463	250	34.6	NM	37.2	0	72	2.65
GILL_RANCH_34-18-202	04039201180000	Tracy	6464	250	NM	42.5	NM	NM	NM	NM
GILL_RANCH_34-18-202	04039201180000	Tracy	6464	250	69.2	NM	37.8	0	65.7	2.66
GILL_RANCH_34-18-202	04039201180000	Tracy	6465	250	NM	46.6	NM	NM	NM	NM
GILL_RANCH_34-18-202	04039201180000	Tracy	6465	250	80.3	NM	37.5	0	67.3	2.65
GILL_RANCH_34-18-202	04039201180000	Tracy	6466	250	NM	85.9	NM	NM	NM	NM
GILL_RANCH_34-18-202	04039201180000	Tracy	6466	250	0.021	NM	38.5	0	67.1	2.66
GILL_RANCH_34-18-202	04039201180000	Tracy	6467	250	NM	0.019	NM	NM	NM	NM
GILL_RANCH_34-18-202	04039201180000	Tracy	6467	250	296	NM	39	0	60.4	2.66
GILL_RANCH_34-18-202	04039201180000	Tracy	6468	250	NM	63	NM	NM	NM	NM
GILL_RANCH_34-18-202	04039201180000	Tracy	6469	250	62.3	NM	36.4	0	87.8	2.66
GILL_RANCH_34-18-202	04039201180000	Tracy	6469	250	NM	173.2	NM	NM	NM	NM
GILL_RANCH_34-18-202	04039201180000	Tracy	6469	250	353.1	NM	37	0	73.3	2.66
GILL_RANCH_34-18-202	04039201180000	Tracy	6470	250	NM	282	NM	NM	NM	NM

Well	UWI	Formation	Depth (feet)	Pressure	KA (mD)	Vertical Perm (mD)	PHIT (%)	SOC (%)	SWC (%)	GD (G/CC)
GILL_RANCH_34-18-202	04039201180000	Tracy	6470	250	197.6	NM	40.1	0	89.7	2.67
GILL_RANCH_34-18-202	04039201180000	Tracy	6471	250	NM	121.1	NM	NM	NM	NM
GILL_RANCH_34-18-202	04039201180000	Tracy	6471	250	76.5	NM	41.9	0	83.2	2.67
GILL_RANCH_34-18-202	04039201180000	Tracy	6472	250	NM	2.6	NM	NM	NM	NM
GILL_RANCH_34-18-202	04039201180000	Tracy	6472	250	93.4	NM	36.4	0	53.6	2.68
GILL_RANCH_34-18-202	04039201180000	Tracy	6473	250	NM	7.5	NM	NM	NM	NM
GILL_RANCH_34-18-202	04039201180000	Tracy	6473	250	279.6	NM	30.7	0	90.6	2.7
GILL_RANCH_34-18-202	04039201180000	Tracy	6474	250	NM	327.6	NM	NM	NM	NM
GILL_RANCH_34-18-202	04039201180000	Tracy	6474	250	194.4	NM	35.4	0	80.4	2.67
GILL_RANCH_34-18-202	04039201180000	Tracy	6475	250	NM	114.3	NM	NM	NM	NM
GILL_RANCH_34-18-202	04039201180000	Tracy	6475	250	173.2	NM	32.3	0	89.4	2.68
GILL_RANCH_34-18-202	04039201180000	Tracy	6475	250	NM	140.4	NM	NM	NM	NM
GILL_RANCH_34-18-202	04039201180000	Tracy	6494	250	99.9	NM	33.9	0	71.9	2.67
GILL_RANCH_34-18-202	04039201180000	Tracy	6495	250	NM	55.8	NM	NM	NM	NM
GILL_RANCH_34-18-202	04039201180000	Tracy	6495	250	70.2	NM	34.8	0	64	2.67
GILL_RANCH_34-18-202	04039201180000	Tracy	6496	250	NM	57.2	NM	NM	NM	NM
GILL_RANCH_34-18-202	04039201180000	Tracy	6496	250	309.4	NM	36.1	0	83.5	2.68
GILL_RANCH_34-18-202	04039201180000	Tracy	6496	250	NM	35.6	NM	NM	NM	NM
GILL_RANCH_34-18-202	04039201180000	Tracy	6497	250	977.4	NM	36.6	0	59.1	2.67
GILL_RANCH_34-18-202	04039201180000	Tracy	6497	250	NM	836.5	NM	NM	NM	NM
GILL_RANCH_34-18-202	04039201180000	Tracy	6498	250	819.6	NM	33.6	0	79.7	2.67
GILL_RANCH_34-18-202	04039201180000	Tracy	6498	250	NM	792.1	NM	NM	NM	NM
GILL_RANCH_34-18-202	04039201180000	Tracy	6499	250	1592.9	NM	35.7	0	78.5	2.67
GILL_RANCH_34-18-202	04039201180000	Tracy	6500	250	NM	2889	NM	NM	NM	NM
GILL_RANCH_34-18-202	04039201180000	Tracy	6500	250	2473	NM	33.8	0	62.1	2.67
GILL_RANCH_34-18-202	04039201180000	Tracy	6501	250	NM	1991.5	NM	NM	NM	NM
GILL_RANCH_34-18-202	04039201180000	Tracy	6501	250	684.4	NM	35.6	0	71.4	2.66

Well	UWI	Formation	Depth (feet)	Pressure	KA (mD)	Vertical Perm (mD)	PHIT (%)	SOC (%)	SWC (%)	GD (G/CC)
GILL_RANCH_34-18-202	04039201180000	Tracy	6502	250	NM	1979.9	NM	NM	NM	NM
GILL_RANCH_34-18-202	04039201180000	Tracy	6502	250	750.4	NM	35	0	75.8	2.66
GILL_RANCH_34-18-202	04039201180000	Tracy	6503	250	NM	524.1	NM	NM	NM	NM
GILL_RANCH_34-18-202	04039201180000	Tracy	6503	250	716	NM	35.3	0	95.2	2.67
GILL_RANCH_34-18-202	04039201180000	Tracy	6504	250	NM	516	NM	NM	NM	NM
GILL_RANCH_34-18-202	04039201180000	Tracy	6504	250	828.9	NM	34.7	0	79.9	2.67
GILL_RANCH_34-18-202	04039201180000	Tracy	6505	250	NM	585.1	NM	NM	NM	NM
GILL_RANCH_34-18-202	04039201180000	Tracy	6505	250	845.8	NM	39.6	0	44.9	2.66
GILL_RANCH_34-18-202	04039201180000	Tracy	6506	250	NM	580.8	NM	NM	NM	NM
GILL_RANCH_34-18-202	04039201180000	Tracy	6506	250	619.1	NM	33.7	0	84.7	2.67
GILL_RANCH_34-18-202	04039201180000	Tracy	6507	250	NM	446.9	NM	NM	NM	NM
GILL_RANCH_34-18-202	04039201180000	Tracy	6507	250	610.4	NM	35.3	0	82.4	2.67
GILL_RANCH_34-18-202	04039201180000	Tracy	6508	250	NM	395.1	NM	NM	NM	NM
GILL_RANCH_34-18-202	04039201180000	Tracy	6508	250	492	NM	35.8	0	82.6	2.66
GILL_RANCH_34-18-202	04039201180000	Tracy	6509	250	NM	295.5	NM	NM	NM	NM
GILL_RANCH_34-18-202	04039201180000	Tracy	6509	250	649.1	NM	36.9	0	76.9	2.66
GILL_RANCH_34-18-202	04039201180000	Tracy	6510	250	NM	495.6	NM	NM	NM	NM
GILL_RANCH_34-18-202	04039201180000	Tracy	6510	250	782.7	NM	34.6	0	76.2	2.66
GILL_RANCH_34-18-202	04039201180000	Tracy	6511	250	NM	591.3	NM	NM	NM	NM
GILL_RANCH_34-18-202	04039201180000	Tracy	6511	250	914.5	NM	36.4	0	58.3	2.66
GILL_RANCH_34-18-202	04039201180000	Tracy	6512	250	NM	470.5	NM	NM	NM	NM
GILL_RANCH_34-18-202	04039201180000	Tracy	6512	250	894.4	NM	34	0	80.9	2.67
GILL_RANCH_34-18-202	04039201180000	Tracy	6513	250	NM	122.3	NM	NM	NM	NM
GILL_RANCH_34-18-202	04039201180000	Tracy	6513	250	239	NM	34.5	0	80.1	2.67
GILL_RANCH_34-18-202	04039201180000	Tracy	6514	250	NM	245	NM	NM	NM	NM
GILL_RANCH_34-18-202	04039201180000	Tracy	6514	250	618.6	NM	32.2	0	88.4	2.67
GILL_RANCH_34-18-202	04039201180000	Tracy	6515	250	539.2	NM	36	0	72.6	2.66

Well	UWI	Formation	Depth (feet)	Pressure	KA (mD)	Vertical Perm (mD)	PHIT (%)	SOC (%)	SWC (%)	GD (G/CC)
GILL_RANCH_34-18-202	04039201180000	Tracy	6515	250	NM	335.6	NM	NM	NM	NM
LE_COMPTE_1	04019231840000	Tracy	6913	NM	27	NM	33.8	0	66	2.59
NAPA_AVE_A1	04019225380000	Tracy	6497	NM	22	NM	33.9	0	89.2	2.64
NAPA_AVE_A1	04019225380000	Tracy	6605	NM	74	NM	33.1	0	83.2	2.64
NAPA_AVE_A1	04019225380000	Tracy	6807	NM	21	NM	32.1	0	72.9	2.63
NAPA_AVE_A1	04019225380000	Tracy	7055	NM	404	NM	26.3	0	84.3	2.51
NAPA_AVE_A1	04019225380000	Tracy	7234	NM	105	NM	28.7	0	85.1	2.59
NAPA_AVE_A1	04019225380000	Tracy	7305	NM	110	NM	33.2	0	83.5	2.65
NLF_POTTER_19-1	04047200700000	Tracy	5958	NM	620	NM	30.4	0	94.1	NM
NLF_POTTER_19-1	04047200700000	Tracy	5976	NM	390	NM	30.4	0	91.3	NM
NLF_POTTER_19-1	04047200700000	Tracy	5981	NM	230	NM	28.6	0	90.8	NM
NLF_POTTER_19-1	04047200700000	Tracy	5986	NM	190	NM	29.1	0	90.4	NM
NLF_POTTER_19-1	04047200700000	Tracy	6024	NM	700	NM	31.9	0	89.3	NM
NLF_POTTER_19-1	04047200700000	Tracy	6036	NM	310	NM	32.4	0	87.9	NM
NLF_POTTER_19-1	04047200700000	Tracy	6060	NM	2260	NM	28	0	92.3	NM
NLF_POTTER_19-1	04047200700000	Tracy	6090	NM	650	NM	28.8	0	88.7	NM
NLF_POTTER_19-1	04047200700000	Tracy	6114	NM	1100	NM	27.4	0	90.3	NM
NLF_POTTER_19-1	04047200700000	Tracy	6146	NM	930	NM	29.2	0	92.7	NM
NLF_POTTER_19-1	04047200700000	Tracy	6226	NM	210	NM	34	0	87.1	NM
NLF_POTTER_19-1	04047200700000	Tracy	6270	NM	270	NM	30.2	0	90.4	NM
NLF_POTTER_19-1	04047200700000	Tracy	6294	NM	510	NM	29.8	0	84.6	NM

NM = No measure

Table 2.4-8. Kreyenhagen, Domengine, Garzas, Blewett and Tracy Formation Thickness and Depth within the AoR

Zone	Formation	Property	Low	High	Mean
Confining Zone	Kreyenhagen Shale	Thickness (feet)	522	659	560
		Depth (feet TVD)	3,627	4,303	3,980
Injection Zone	Domengine	Thickness (feet)	1,078	1,335	1,189
		Depth (feet TVD)	4,200	4,828	4,542
	Garzas	Thickness (feet)	958	1,440	1,216
		Depth (feet TVD)	5,836	6,391	6,001
	Blewett	Thickness (feet)	546	1,052	791
		Depth (feet TVD)	7,574	8,402	7,987
	Tracy	Thickness (feet)	136	482	291
		Depth (feet TVD)	8,665	9,500	9,232

Table 2.5-1. Wells Used for the Overburden Stress Gradient Calculation

Well	UWI
ADAMS_1_WESTLANDS	04019231020000
B&N_1	04019231910000
B&N_1_RD1	04019231910010
B&N_2-25	04019234900000
B&N_2-25_RD1	04019234900100
BERTAO_1-30	04047200940000
BERTAO_1-31	04047200860000
BLUE_AGAVE_1_RD1	04019242250100
BOREL_64X-1	04047200870000
BRAVO_1_UNION	04019217460000
BRONSTEIN_1-8	04019236460000
BUIE_1-30	04047201220000
BUIE_1-36	04047200950000
CLARK_BROS_11-1	04047200730000
CLAYTON_75X-1	04039200880000
CODERNIZ_1-14	04019234320000
DODD_1-14	04019235290000
DODD_2-14	04019235310000
FIALHO_1	04047200080000
FOURCHY_1-25	04019235300000
FOURCHY_1-25_RD1	04019235300100
GILL_38X-17	04039200850000
GILL_RANCH_11-21-101	04039201160000
GILL_RANCH_34-18-202	04039201180000
GROPPETTI_1_PHILLIPS	04019231810000
HAMBURG_1-1	04019221270000
KIMBERLIN_18-1	04019215510000
KINDERGARTEN_COP_1-3	04047201140000
LE_COMPTE_1	04019231840000
LECOMPTE_1-13	04019235320000
LECOMPTE_1-13_RD1	04019235320100
LITTLE_PANOCHE_1	04019215740000
LORENZETTI_23X-22	04019212770000
MOFFAT_48X-7	04039201090000
MURRIETA-STEELE_1	04019214340000
NAPA_AVE_A1	04019225380000
O'BANION_1	04019231180000
O'BANION_2	04019231850000

Well	UWI
O'BANION_2_RD1	04019231850100
O'BANION_3	04019232040000
O'BANION_4	04019232700000
O'BANION_5	04019235330000
O'BANION_7-25	04019236500000
RED_HEAT_1	04019244150000
REDFERN_RANCHES_A_1	04019206590000
SEQUEIRA_1-16	04047200890000
SOUZA_1	04019219240000
SWINDLE_1-5	04019247720000
TEIXEIRA_1	04047200410000
VON_ALLMAN_1-23_RD1	04019236470100
WICK_18-34	04039200900000
WICK_55X-7	04039200870000
YOUNG_ET_AL_1	04019204110000

Table 2.6-1. Data from USGS Earthquake Catalog for Historical Seismicity within the Model Boundary and a 7-mile Radius Around the Edge of the AoR

Date	Magnitude	Last Updated	Locale	Type	Status	Depth (km)
9/26/1976	2.65	12/15/2016	13 km S of South Dos Palos, California	earthquake	reviewed	-0.245
11/27/1976	2.83	12/15/2016	18 km S of South Dos Palos, California	earthquake	reviewed	6.585
6/28/1980	2.87	4/2/2016	6km WNW of Mendota, CA	earthquake	reviewed	6
1/11/1982	2.62	12/12/2016	9 km S of South Dos Palos, California	earthquake	reviewed	-0.629
2/16/1989	2.59	12/8/2016	17 km WSW of Mendota, California	earthquake	reviewed	-0.406
3/18/1990	2.54	12/17/2016	10 km ESE of Dos Palos, California	earthquake	reviewed	0.8
11/2/1998	2.81	12/29/2016	11 km S of South Dos Palos, California	earthquake	reviewed	-0.369
4/8/2005	2.85	1/11/2017	12 km SW of Firebaugh, California	earthquake	automatic	11.278
3/24/2012	2.63	1/27/2017	9 km SSE of South Dos Palos, California	earthquake	reviewed	1.535

Table 2.7-1. Injectate Compositions

Component	Injectate 1 (Mass %)	Injectate 2 (Mass %)
CO_2	99.21%	99.88%
H_2	0.05%	0.01%
N_2	0.64%	0.00%
H_2O	0.02%	0.00%
CO	0.03%	0.00%
Ar	0.03%	0.00%
O_2	0.00%	0.00%
SO_2+SO_3	0.00%	0.00%
H_2S	0.00%	0.01%
CH_4	0.00%	0.04%
NOx	0.00%	0.00%
NH_3	0.00%	0.00%
C_2H_6	0.00%	0.05%
Ethylene	0.00%	0.00%
Total	100.00%	100.00%

Table 7.2-2. Simplified Four-Component Composition for Injectate 1 and Injectate 2

Injectate 1	
Component	Mass %
CO_2	99.213%
N_2	0.643%
SO_2+SO_3	0.003%
H_2S	0.001%

Injectate 2	
Component	Mass %
CO_2	99.884%
CH_4	0.039%
C_2H_6	0.053%
H_2S	0.014%

Table 7.2-3. Injectate Properties Range at Downhole Conditions for Injectate 1 and Injectate 2

Injectate property at downhole conditions	Injectate 1	Injectate 2
Viscosity, cp	0.05–0.06	0.05–0.06
Density, lb/ft^3	35.87–44.45	37.78–45.55
Compressibility factor, Z	0.43–0.68	0.41–0.67